Remote File
Posted
E&B

GEORGIA INSTITUTE OF TECHNOLOGY
OFFICE OF RESEARCH ADMINISTRATION

RESEARCH PROJECT INITIATION

Date: July 12, 1974

Project Title: Physical Structure of Porous Catalysts & Adsorbents

Project No: E-19-625

Principal Investigator: Dr. Clyde Orr, Jr.

Sponsor: National Science Foundation

Agreement Period: From May 1, 1974 Until Oct. 31, 1976*

*24 months budget period plus 6 months for submission of required reports etc.

Type Agreement: Grant GK-43616

Amount: $38,900 - NSF Funds (E-19-625)
11,302 - GIT Contrib. (E-19-325)
$50,202 - Total

Reports Required: Annual Letter Technical; Final Report

Sponsor Contact Person (s):

Administrative Matters
Mr. F. G. Naughten
Grants Manager, Area 4
National Science Foundation
Washington, D. C. 20550
Phone: (202) 632-5965

Technical Matters
Dr. Marshall M. Lih, Director
Thermodynamic and Mass Transfer Program
Division of Engineering
National Science Foundation
Washington, D. C. 20550
Phone: (202) 632-5867

Assigned to: School of Chemical Engineering

COPIES TO:

- Principal Investigator
- School Director
- Dean of the College
- Director, Research Administration
- Director, Financial Affairs (2)
- Security-Reports-Property Office
- Patent Coordinator
- Library
- Rich Electronic Computer Center
- Photographic Laboratory
- Project File
- Other

RA-3 (6-71)

GEORGIA INSTITUTE OF TECHNOLOGY
OFFICE OF CONTRACT ADMINISTRATION

Posted

SPONSORED PROJECT TERMINATION

Date: June 20, 1977

Project Title: "Physical Structure of Porous Catalysts and Adsorbents."

Project No: E-19-625

Project Director: Dr. Clyde Orr, Jr.

Sponsor: National Science Foundation

Effective Termination Date: 10/31/76

Clearance of Accounting Charges: 10/31/76

Grant/Contract Closeout Actions Remaining: NONE

_ Final Invoice and Closing Documents
_ Final Fiscal Report
_ Final Report of Inventions
_ Govt. Property Inventory & Related Certificate
_ Classified Material Certificate
_ Other _____

Assigned to: Chemical Engineering (School/Laboratory)

COPIES TO:

Project Director
Division Chief (EES)
School/Laboratory Director
Dean/Director–EES
Accounting Office
Procurement Office
Security Coordinator (OCA)
Reports Coordinator (OCA)
Library, Technical Reports Section
Office of Computing Services
Director, Physical Plant
EES Information Office
Project File (OCA)
Project Code (GTRI)
Other _____

CA–4 (3/76)

ANNUAL REPORT

INVESTIGATION INTO THE PHYSICAL STRUCTURE OF POROUS CATALYSTS AND ADSORBENTS

Grant No. GK–43616

Project No. E–19–625

by

Clyde Orr, Jr. and Albert A. Liabastre

June, 1975

1975

School of Chemical Engineering

GEORGIA INSTITUTE OF TECHNOLOGY

Atlanta, Georgia

Annual Report

INVESTIGATION INTO THE PHYSICAL STRUCTURE OF POROUS CATALYSTS AND ADSORBENTS

Grant No. GK-43616

Project No. E-19-625

by

Clyde Orr, Jr. and Albert A. Liabastre

School of Chemical Engineering

Georgia Institute of Technology

Atlanta, Georgia 30332

June, 1975

TABLE OF CONTENTS

LIST OF TABLES

LIST OF FIGURES

I. SUMMARY

The structure of porous solids, while of great importance to technology, cannot presently be determined without the inclusion of assumptions of questionable merit, making for ambiguities and disagreement of results. This research sought to assess the validity of the several assumptions by subjecting materials with regular and well-defined pore characteristics to evaluation techniques and examining the results in terms of the defined structures.

Obtaining or producing materials with the desired pores constituted the first phase of the research. Ultimately two very different materials, controlled-pore glass and Nuclepore membranes of polycarbonate, were selected. Both were obtained with nearly cylindrical pores in a variety of diameter ranges, and techniques were developed whereby pore diameters could be reliably measured by microtomy and electron microscopy. Evaluation was then initiated by the two primary test methods available, mercury penetration and low-temperature gas adsorption and desorption.

Definitive conclusions from this research can only be reached when more data are accumulated and comparisons with theory are compiled. Enough has been accomplished to confirm measurable differences and patterns of disagreement, suggesting that modifications of theory are possible. This report contains primarily a presentation of the data so far obtained.

II. INTRODUCTION

Porous solid materials play an important role in todays economy. They are used in the chemical process industry in pollution control, in life support systems, and in chemical research, to name only a few. Among the specific applications of porous solids are filters, adsorbents, chromatographic column packings, and catalyst supports. In most instances the size and shape of the pores are of primary concern, since they influence the efficiency of the solid in its specific role. The size and shape features of porous solids are usually determined by one of two analytical techniques- - mercury penetration and low temperature gas adsorption. These techniques rely on extrapolations of theoretical hypotheses and physical constants to determine pore size and shape features. As a result they give information based on various assumptions having practical limitations, and do not give unambigous results. Quite often in cases where both analytical techniques are applied they give very different results.

This research was concerned with the validity of the several assumptions and with ways of determining how to make the results coincide with actual values. The problem was approached by carefully examining results from available materials that had nearly cylindrical pores of relatively uniform diameters. By so testing the validity of the assumptions and extrapolations it is expected that the evaluation of porous solids can be put on a firmer foundation.

III. EXPERIMENTAL WORK

The experimental work breaks down into four general categories: porous material selection or preparation, electron microscopic examination, mercury penetration tests, and low temperature gas adsorption studies. Electron microscope techniques and results of microscopic analyses are included in the section describing material selection.

A. Material Selection

Much of the effort expended in this research has been directed toward selecting and characterizing the geometrical features of various solid materials. These efforts have enabled the selection (or exclusion) of solid materials with which to conduct further experimentation.

Considerable time and effort was devoted to the analysis of a CeO_2 doped Gd_2O_3-Mo composite, which is a unidirectionally solidified oxide-metal composite consisting of metal fibers grown in a refractory matrix. This material is grown from a molten eutectic which is cooled at a controlled rate so that different freezing points cause one component to nucleate first and to grow as needles or fibers in the other. Such a composite material was previously grown and analyzed by Rieger,[1] who found that the molybdenum fibers were present in the ceria-gadolina matrix in roughly a hexagonal array and that the molybdenum could be etched away leaving essentially cylindrical pores. A cylindrical ingot of such a composite was sectioned, etched, and examined microscopically. Analyses regarding pore size and density obtained in this research agree with the previous results of Rieger.[1] It was hoped that several ingot sections could be crushed to a powder and then etched in order to obtain sufficient pores to conduct meaningful pore-evaluation experiments. However, in examining the composite sections it was discovered that large areas of inhomogeneity existed which, when taken together with the low pore density, excluded this material from further consideration, as it was calculated that a minimum of 50 grams of material without inhomogeneity would be required.

Among other systems investigated and excluded from further consideration were Vycor glass and some catalysts due to the complexity of their pore structures.

An important system chosen for investigation was controlled pore glass* (porous glass) with pores ranging in nominal** diameter from 75 Å to 2000 Å. Porous glasses were selected because their pores were thought to be relatively uniform in size, they are widely used in many applications, and without their inclusion any study of this type would be incomplete. Considerable effort was devoted to developing an improved technique to elucidate the glass structure. That finally selected was to grind the glass to a fine powder, heat the powder under vacuum to 180°C for one hour, raise the temperature to 250°C for 15 minutes, then cool to room temperature while still in vacuum. The samples were then placed in polyethylene mounting block forms which had previously

---

* From Electro-Nucleonics, Inc., Fairfield, New Jersey.

** The nominal diameter as supplied by the manufacturer is used throughout for identification purposes even though subsequent measurements revealed it to be only approximately correct in many instances.

been dried, Spurr resin* was poured in, and the blocks were again exposed to a vacuum. The system was evacuated for 15 min. to aid pore penetration. Then the system was filled with nitrogen and allowed to remain overnight. The next day the samples were allowed to cure at 70°F for 12 hrs. The cured samples were finally sectioned (600-1000 Å) and electron micrographs made at 80 and 100 kv.

The resulting micrographs appear similar to those of Barrall and Cain[2] who also investigated porous glass. Figures 1 and 2 show two typical electron micrographs obtained in this work. It should be noted that the subsequent analysis of the micrographs is not unambigous since the structure of the glass seems quite complex. Wantanabe, Noake, and Aiba[3] have suggested that porous glass has a honeycomb structure, that is, linked cavities. It has been suggested by Karnaukhov[4] that the structure of porous glass is composed of cylindrical or close-to-cylindrical pores, closed and open pores, and bottle shaped pores. The only other attempt to evaluate pore sizes from micrographs is that of Barrall and Cain;[2] their work indicated the open pores to be irregular, interconnected channels which penetrate the entire glass structure. Widths of the channels were measured along lines oriented as nearly perpendicular to one wall as possible. The resulting micrography pore dimensions compared quite well with mercury porosimetry results on the same samples.

The analyses of this study were conducted along the same lines except that the size distribution of the pores that go through and into the material was determined. In the case of the nominal 160 Å glass, this method and the method of Barrall and Cain[2] were compared and yielded the same result. Results for the analyses of the porous glasses are included in Table 1.

The only system which lends itself to straightforward analysis is Nuclepore membrane filters.** Microscopic analysis indicates that here the pores run essentially straight through the material, display very little narrowing in going through the material, and have sufficient pore density for the low temperature gas adsorption and mercury porosimetry experiments. At this junction it should be noted that it is extremely difficult to obtain transmission electron microscopy results where the features of interest are smaller than 1000 Å. For samples having pores of 1000 Å and larger scanning electron microscopy may be used, however the limit of detection of this technique is about 200 $\pm$ 100 Å. The materials of interest for low temperature gas adsorption studies in this work are

---

* From Polyscience Inc., Warrington, Pennsylvania.

** Nuclepore Corporation, Pleasanton, California.

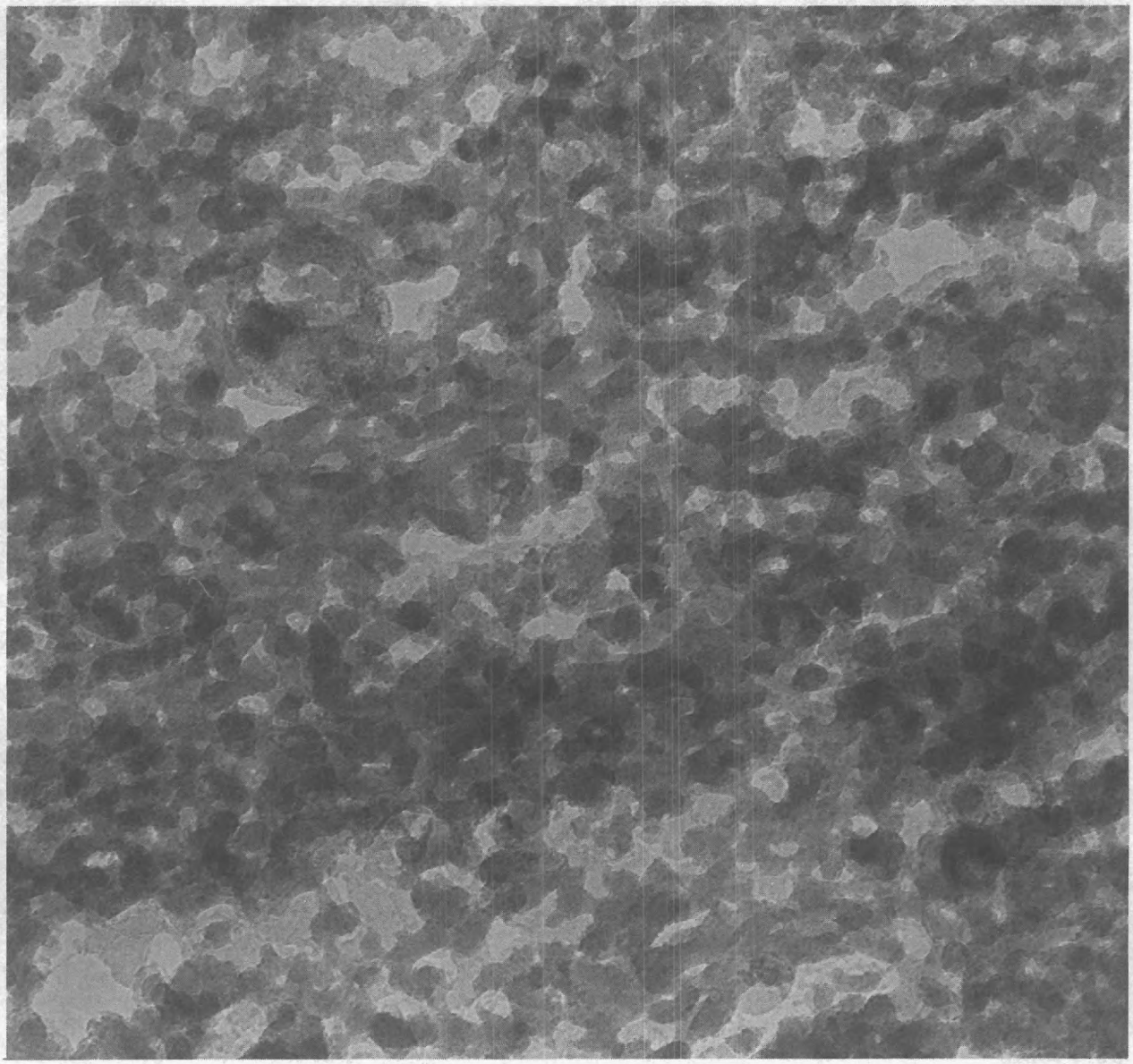

1000Å

192,000x

Figure 1. Transmission Electron Micrograph of Nominal 160 Å Controlled Pore Glass Using Ultramicrotomy.

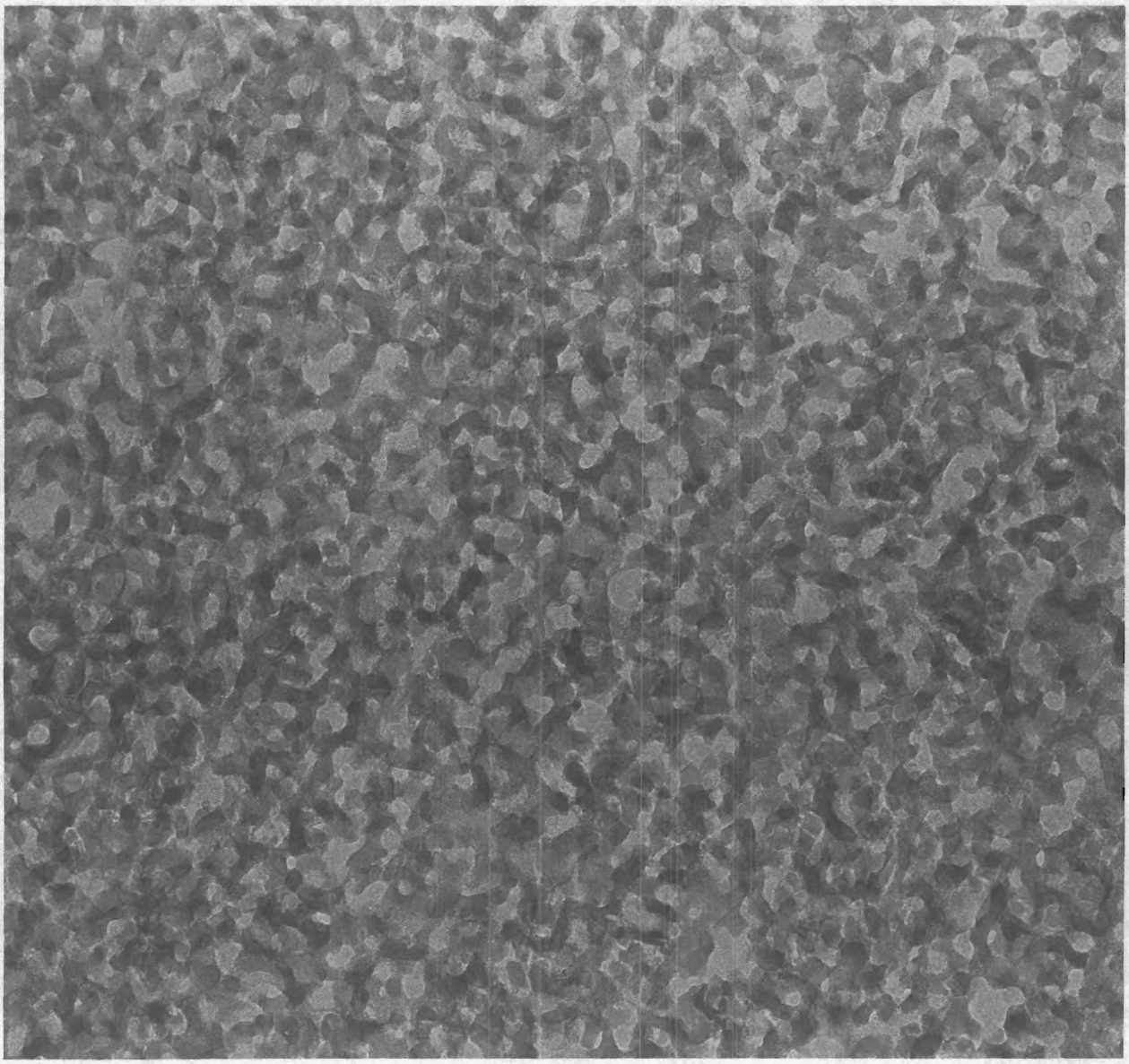

Figure 2. Transmission Electron Micrograph of Nominal 215 Å Controlled Pore Glass Using Ultramicrotomy.

Table I. Results of Electron Microscopic Analyses of Various Materials*

Nominal Pore Diameter (Å)	Measured Modal Diameter (Å)	Pore Density (Pores/cm^{2}x10^{-9})
Porous Glass		
75	**	- -
160	122	- -
170	**	- -
215	220	- -
350	**	- -
475	490	- -
1093	1230	- -
1223	∿1300	- -
1933	∿1969	- -
Nuclepore Membrane		
150***	∿310	3.0
300***	∿630	3.0
2000	**	**
4000	**	**
6000	**	**
10,000	**	**
50,000	**	**

* All results are based on limited statistical data and are subject to minor alterations as additional data are obtained.

** Analysis in progress.

*** Specially prepared by the Nuclepore Corporation for this study.

smaller than 600 Å. This has resulted in very tedious and time consuming sample handling and preparation procedures for microscopic analysis. Nevertheless, techniques have been developed to analyze the Nuclepore material for transmission electron microscopy.

Two methods were developed, one involving ultramicrotomy and the other a carbon replication technique. The untramicrotomy technique involved preparing the Nuclepore membranes containing nominal 150 Å and 300 Å diameter pores by embedding the material in a suitable resin. Three types of resin were tried: Spurr, methylmethacrylate, and Araldite.**** The Spurr and methylmethacrylate formed unsuitable bonds with the Nuclepore membrane while the Araldite formed a weak but usable bond. A typical sample preparation follows. The membrane was cut into five, 6-mm diameter discs and soaked for one minute in water to

**** From Cargille Sons, Little Falls, New Jersey.

remove the static charge. The discs were then soaked 1 hr in a 1% uranyl acetate in methanol solution, in order to dye the pores for viewing in the electron microscope. After drying at room temperature, the discs were placed one at a time in a 20-mm diameter drop of Araldite, exercising caution not to entrap air. The Araldite, disc composite was sandwiched between two pieces of Teflon and cured overnight at 70°C. The composite was re-embedded in a capsule of Araldite and again cured overnight at 70°C. The capsule was then microtomed, using a diamond knife, into 600 to 900 Å thick sections. Figures 3 and 4 show two typical electron micrographs obtained by this method

The other method employed was that of making carbon replicas of the Nuclepore membrane surface. This involved coating the membrane surface with a layer of carbon and then dissolving the membrane away using chloroform.

Because of the ease of preparation and absence of distortion due to microtoming it is believed this latter method is best for the Nuclepore membrane. Typical transmission electron micrographs are shown in Figures 5 through 8.

All pores of size greater than 800 Å were analyzed using standard scanning electron microscopic techniques. Typical scanning electron micrographs are shown in Figures 9 through 12.

B. Mercury Porosimetry

The results of the completed mercury porosimetry experiments are shown in Table II. These experiments were conducted using a Micromeritics* mercury penetration porosimeter, Model 905-1. The mercury** was triply distilled and discarded after use. Where repetative analyses have been conducted, good reproducibility has been achieved. In the case of the 1200 Å controlled pore glass, an analysis similar to that of Svatá[5] was carried out. This technique is presently being evaluated but no conclusions about the technique are available at this time. The purpose of this test is to attempt to evaluate the distribution of "ink-bottle" pores. However, it appears that hysteresis exhibited by porous substances is due both to structural considerations and to contact angle hysteresis (the fact that the advancing and receding contact angles differ). These features should be resolvable by analyzing a

* Micromeritics Instrument Corporation, Norcross, Georgia.

** Bethlehem Apparatus Co., Inc., Hellertown, Pennsylvania.

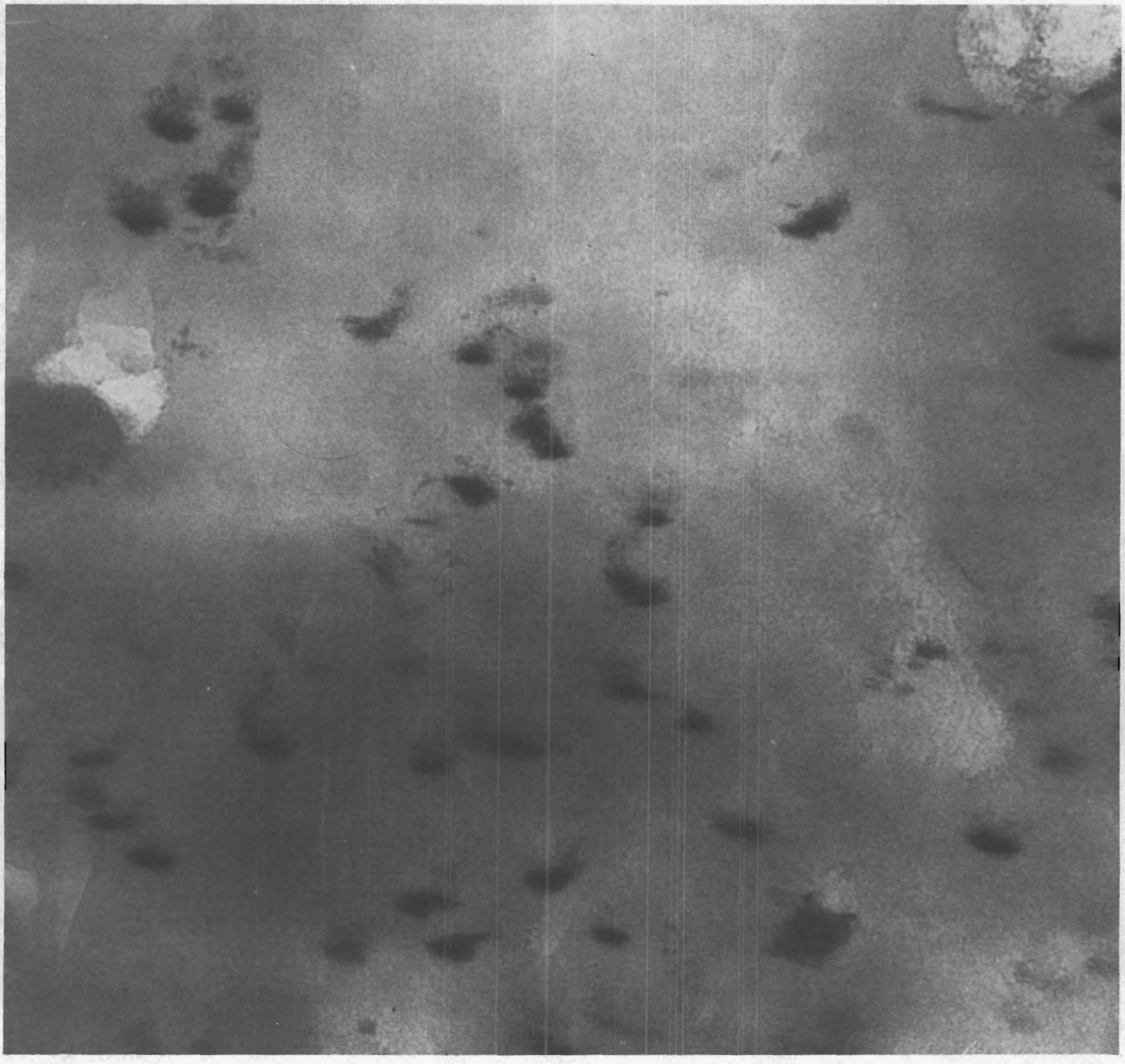

1000 Å

192,000x

Figure 3. Transmission Electron Micrograph of Nominal 150 Å Nuclepore Membrane Using Ultramicrotomy.

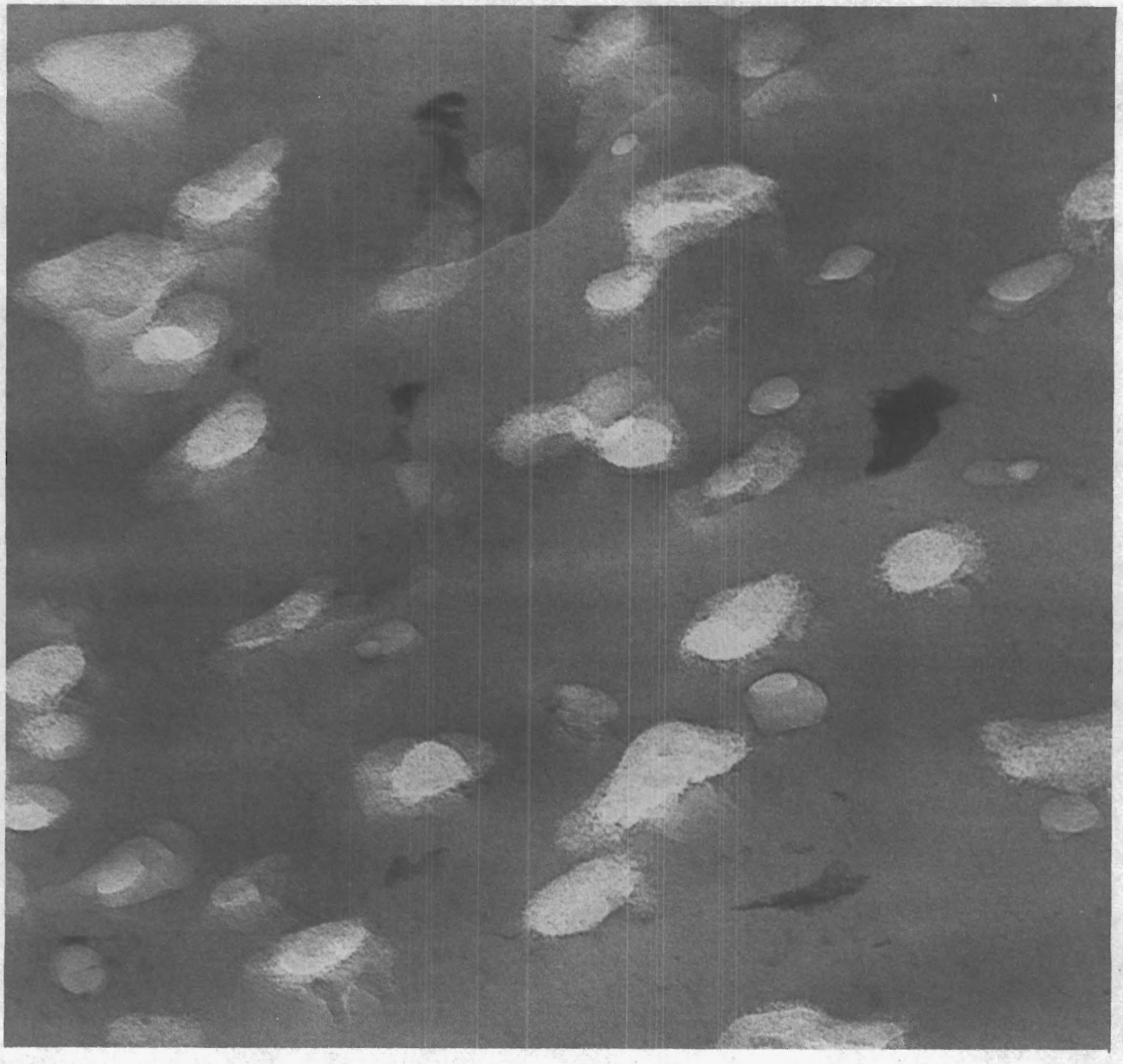

Figure 4. Transmission Electron Micrograph of Nominal 300 Å Nuclepore Membrane Using Ultramicrotomy.

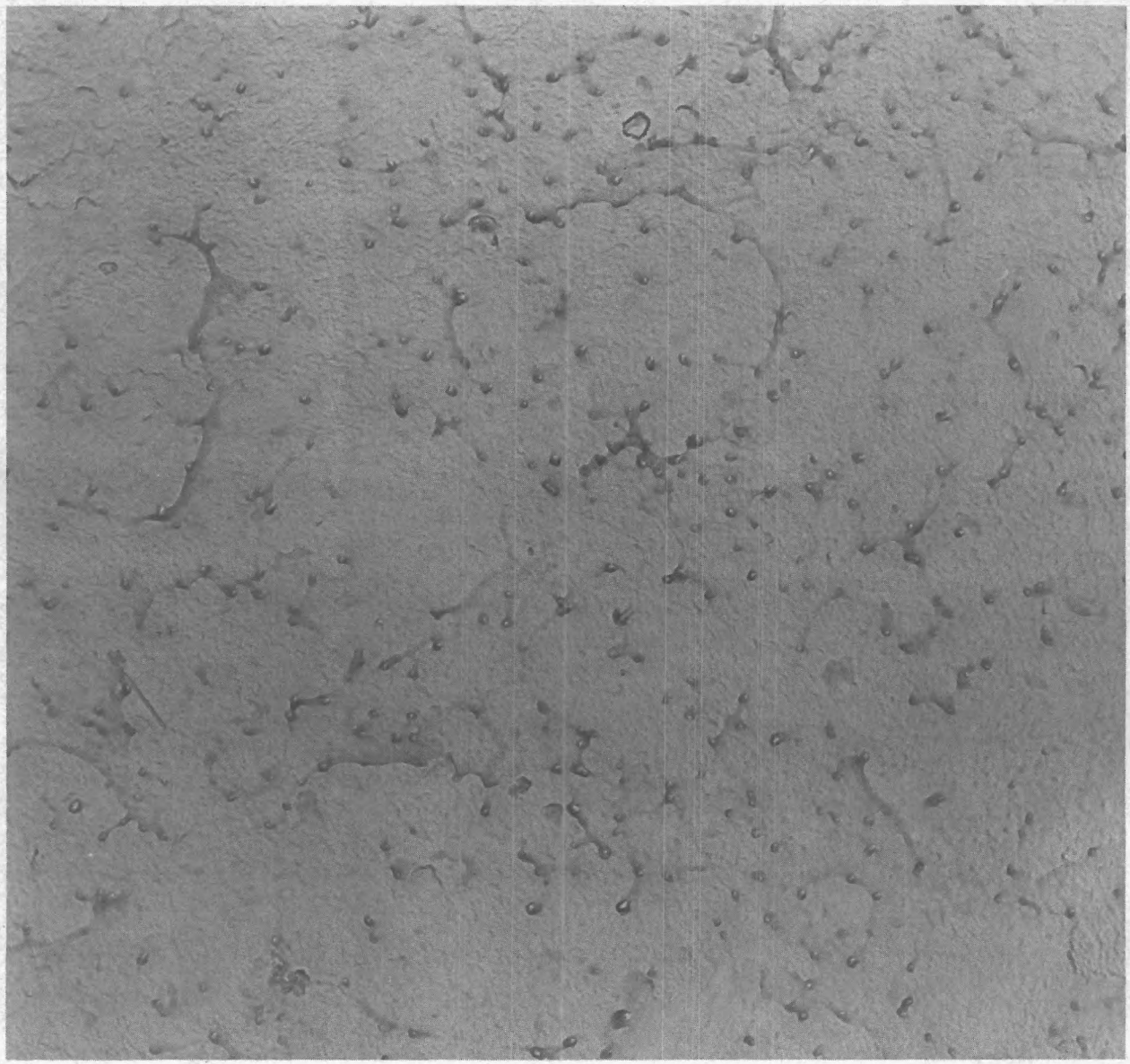

Figure 5. Transmission Electron Micrograph of Nominal 150 Å Nuclepore Membrane Using Carbon Replica, Smooth Side.

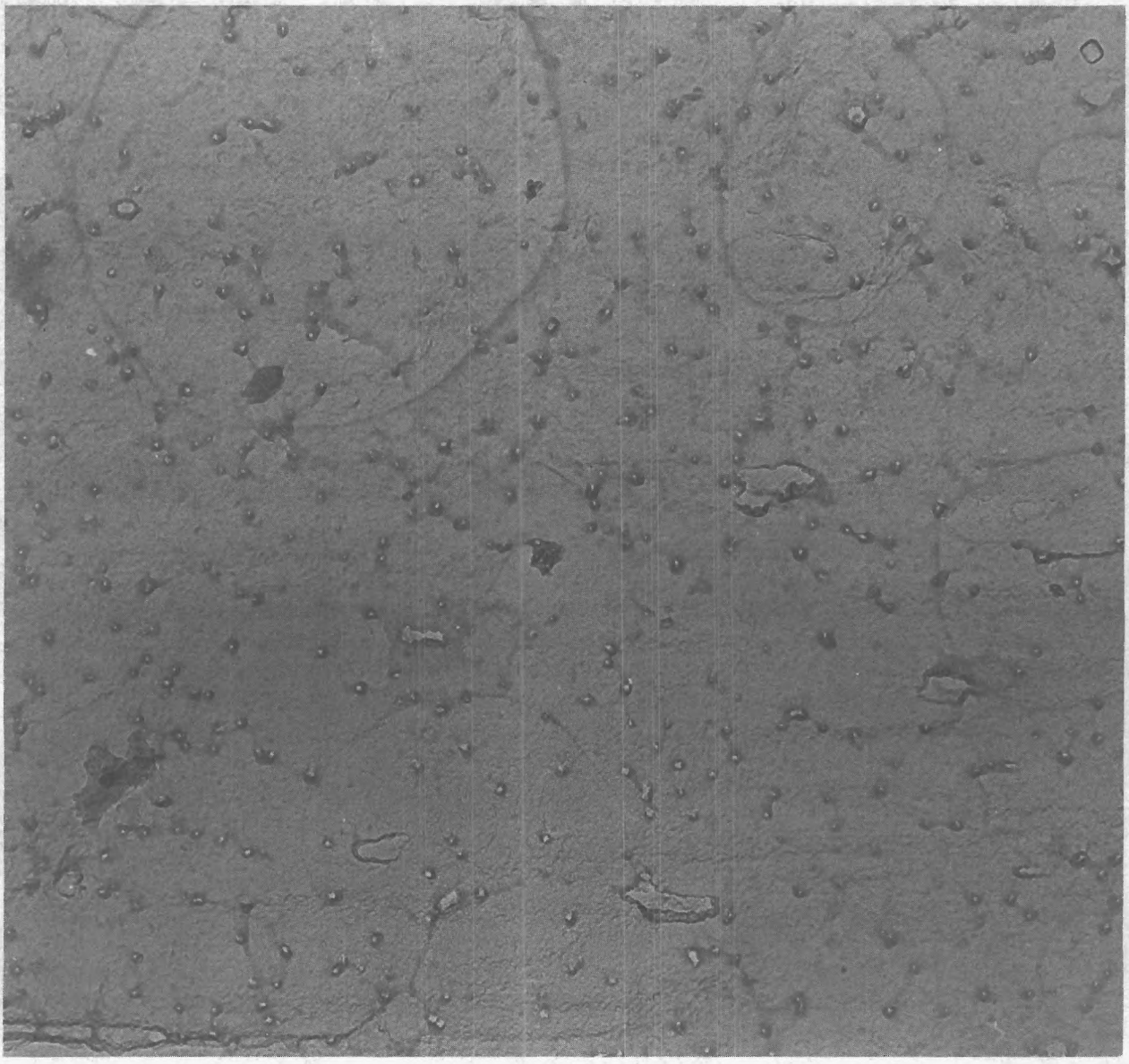

10,000 Å

46,700x

Figure 6. Transmission Electron Micrograph of Nominal 150 Å Nuclepore Membrane Using Carbon Replica, Rough Side.

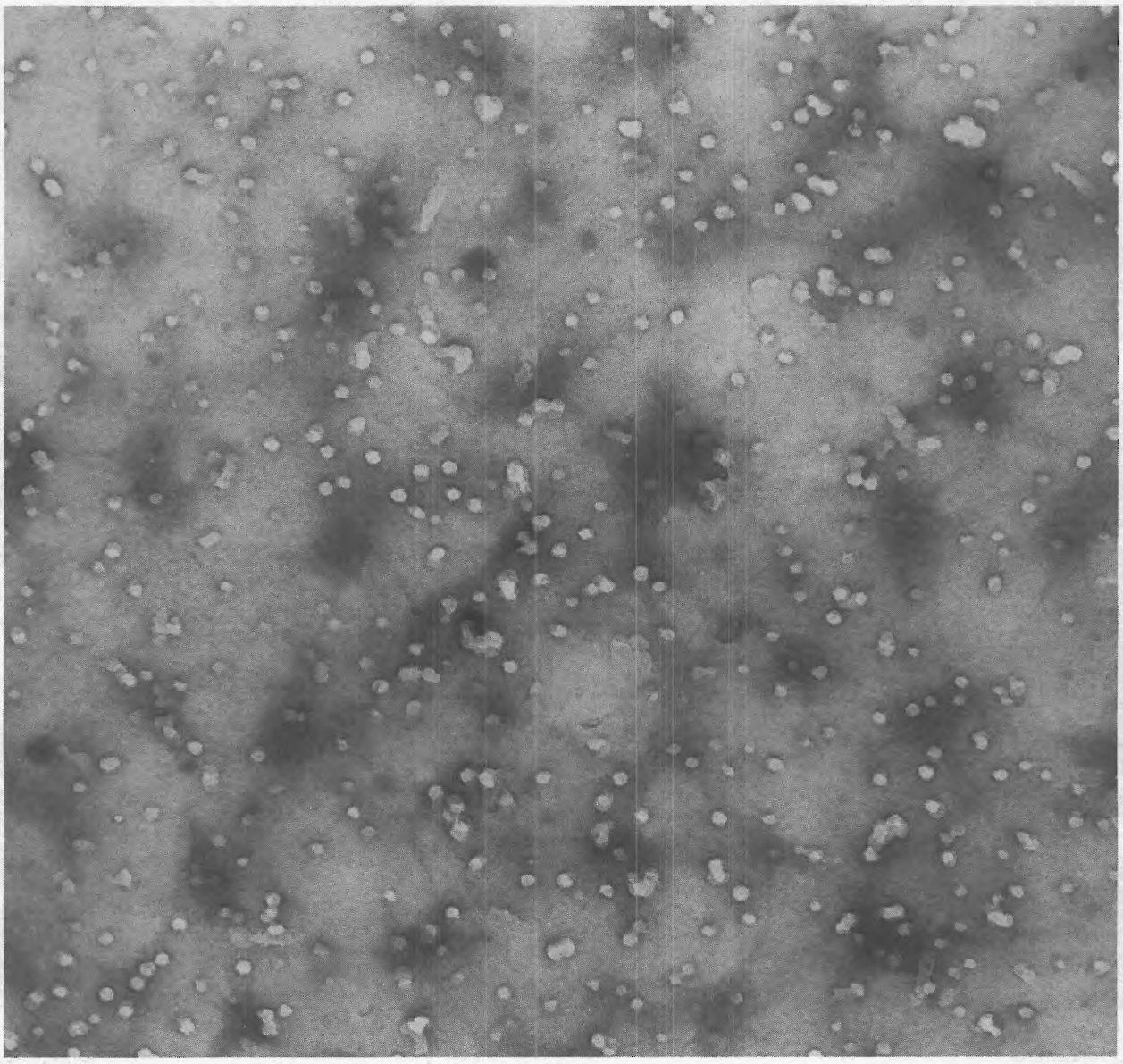

Figure 7. Transmission Electron Micrograph of Nominal 300 Å Nuclepore Membrane Using Carbon Replica, Smooth Side.

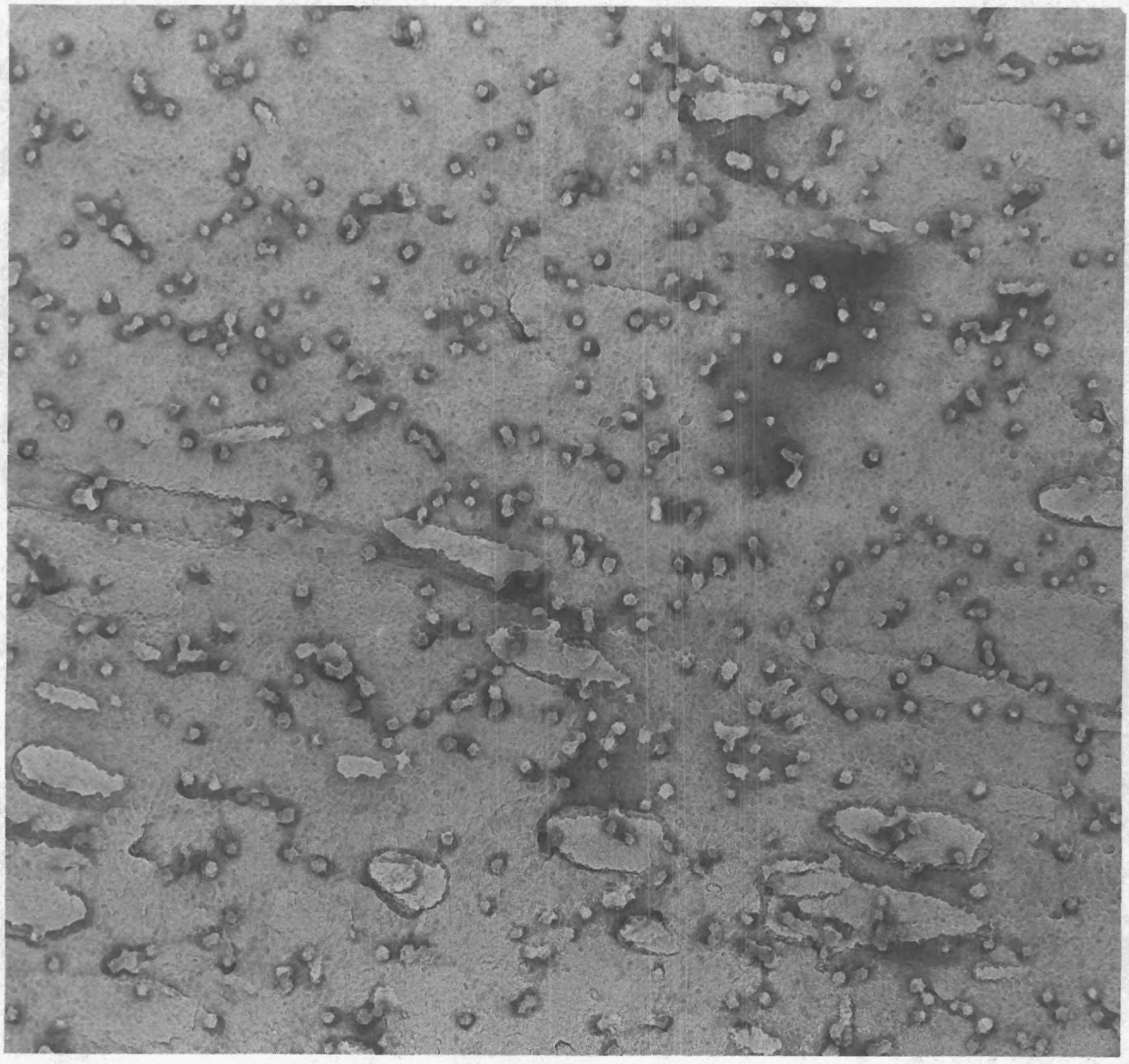

10,000 A

46,700x

Figure 8. Transmission Electron Micrograph of Nominal 300 A Nuclepore Membrane Using Carbon Replica, Rough Side.

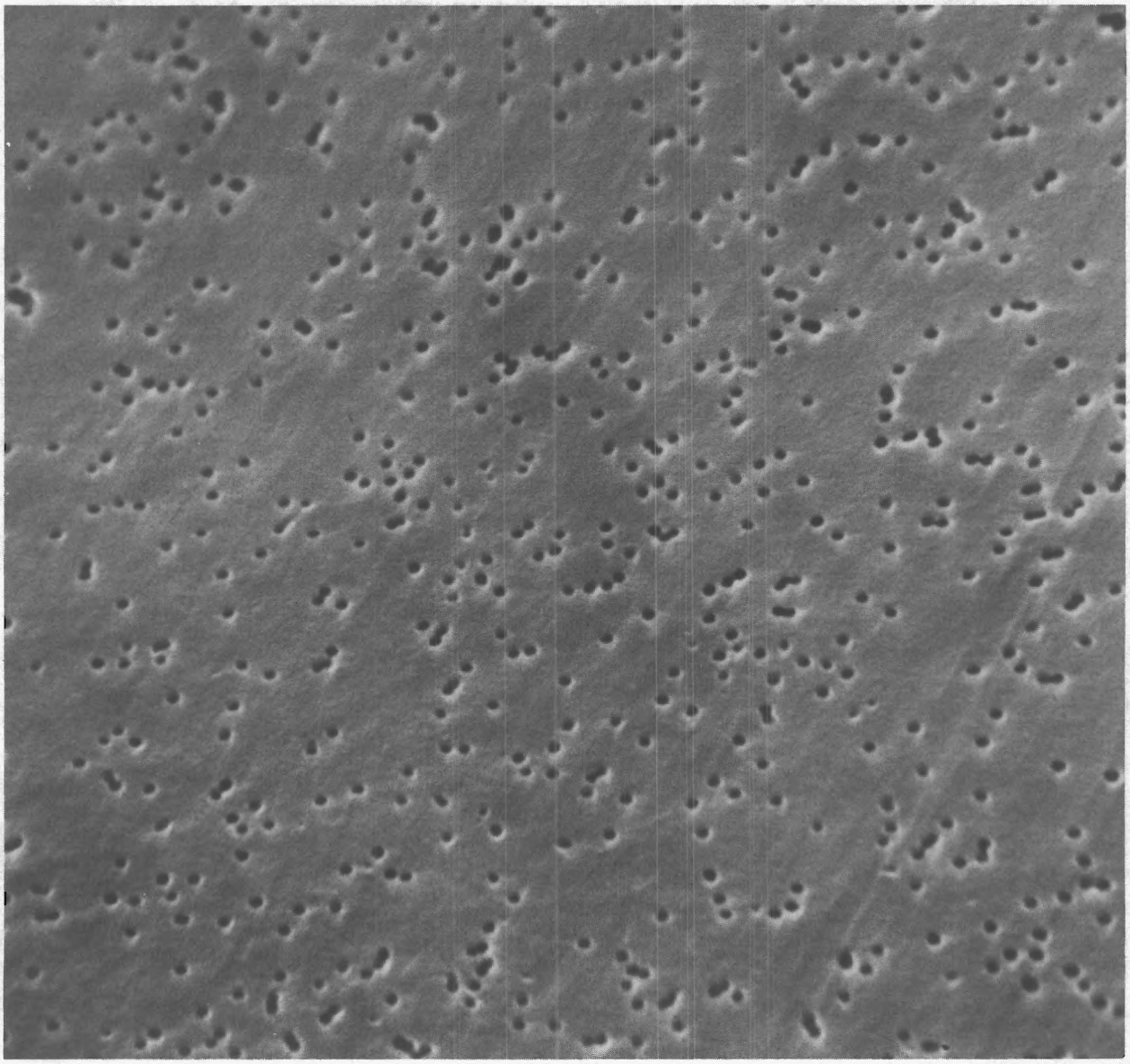

10,000 Å

13,200x

Figure 9. Scanning Electron Micrograph of Nominal 2000 Å Nuclepore Membrane, Smooth Side.

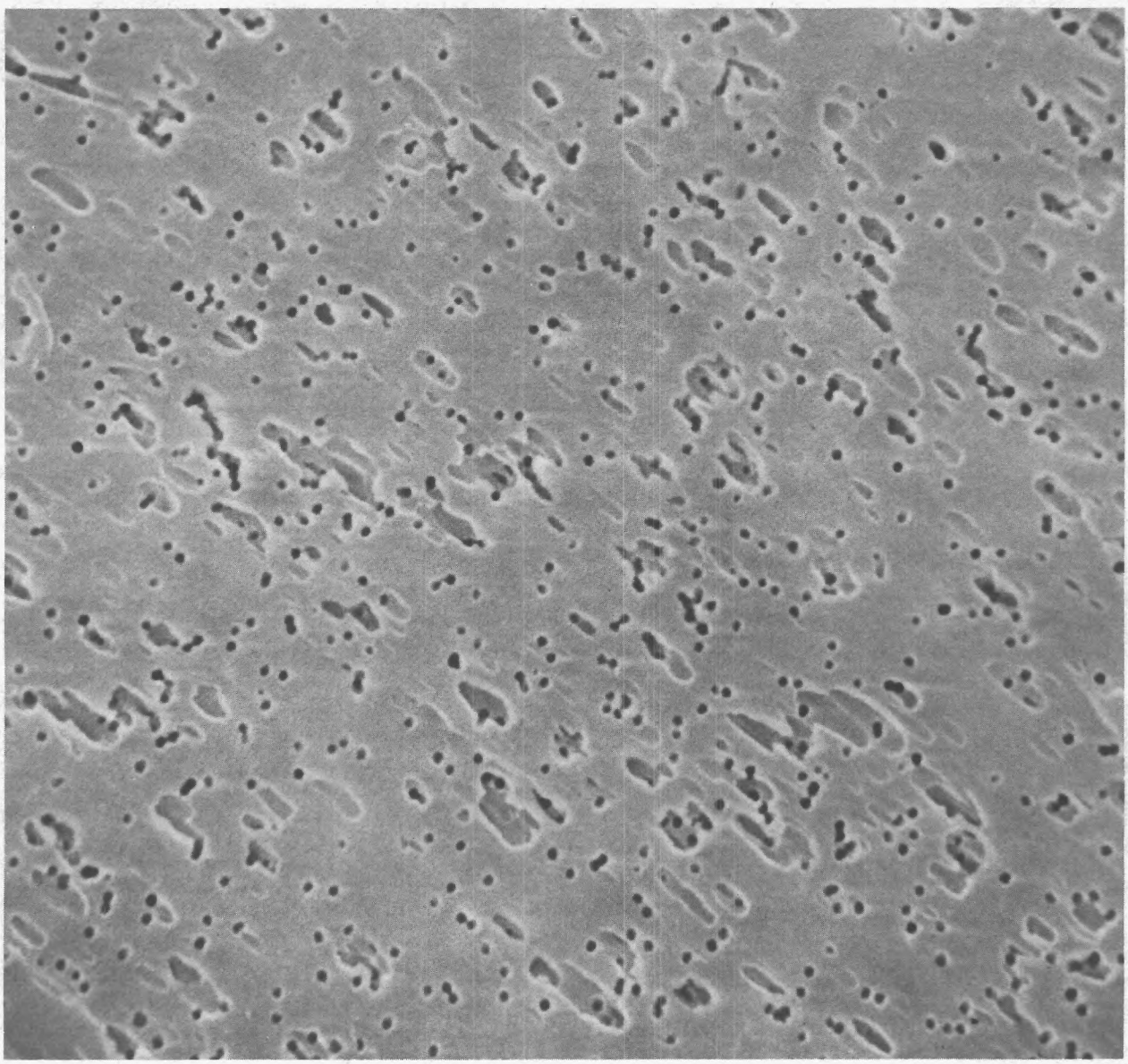

10,000 Å

10,472x

Figure 10. Scanning Electron Micrograph of Nominal 2000 Å Nuclepore Membrane, Rough Side.

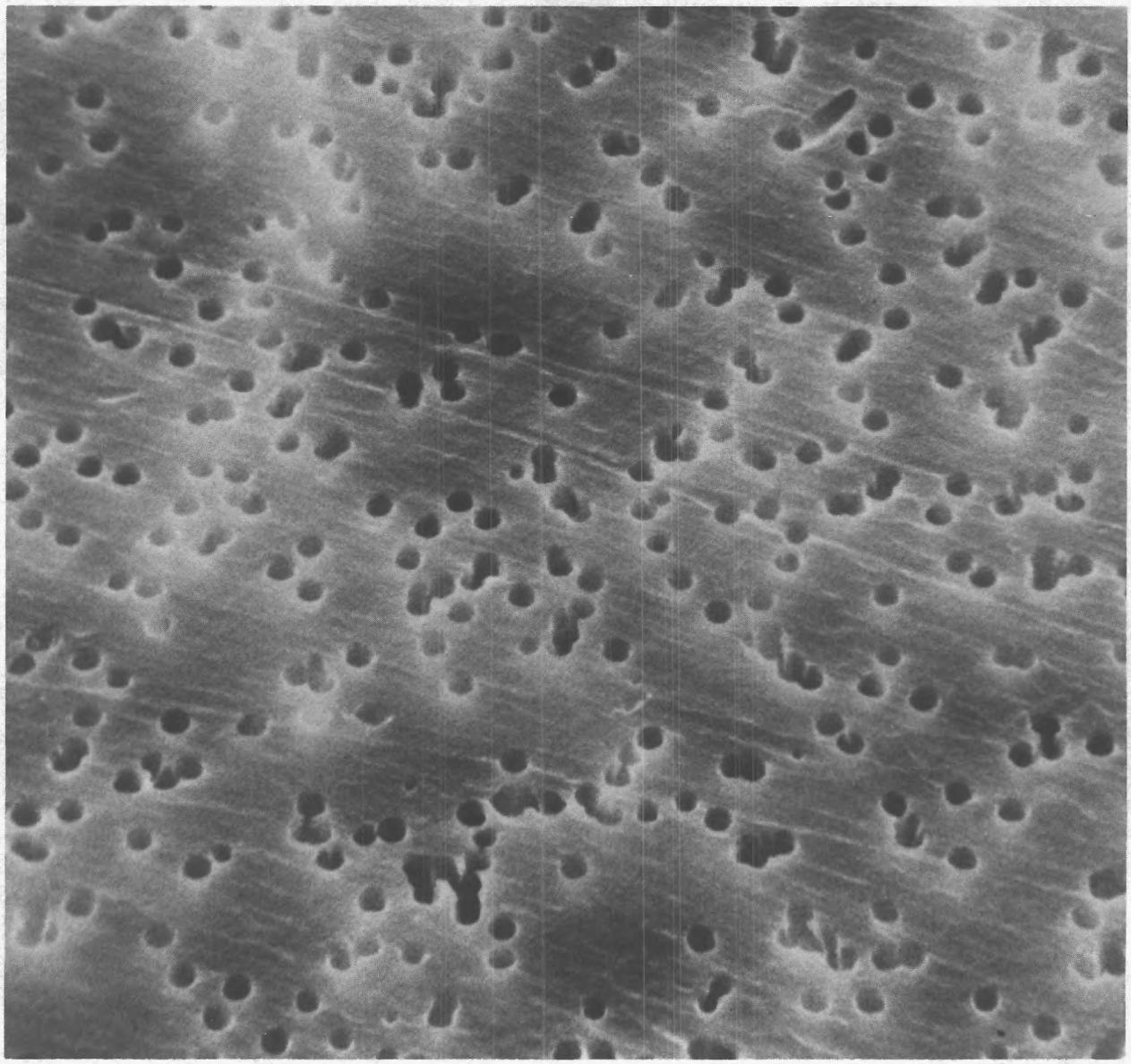

10,000 Å

4,158x

Figure 11. Scanning Electron Micrograph of Nominal 10,000 Å Nuclepore Membrane, Smooth Side.

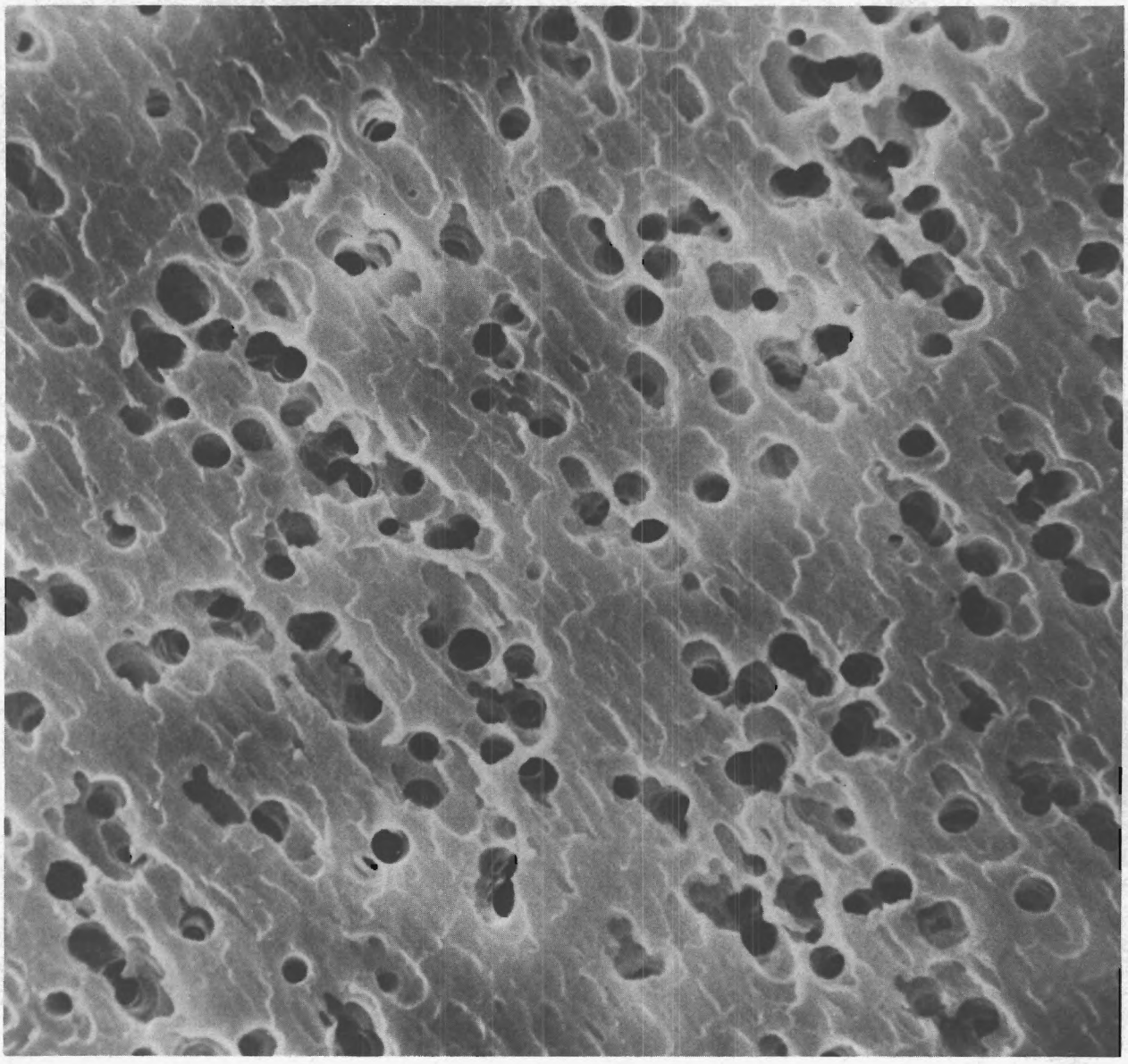

10,000 Å

5,060x

Figure 12. Scanning Electron Micrograph of Nominal 10,000 Å Nuclepore Membrane, Rough Side.

Table II. Mercury Porosimetry Results

Nominal Pore Diameter (Å)	Measured Modal Diameter (Å)
Porous Glass	
75	*
160	121
170	*
215	220
350	*
475	492
1093	1235
1223	1297
1993	2044
Nuclepore Membrane	
150**	*
330**	*
2000	*
4000	*
6000	*
10,000	*
50,000	*

* Analysis in progress

** Specially prepared for this study

series of Nuclepore membrane filters ranging in pore diameter from 0.2 to 8×10^4 Å, in order to evaluate the influence of contact angle hysteresis. Once this evaluation is made, the analysis of Svatá may then be conducted with greater assurance of reliability on the porous glasses.

The results obtained for the Nuclepore materials thus far have not been as reproducible as desired due to experimental difficulties which appear now to have been resolved.

The results for the mercury penetration experiments (volume versus pressure) are shown in Figures 13 through 18.

C. Gas Adsorption and Desorption

Gas adsorption experiments are limited to materials having pore diameters less than 600 Å. The experiments in this research were conducted using a Surface Area and Pore Volume Analyzer called the Digisorb 2500.* The gas

* Micromeritics Instrument Corporation, Norcross, Georgia.

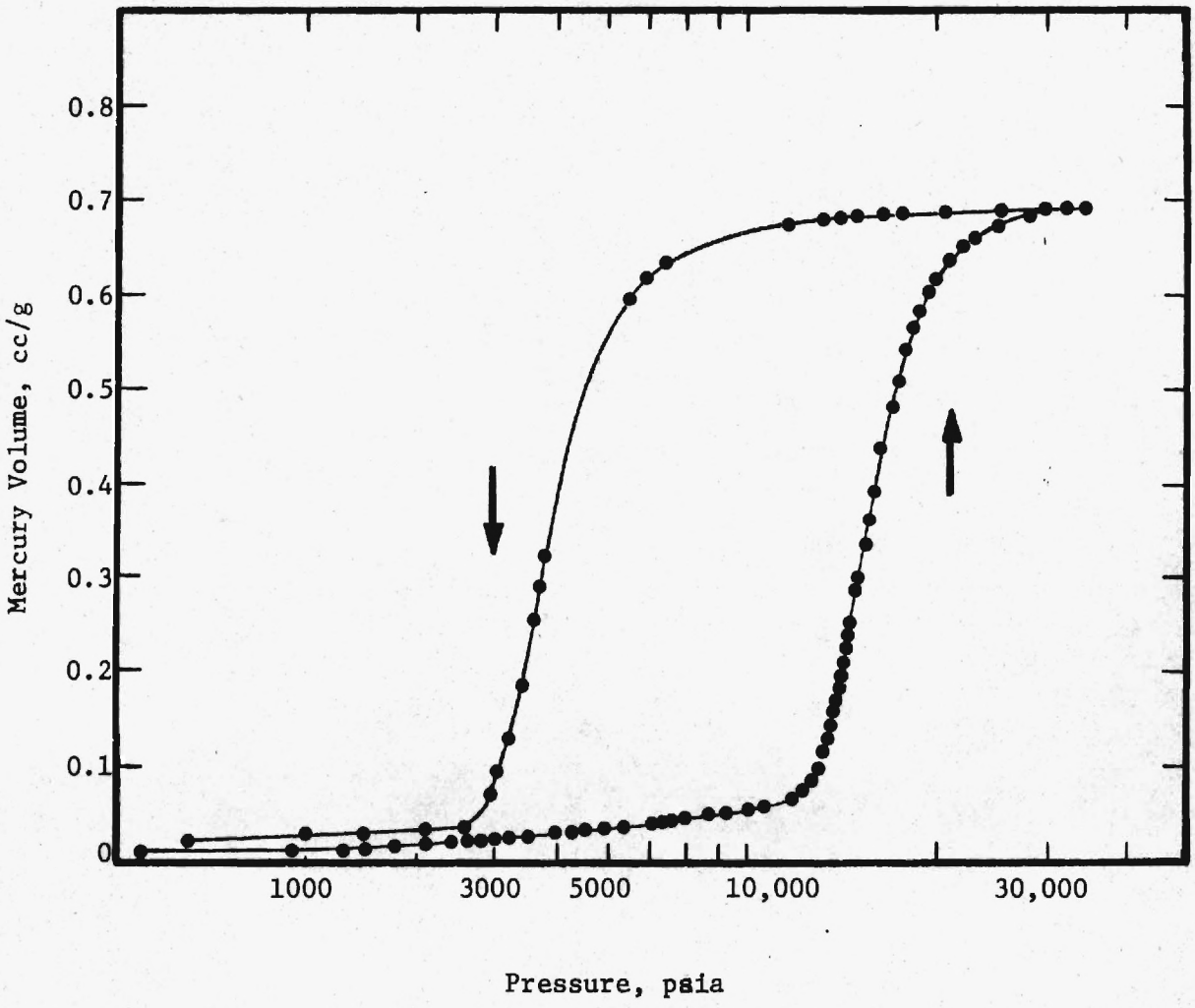

Figure 13. Mercury Penetration of Nominal 160 Å Porous Glass.

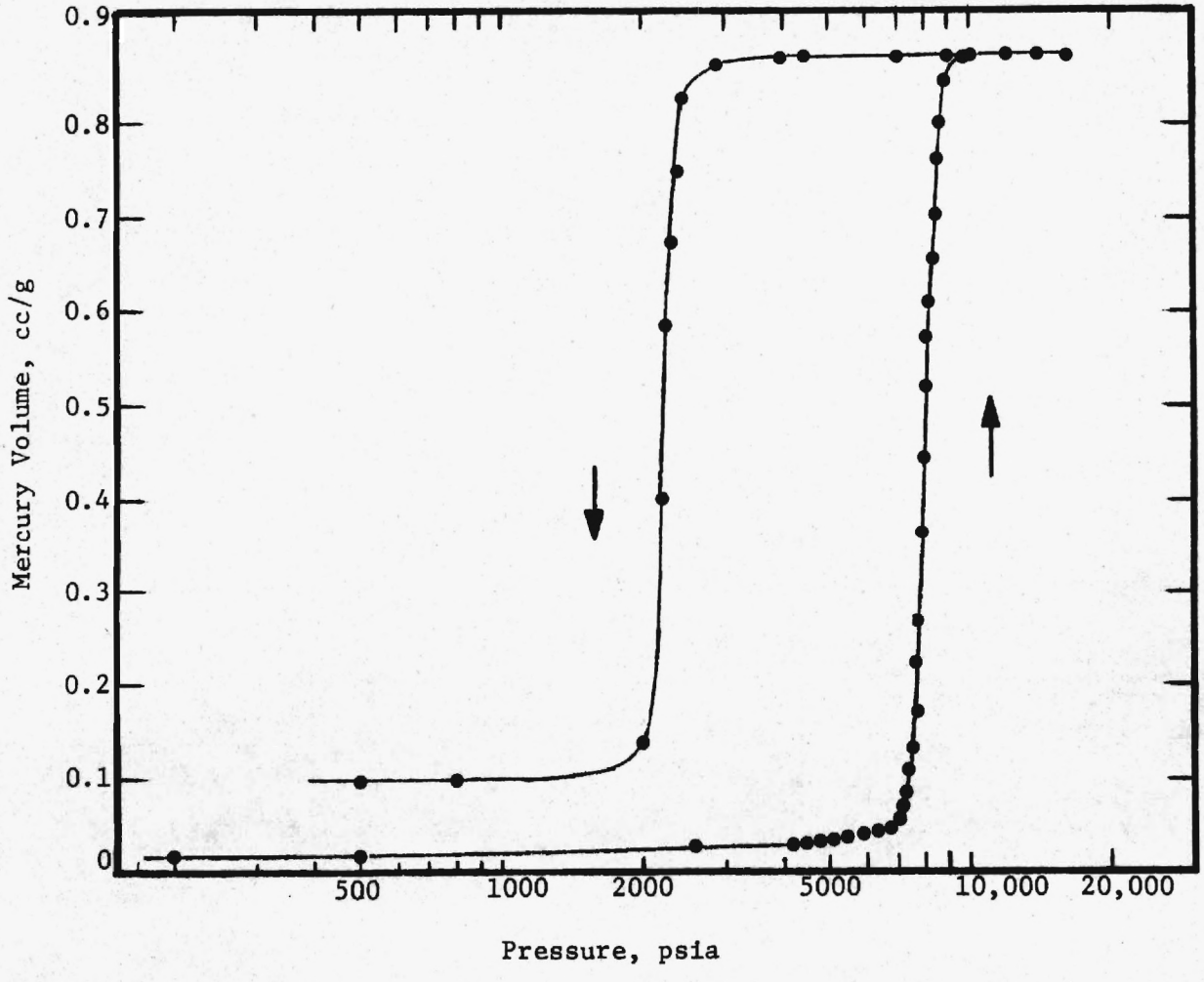

Figure 14. Mercury Penetration of Nominal 215 Å Porous Glass.

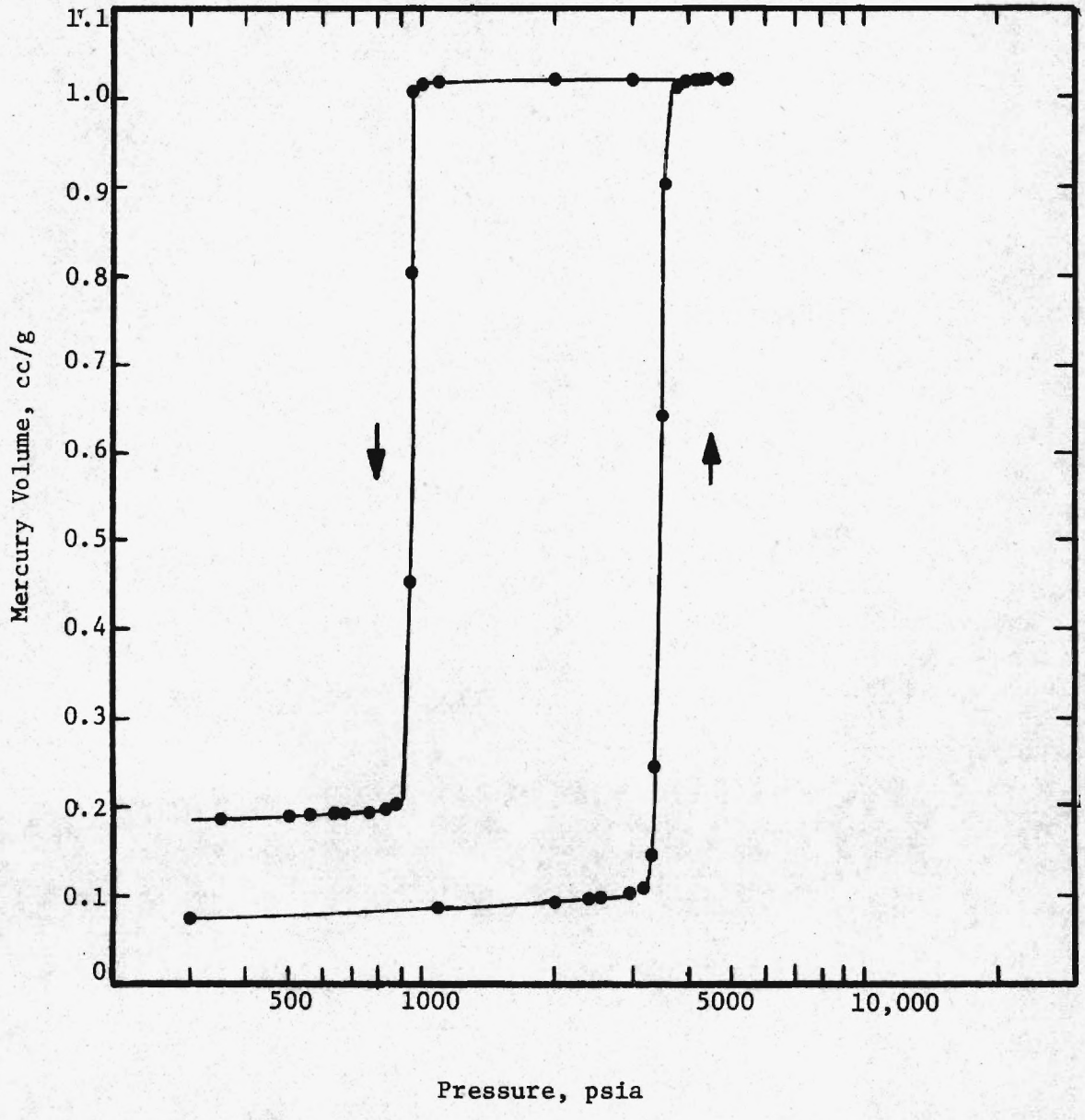

Figure 15. Mercury Penetration of Nominal 475 Å Porous Glass .

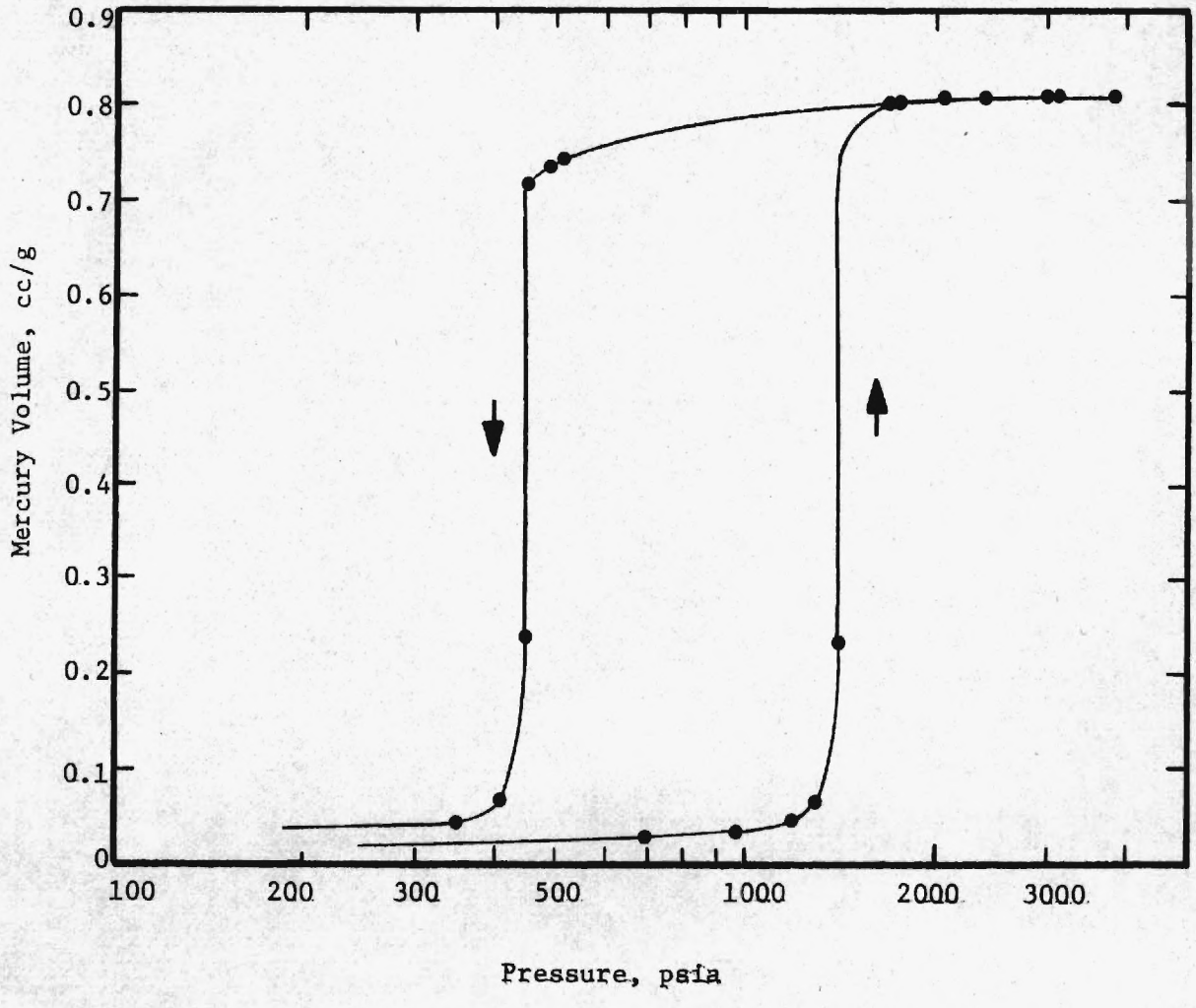

Figure 16. Mercury Penetration of Nominal 1093 Å Porous Glass.

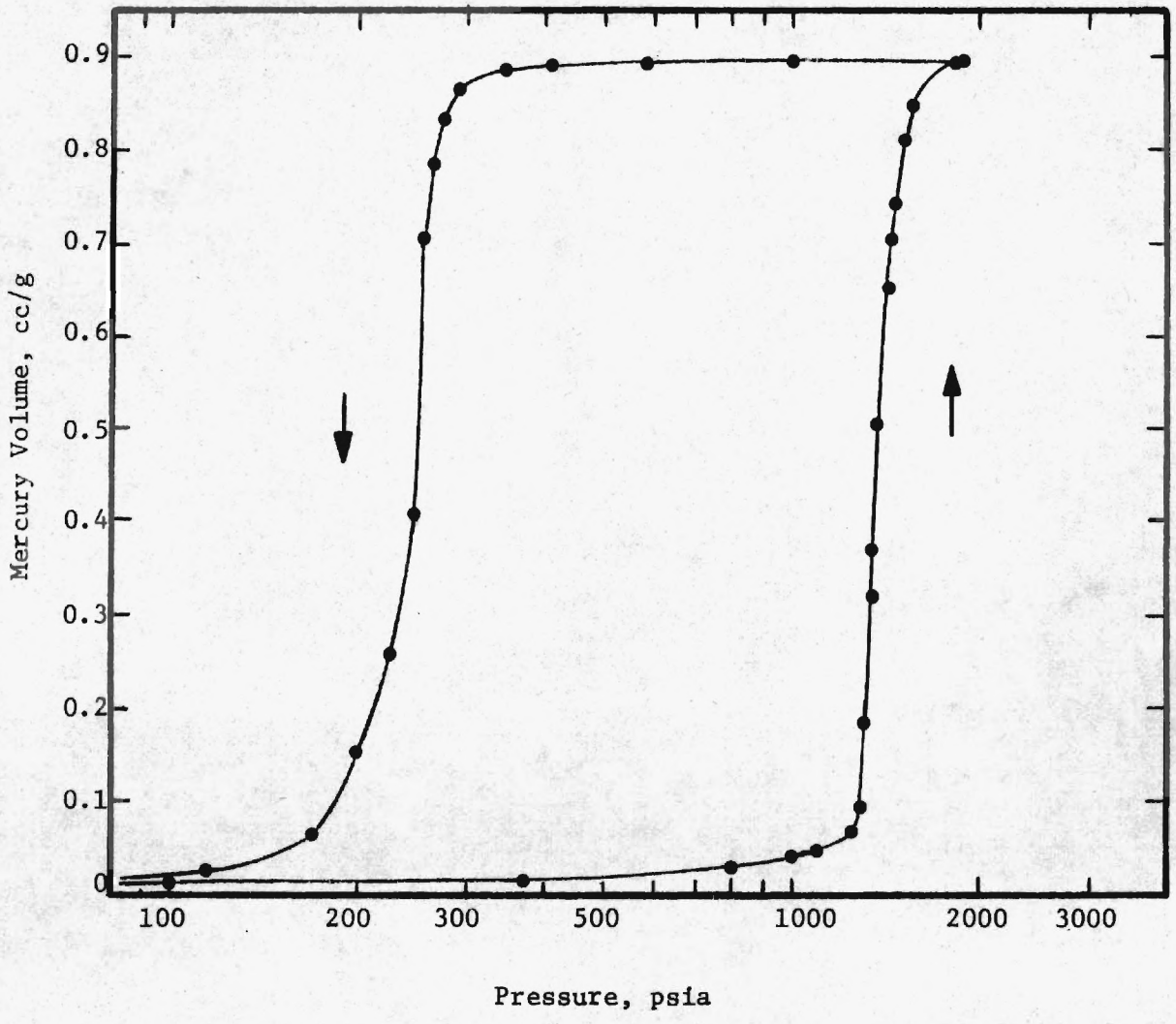

Figure 17. Mercury Penetration of Nominal 1223 Å Porous Glass.

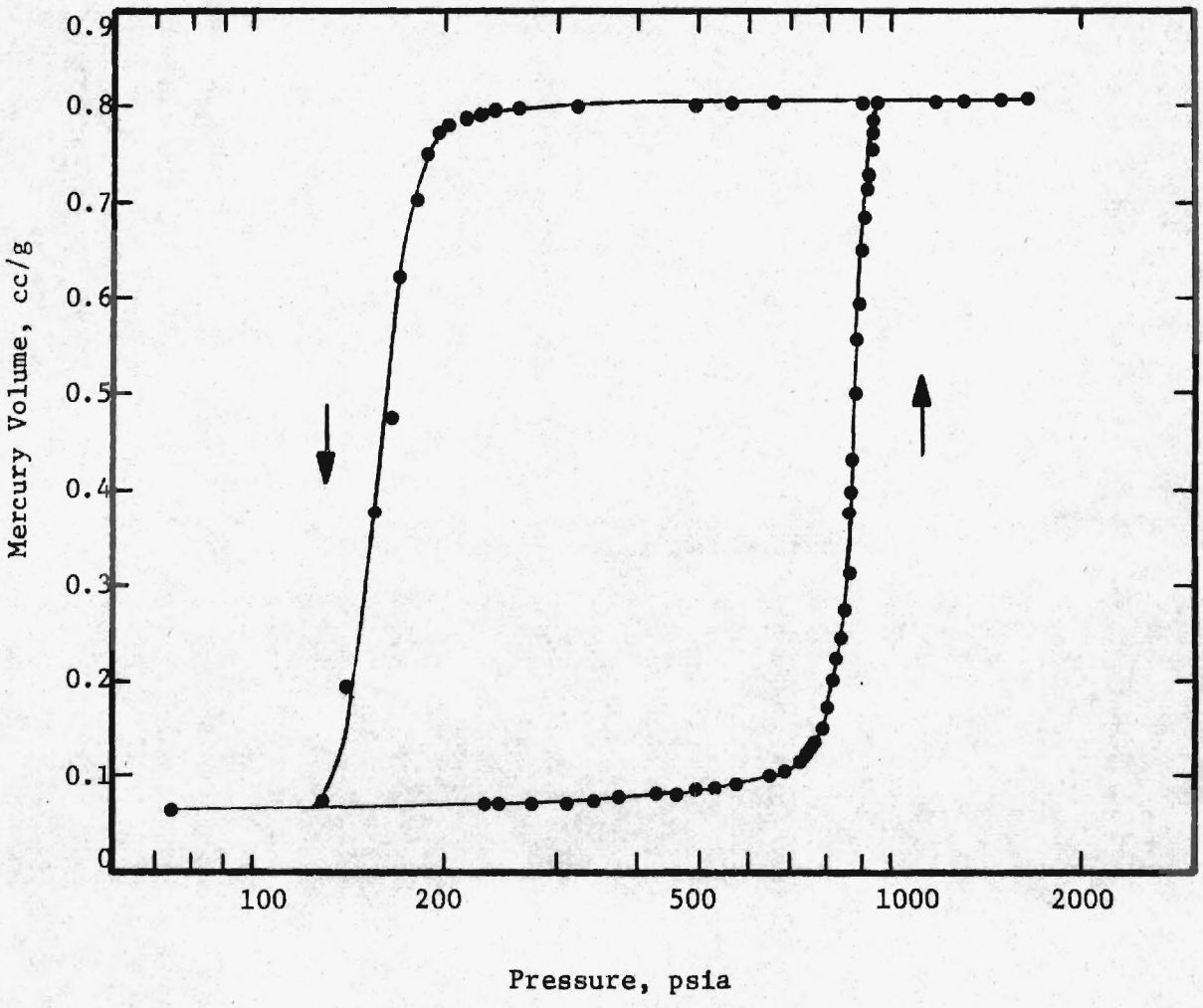

Figure 18. Mercury Penetration of Nominal 1933 Å Porous Glass.

adsorption-desorption isotherms are shown in Figures 19 through 23, and the results for the pore distribution maxima are shown in Table III.

Table III. Nitrogen Adsorption-Desorption Results

Nominal Pore Diameter (Å)	Modal Diameter from Adsorption (Å)	Modal Diameter from Desorption (Å)
Porous Glass		
75	*	*
160	250	155
170	350	230
215	475	270
Nuclepore Membrane		
150**	350	190
300**	- -	- -

* Analysis in progress.

** Specially prepared for this study.

In comparing results from the Nuclepore materials with the modal calculations of Linsen and Heuvel[6] for straight-walled cylindrical pores open at both ends, the agreement was found to be good. Results obtained for the controlled pore glass samples support the structure proposed by Karnaukhov,[4] Watanabe, et al.,[3] and Barrall and Cain,[2] in that the isotherm shapes are similar to those obtained for the Nuclepore material. This method of isotherm shape assignment has been used by de Boer[7] in correlating experimental isotherm shapes with those generated from pore shape models.

IV. DISCUSSION AND CONCLUSIONS

Table IV presents comparisons of pore sizes determined by the various methods referred to in preceding sections. The table is incomplete and some of the values must be regarded as unconfirmed. This situation has arisen because this grant was terminated one year early.

To date the main thrust of this research has been directed toward determining size distributions of pores and pore geometries of the various materials from electron micrographs. Much tedious and time consuming effort has been required to develop the techniques necessary to characterize properly the materials of interest. These difficulties were compounded by the fact that the pores of

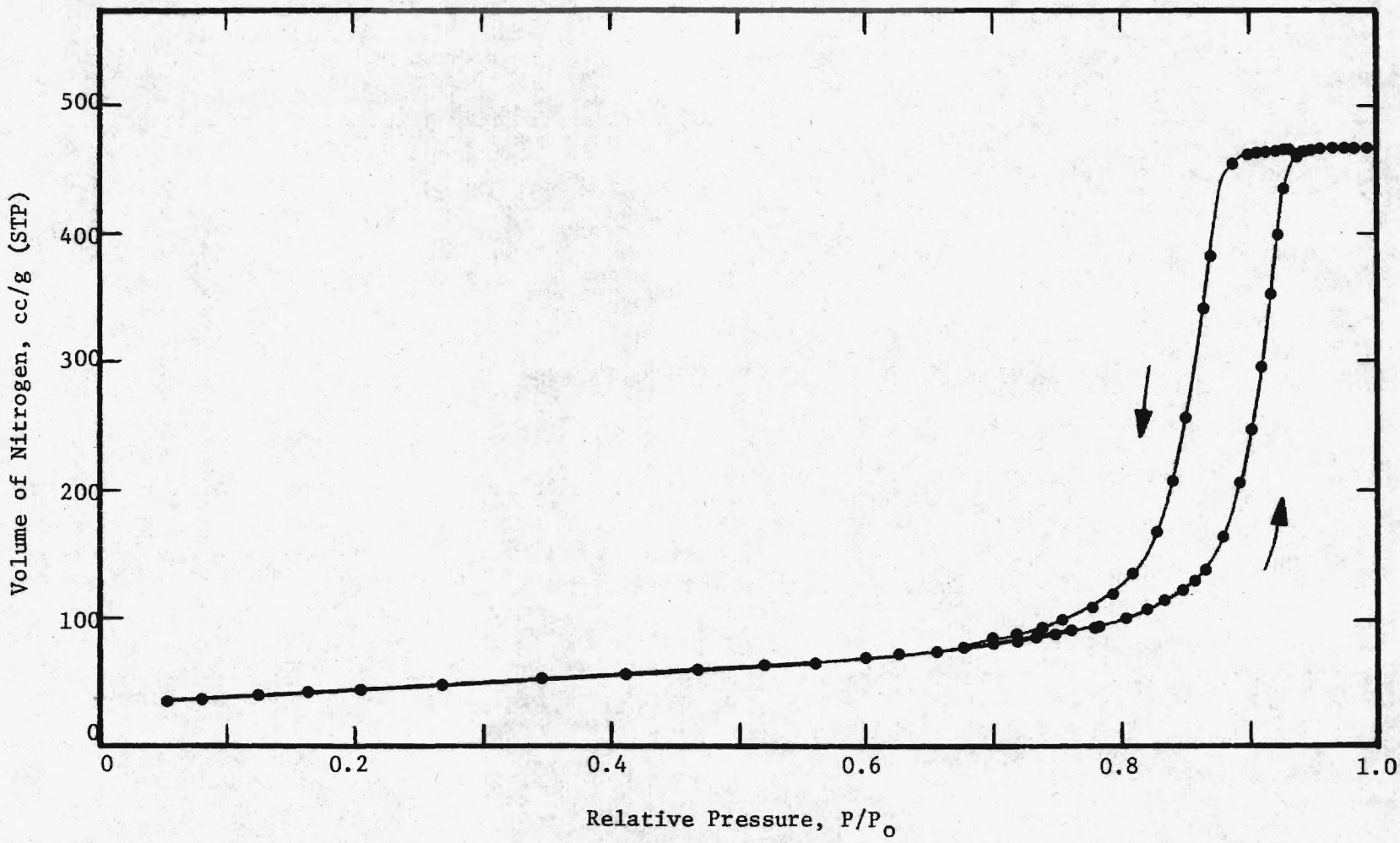

Figure 19. Adsorption-Desorption Isotherm for Nominal 160 Å Porous Glass.

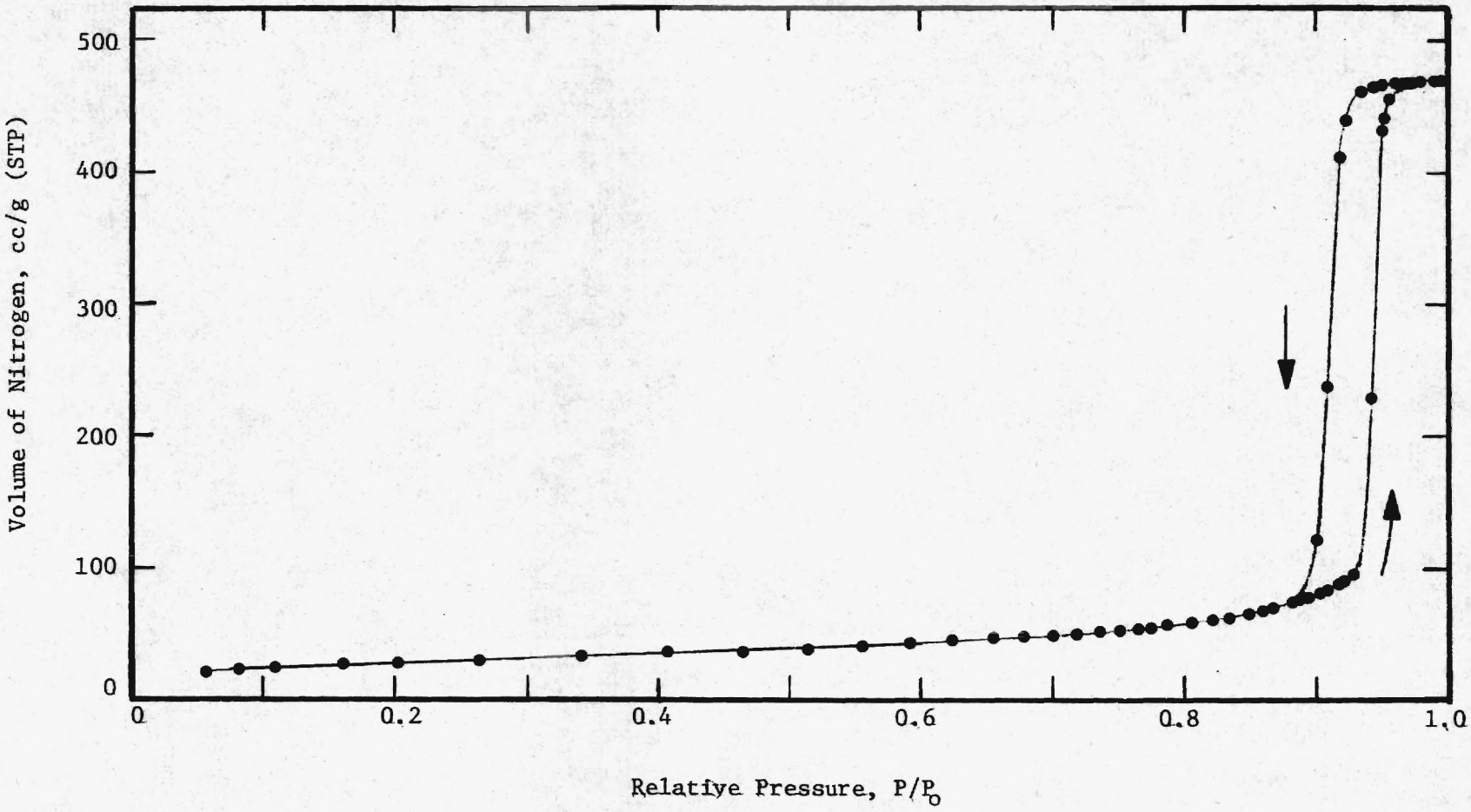

Figure 20. Adsorption-Desorption Isotherm for Nominal 170 Å Porous Glass.

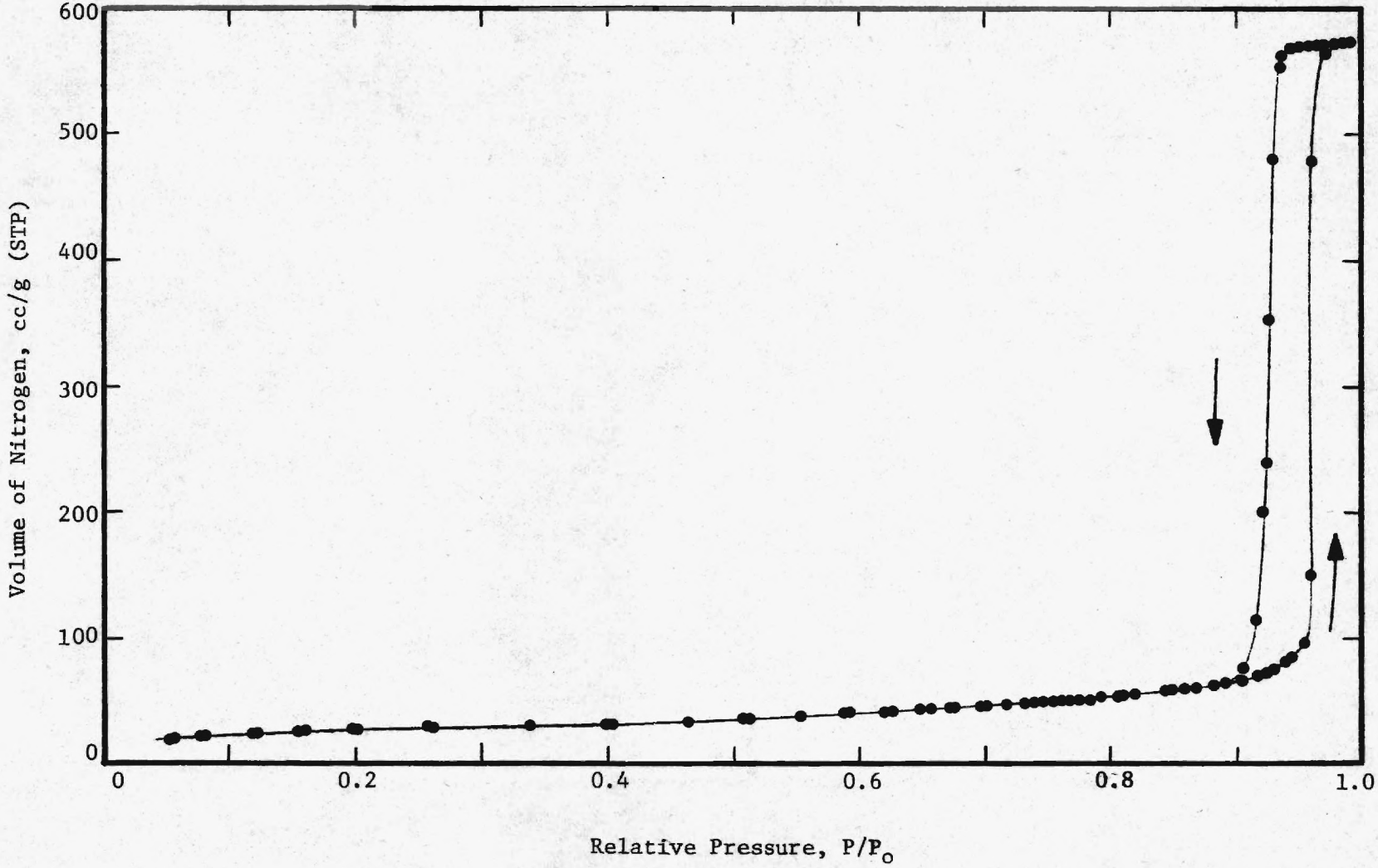

Figure 21. Adsorption-Desorption Isotherm for Nominal 215 Å Porous Glass.

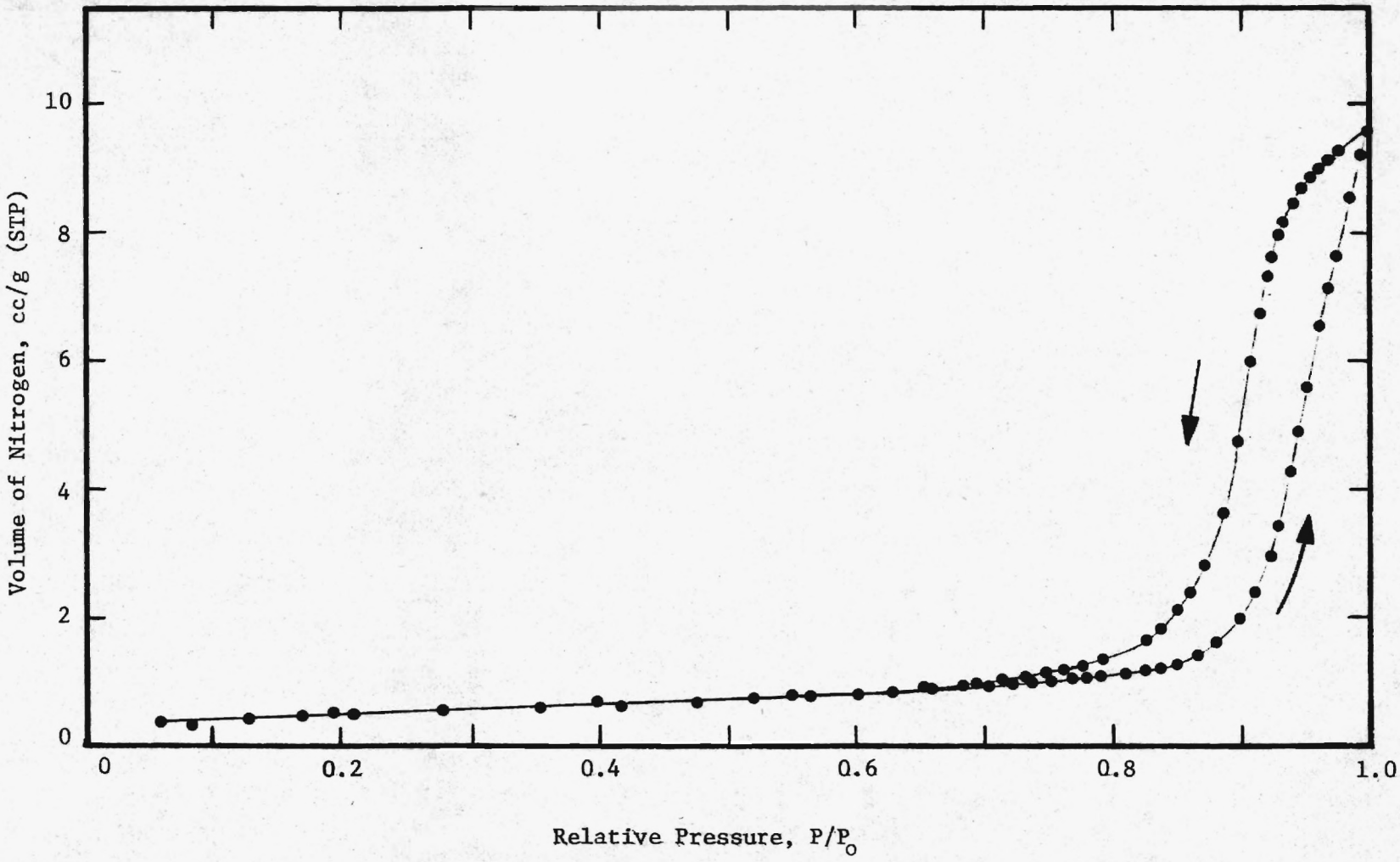

Figure 22. Adsorption-Desorption Isotherm for Nominal 150 Å Nuclepore Membrane.

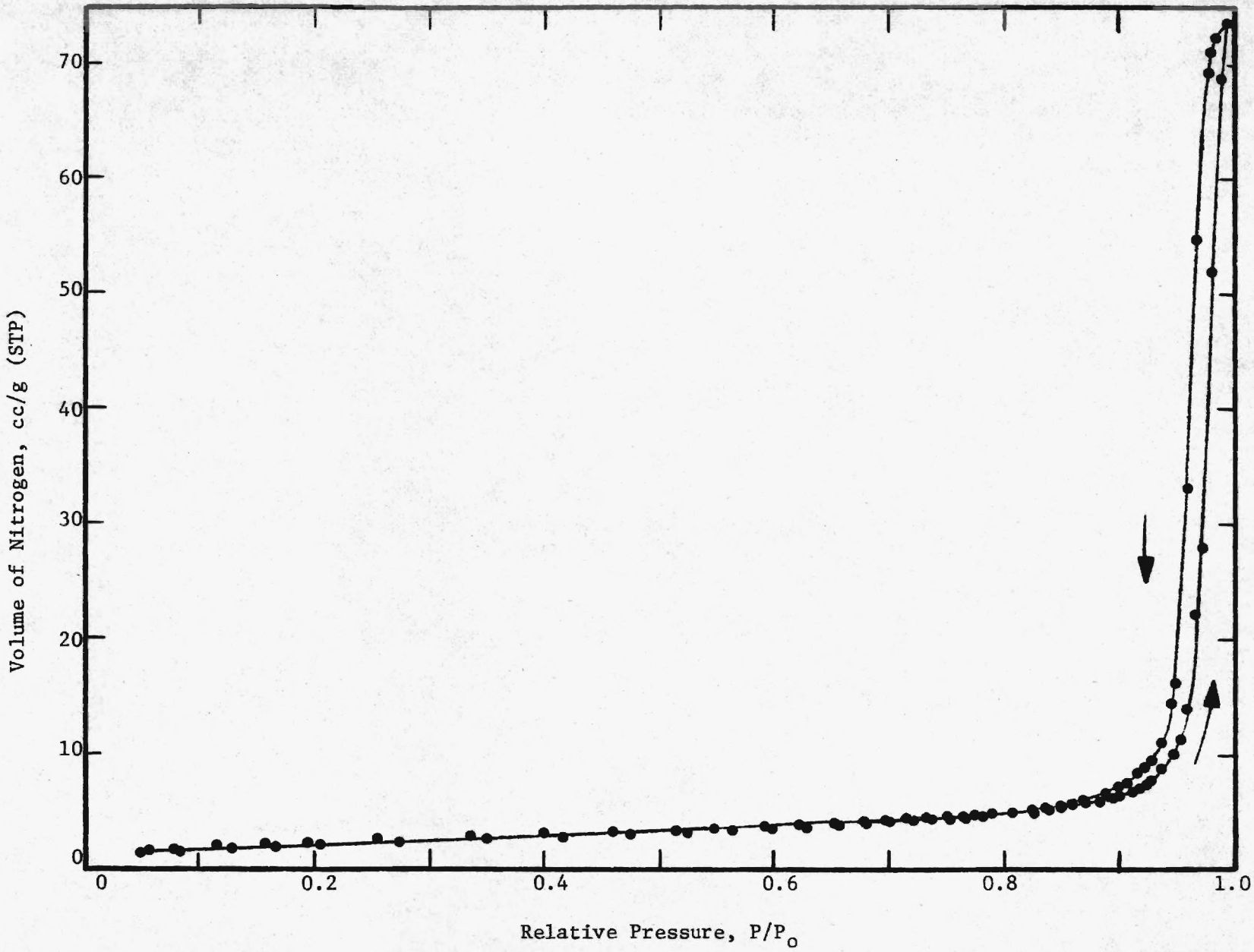

Figure 23. Adsorption-Desorption Isotherm for Nominal 300 Å Nuclepore Membrane.

primary interest were so small (less than 600 Å) that they required working at the limit of detection of electron microscopy.

Table IV. Comparison of Pore Modal Diameters Determined by Various Methods

Nominal Pore Diameter (Å)	Modal Diameter as Determined by: Electron Micrographs (Å)	Mercury Porosimetry (Å)	Nitrogen Adsorption (Å)	Nitrogen Desorption (Å)
Porous Glass				
75	*	*	*	*
160	122	121	250	155
170	*	*	350	230
215	220	220	475	270
350	*	*	- -	- -
475	490	492	- -	- -
1093	1230	1235	- -	- -
1223	∿1300	1297	- -	- -
1993	∿1969	2044	- -	- -
Nuclepore Membrane				
150**	∿310	*	350	190
330**	∿610	*	- -	- -
2000	*	*	- -	- -
4000	*	*	- -	- -
6000	*	*	- -	- -
10,000	*	*	- -	- -
50,000	*	*	- -	- -

* Analysis in progress.

** Specially prepared for this study.

Much experimental work remains to be done. This includes the following: examination of Nuclepore material in the size range 0.2 to 8 x 10^4 Å by mercury porosimetry; re-examination of selected glass samples by mercury porosimetry; analyzing the Nuclepore and glass samples using the t-method[8] and the α_s[9,10] method which will require gas adsorption experiments on non-porous glass and Nuclepore material; re-examination of electron micrographs for repeatability; analysis of hystersis loops by the method of Svatá[5]; and attempts to close one pore end in the smaller Nuclepore material and conduct gas adsorption experiments on closed cylinders.

A. Nuclepore Membrane

The Nuclepore membranes have been exhaustively examined by electron microscopy. The material has been viewed from both sides, that is, the front or smooth side (see Figures 5, 7, 9 and 11) and the back or rough side (see Figures 6, 8, 10 and 12), both with and without pores. The material without pores is shown in Figures 24 and 25. Gross-sections of the Nuclepore membrane have been viewed both with and without pores and are shown in Figures 26 through 29.

In viewing the cross-sections of the Nuclepore membranes (Figures 26 through 28), it is evident that their texture changes from front to back. It is thought that this texture difference gives rise to preferential etching, thus the appearance of the rough side (see Figures 5 through 12). As indicated in Figures 27 and 28, the terminal dimensions of nominal 150 and 300 Å pores are very much longer than their primary diameters (>100x).

The adsorption-desorption isotherms shown in Figures 22 and 23 are like those referred to by Linsen and Heuver[9] as type A, tubular capillaries open at both ends. Theory indicates that pores of this geometry obey the relationship:

$$P_d/P_o = (P_a/P_o)^2 \qquad (1)$$

where

P_d = Desorption Pressure
P_a = Adsorption Pressure
P_o = Vapor Pressure

It was found that this relationship was obeyed.

B. Porous Glass

The mercury penetration data presented in Figures 13 through 18 indicate generally that, if a 30° correction is applied to the contact angle of mercury for the release from glass, the pore distribution maxima for penetration and release will be approximately equal.

The adsorption-desorption isotherms presented in Figures 19 through 21 have the same general shape as that referred to by Linsen and Heuvel[6] and that exhibited by the Nuclepore material. However, no attempt as yet has been made to see if equation 1 is also obeyed as it was in the Nuclepore case.

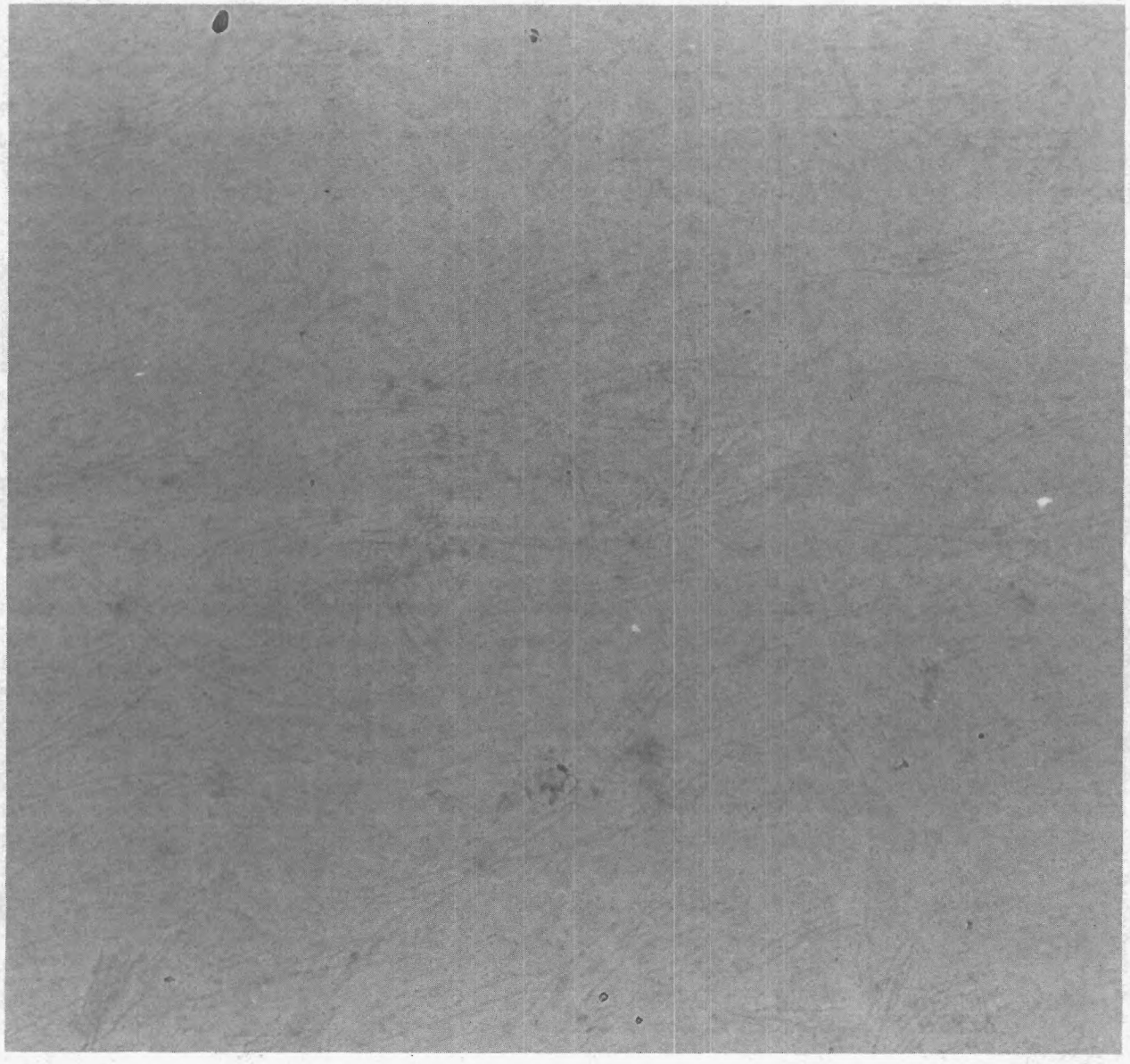

Figure 24. Transmission Electron Micrograph of Poreless Nuclepore Membrane Using Carbon Replica, Smooth Side.

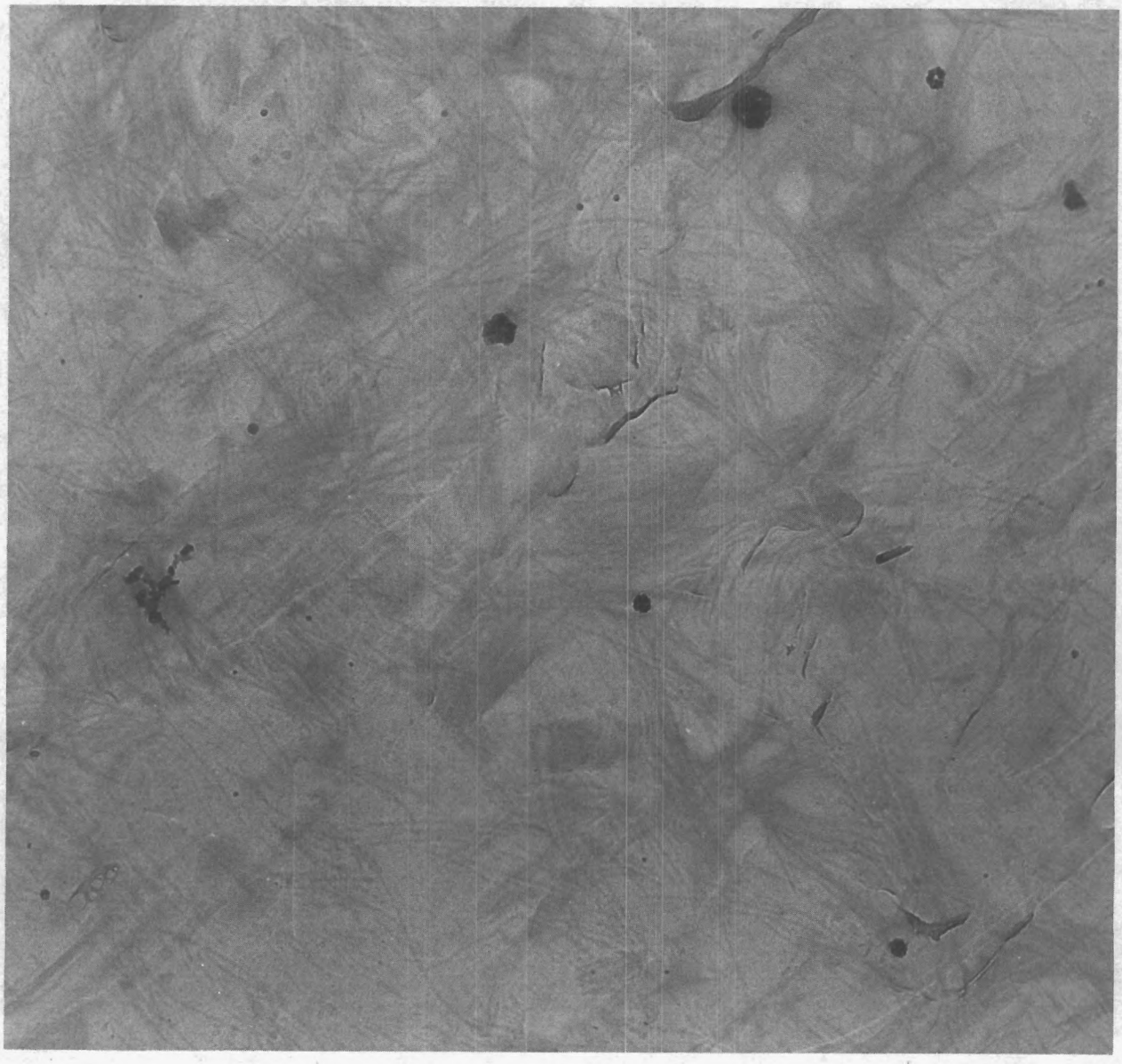

Figure 25. Transmission Electron Micrograph of Poreless Nuclepore Membrane Using Carbon Replica, Rough Side.

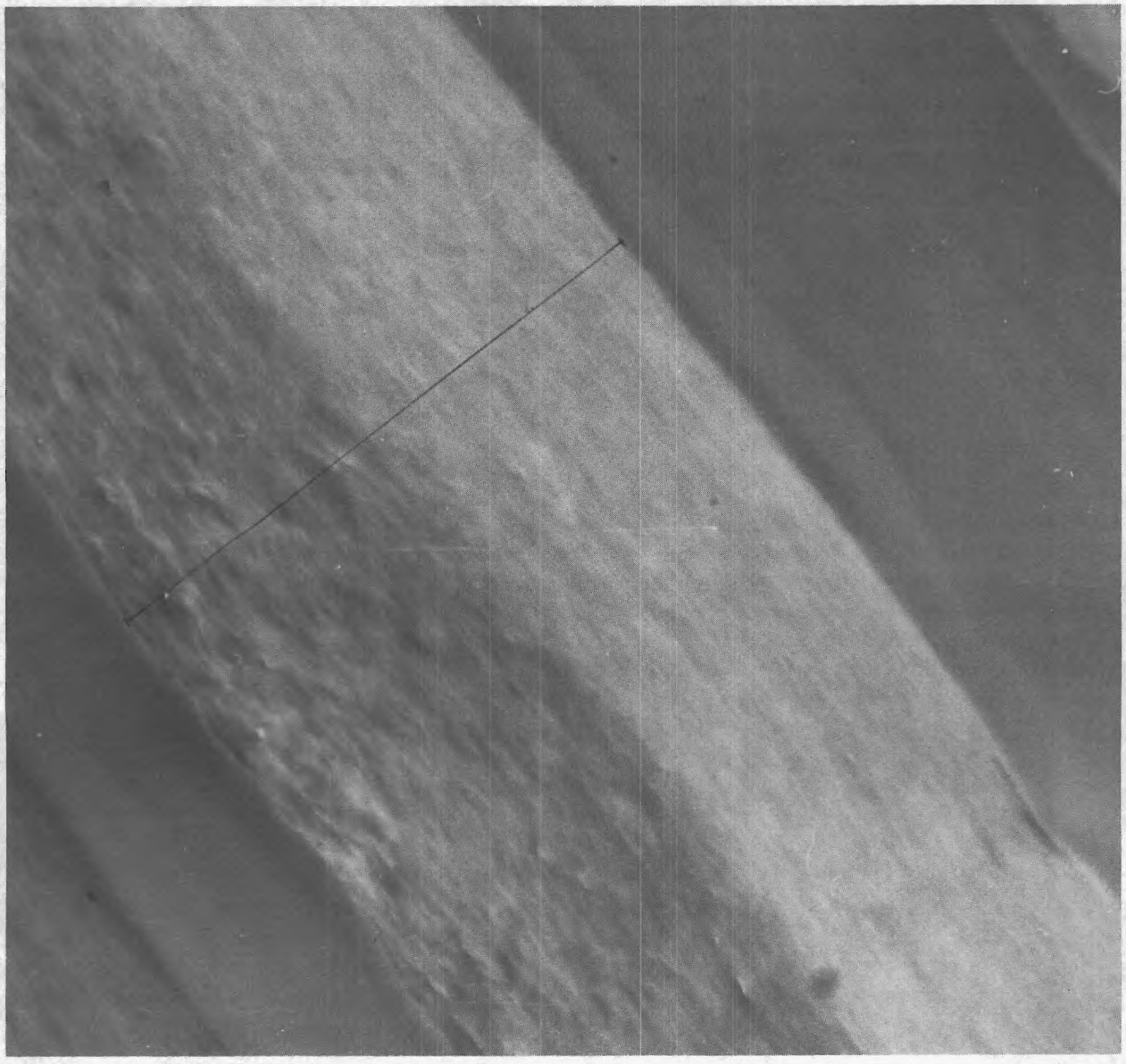

10,000 A

12,800x

Figure 26. Transmission Electron Micrograph of Cross Section of Poreless Nuclepore Membrane Using Ultramicrotomy. The line marks one Membrane Thickness.

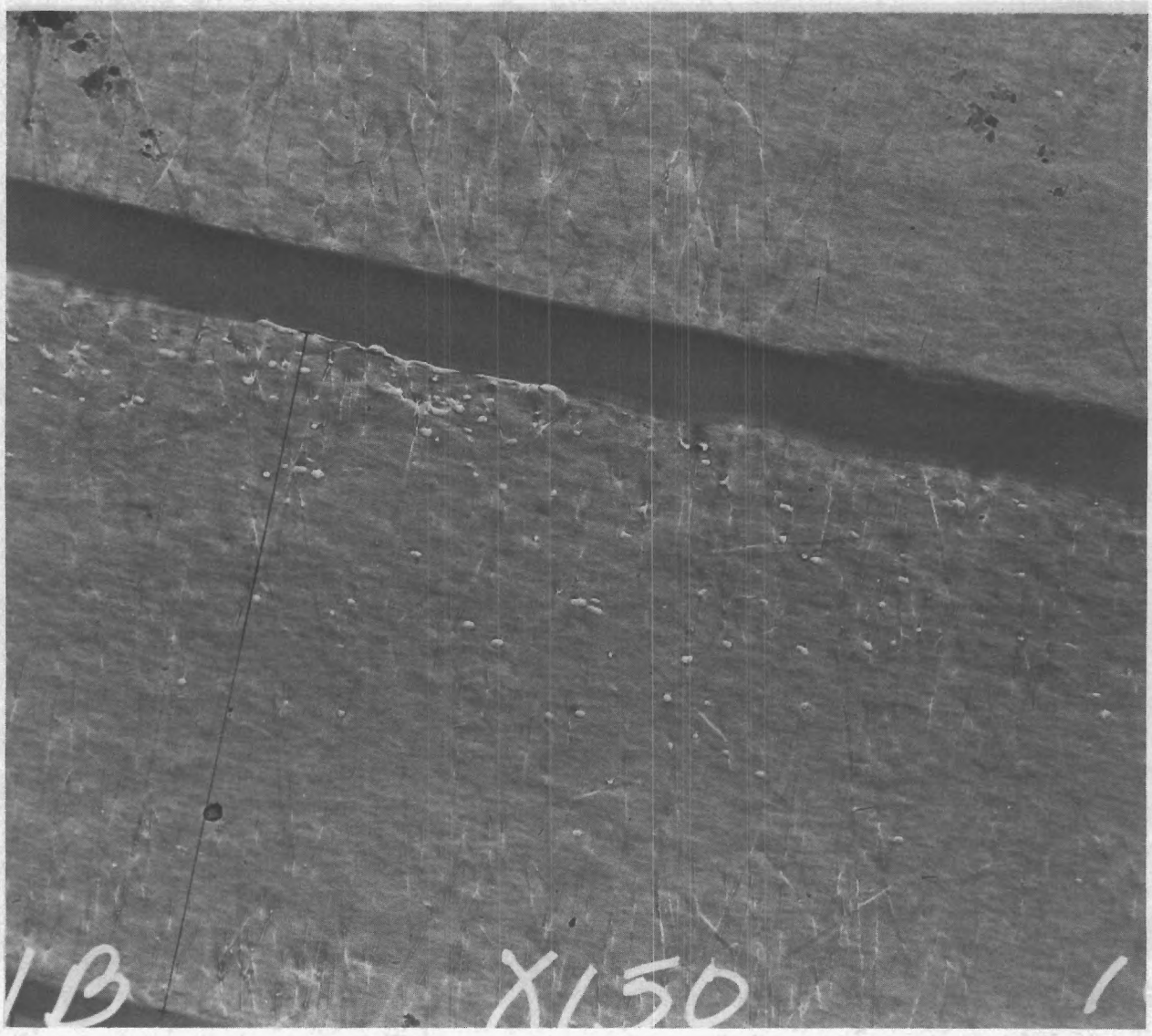

10,000 Å

12,800x

Figure 27. Transmission Electron Micrograph of Cross Section of Nominal 150 Å Nuclepore Membrane Using Ultramicrotomy. The line marks one membrane thickness.

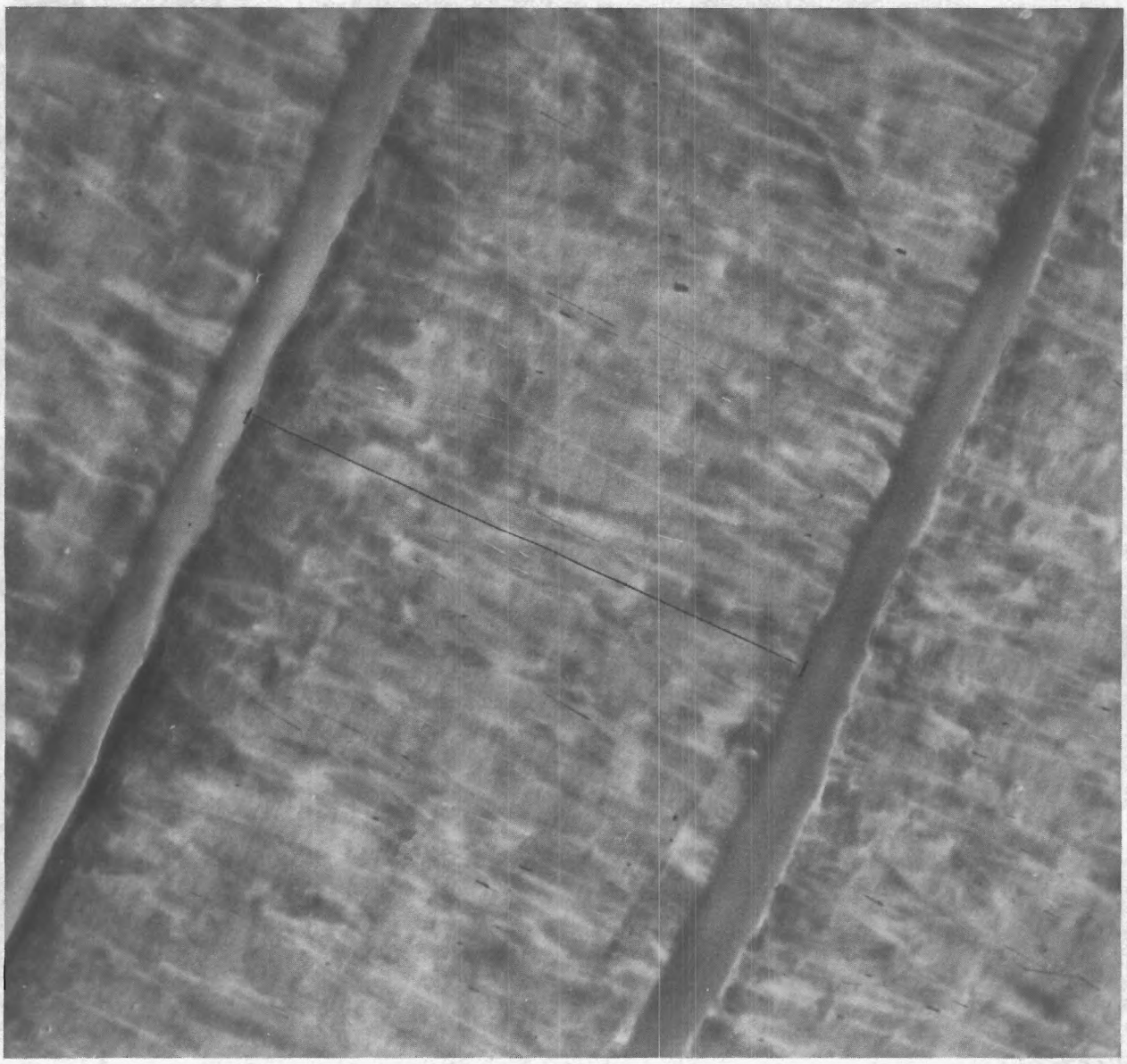

10,000 Å

12,800x

Figure 28. Transmission Electron Micrograph of Cross Section of Nominal 300 Å Nuclepore Membrane Using Ultramicrotomy. The line marks one membrane thickness.

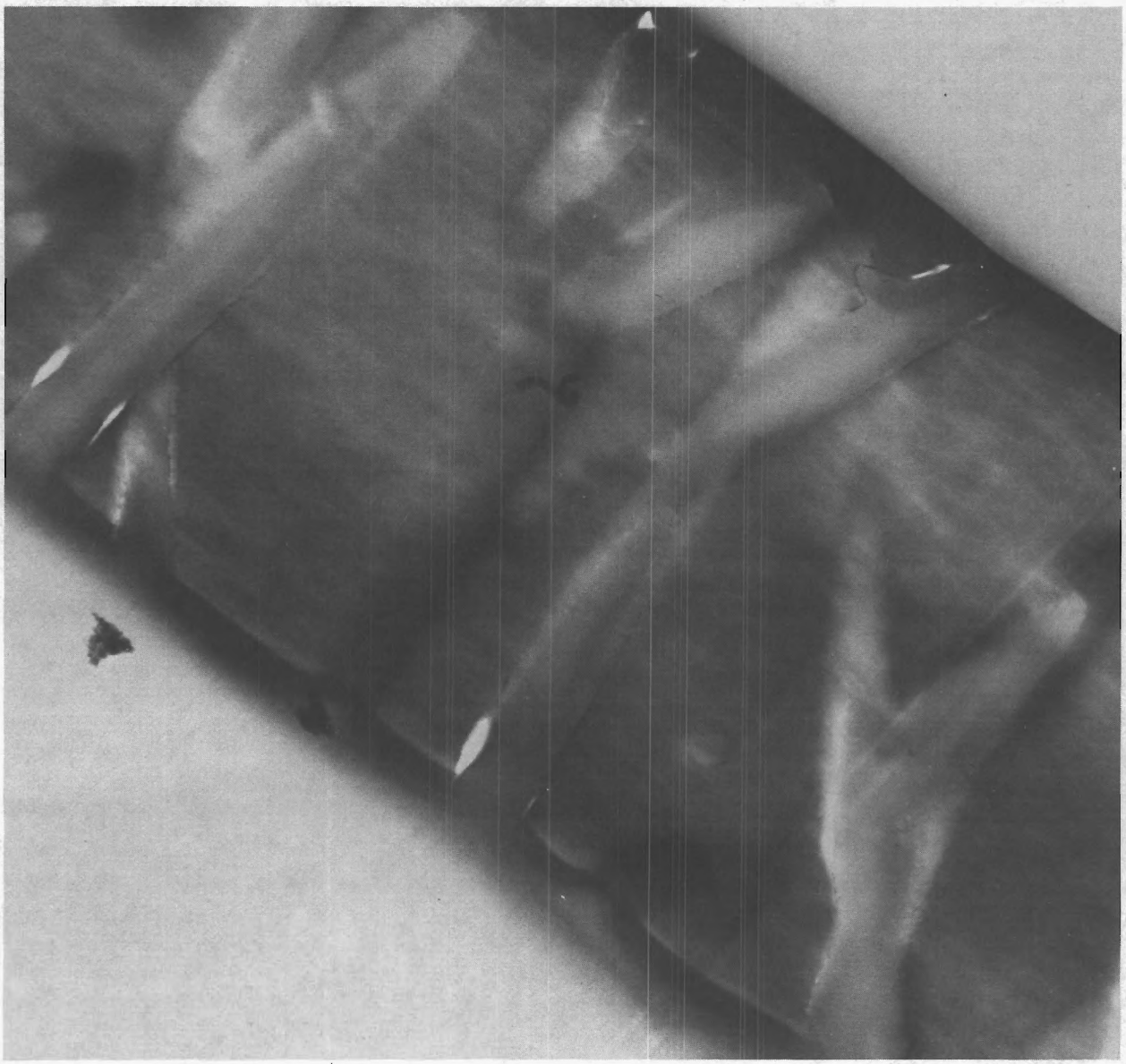

10,000 Å

10,400x

Figure 29. Transmission Electron Micrograph of Cross Section of Nominal 10,000 Å Nuclepore Membrane Using Ultramicrotomy.

Furthermore, it should be noted that the structure of the glass is by no means simple nor truly represented by the simple models presented to date. However, the simple models may well represent the average features which the experimental data support.

C. Pore Distributions

Pore distributions are presented as volume percent versus radius for the Nuclepore materials and the porous glasses. Figures 30 through 33 show the volume versus radius plots for the gas adsorption and desorption isotherms. Figure 34 shows a plot of volume percent versus radius for adsorption on all material studied, and Figure 35 shows an identical plot for desorption. Final analysis of these data is incomplete but it is apparent, at least, that there are marked similarities among the glass samples and differences between the glass and Nuclepore, probably due entirely to structural differences.

Figures 36 through 41 depict volume percent versus radius for mercury uptake and release from the porous glass samples. These figures indicate a smooth change in features with increasing radius of the sample.

The pore maxima from electron micrographs for the various materials investigated in this research are included in Table IV; distributions as such are not included since duplicate analyses are not complete.

V. PERSONNEL

This research is primarily the contribution of seven individuals. Mr. Marco Morales, a graduate student of Chemical Engineering, has largely conducted the mercury penetration tests and made the measurements of pore dimensions from electron micrographs. The early efforts seeking to prepare porous media from the ceria-gadolina composite were conducted by Mr. Edward Keng. The ultramicrotomy, replication, and electron and scanning microscopy of the porous media has been conducted under the direction of Mr. John L. Brown of the Georgia Tech Engineering Experiment Station and his staff, primarily Mrs. Kathryn Logan and Mr. Wayne Cooper, with guidance from Dr. Albert A. Liabastre. Dr. Liabastre, a post-doctoral fellow is coordinating the several efforts, analyzing the results, and generally supervising the testing. Overall direction is being supplied by Dr. Clyde Orr.

VI. PAPERS AND PRESENTATIONS

A review paper (copy included) prepared to meet an April, 1975, deadline for presentation this coming September contains mention of some of the early information uncovered in this work. An oral presentation at a Surface Science Colloquium, 77th National Meeting of the American Ceramic Society, Washington, D. C., May 5, 1975, contained some of the material of this report. And a paper currently being prepared for presentation and inclusion in the proceedings report of an NSF sponsored Workshop on Particle Technology to be held in Philadelphia, August 21 and 22, 1975, will contain even more of the results of the research.

Scientific journal articles can only be prepared when conclusive evidence is gained. There is already much interest in this work because of the unique nature of the pores being investigated.

Respectfully submitted:

Clyde Orr
Project Director

Approved:

Clyde Orr
Acting Director,
School of Chemical Engineering

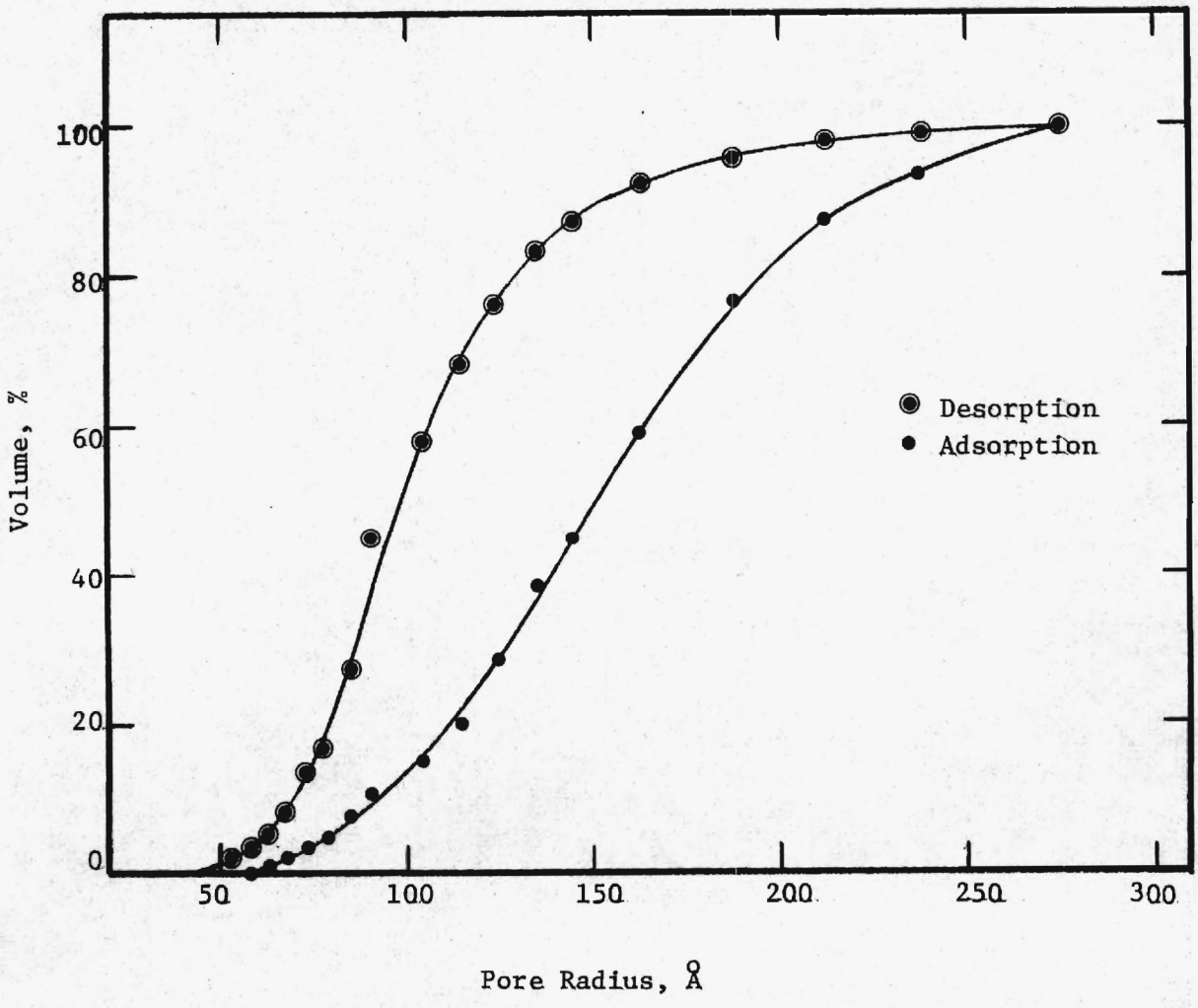

Figure 30. Pore Volume as a Function of Radius for Nominal 150 Å Nuclepore Membrane from Adsorption-Desorption.

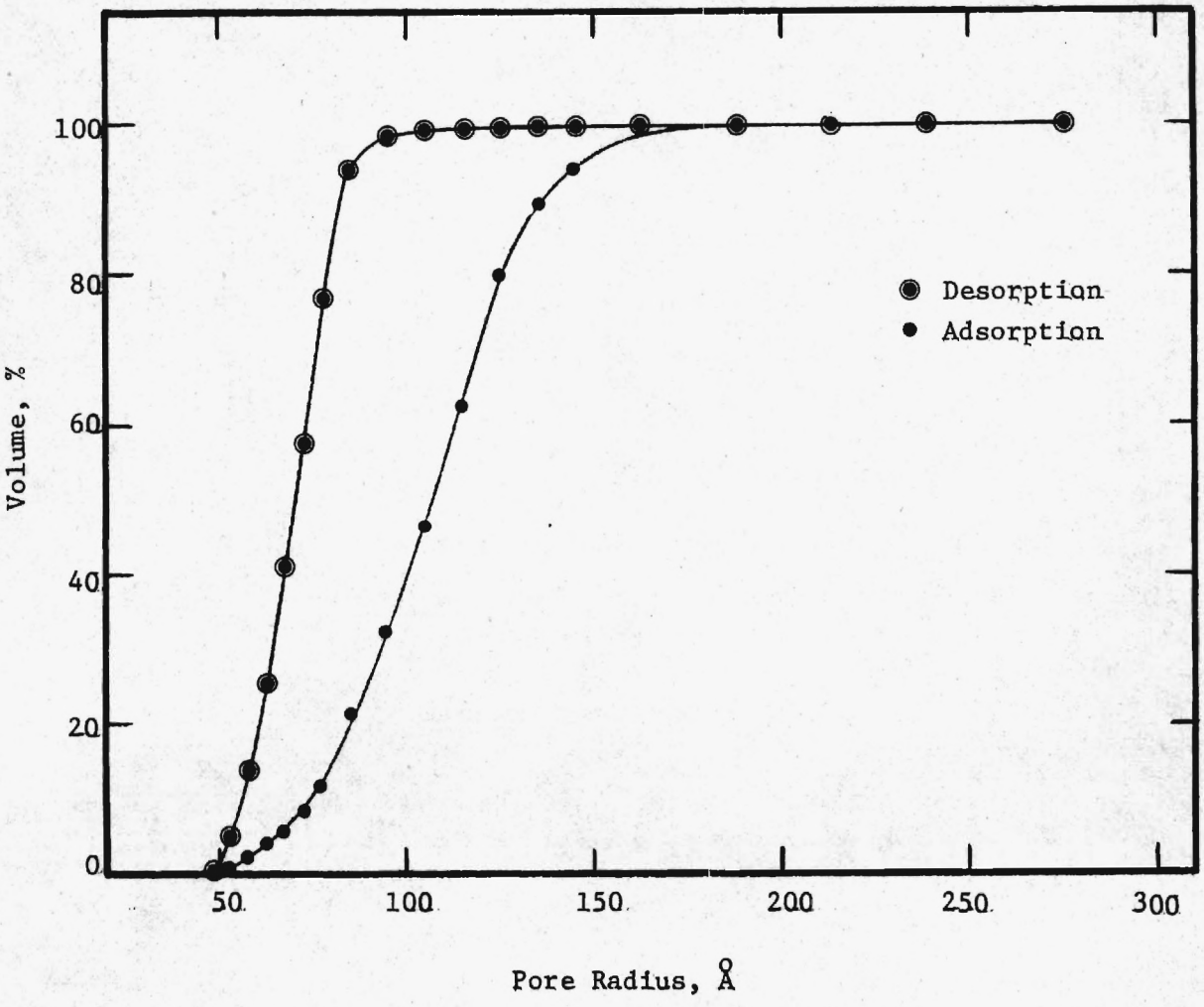

Figure 31. Pore Volume as a Function of Radius for Nominal 160 Å Porous Glass from Adsorption-Desorption.

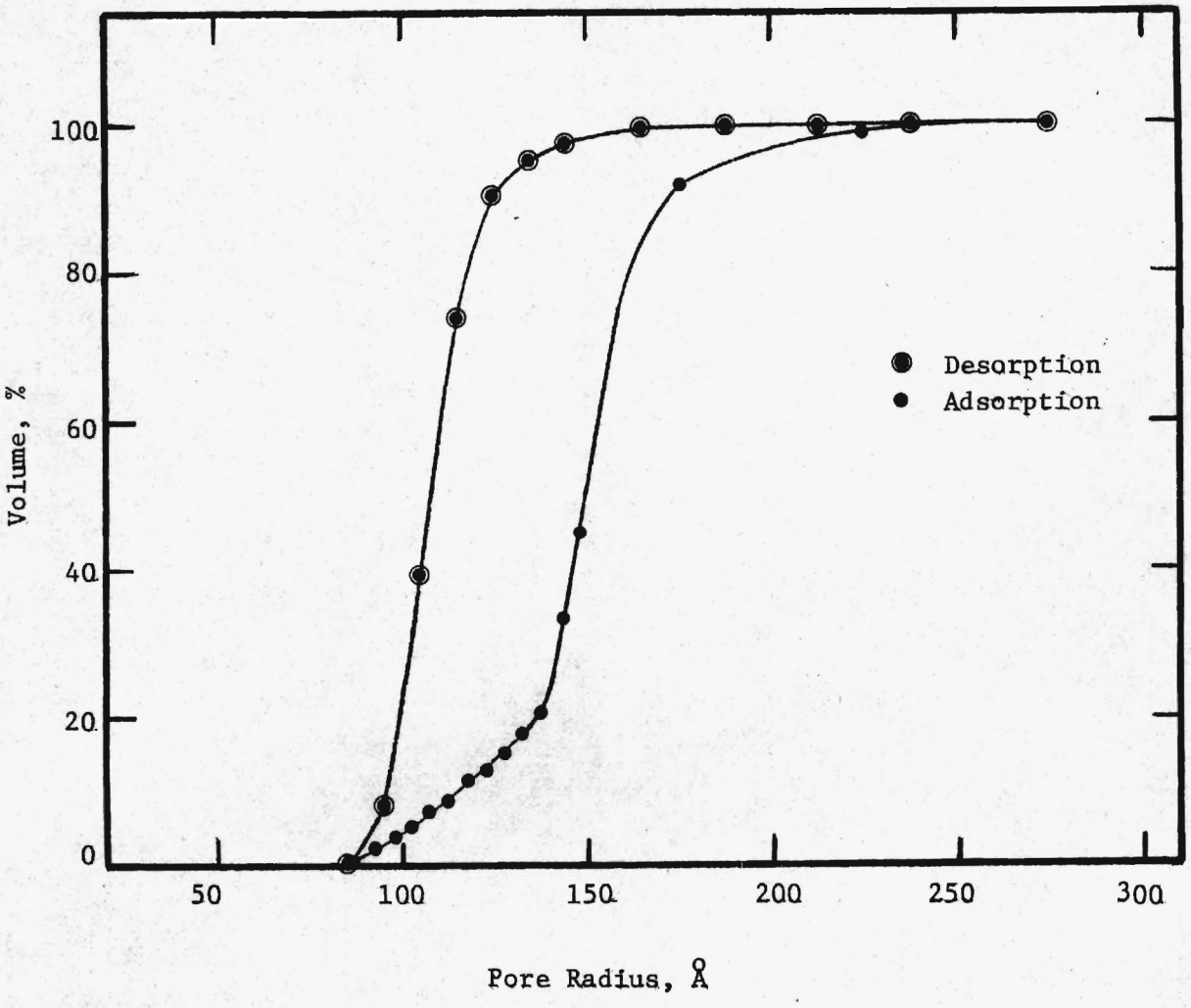

Figure 32. Pore Volume as a Function of Radius for Nominal 170 Å Porous Glass from Adsorption-Desorption.

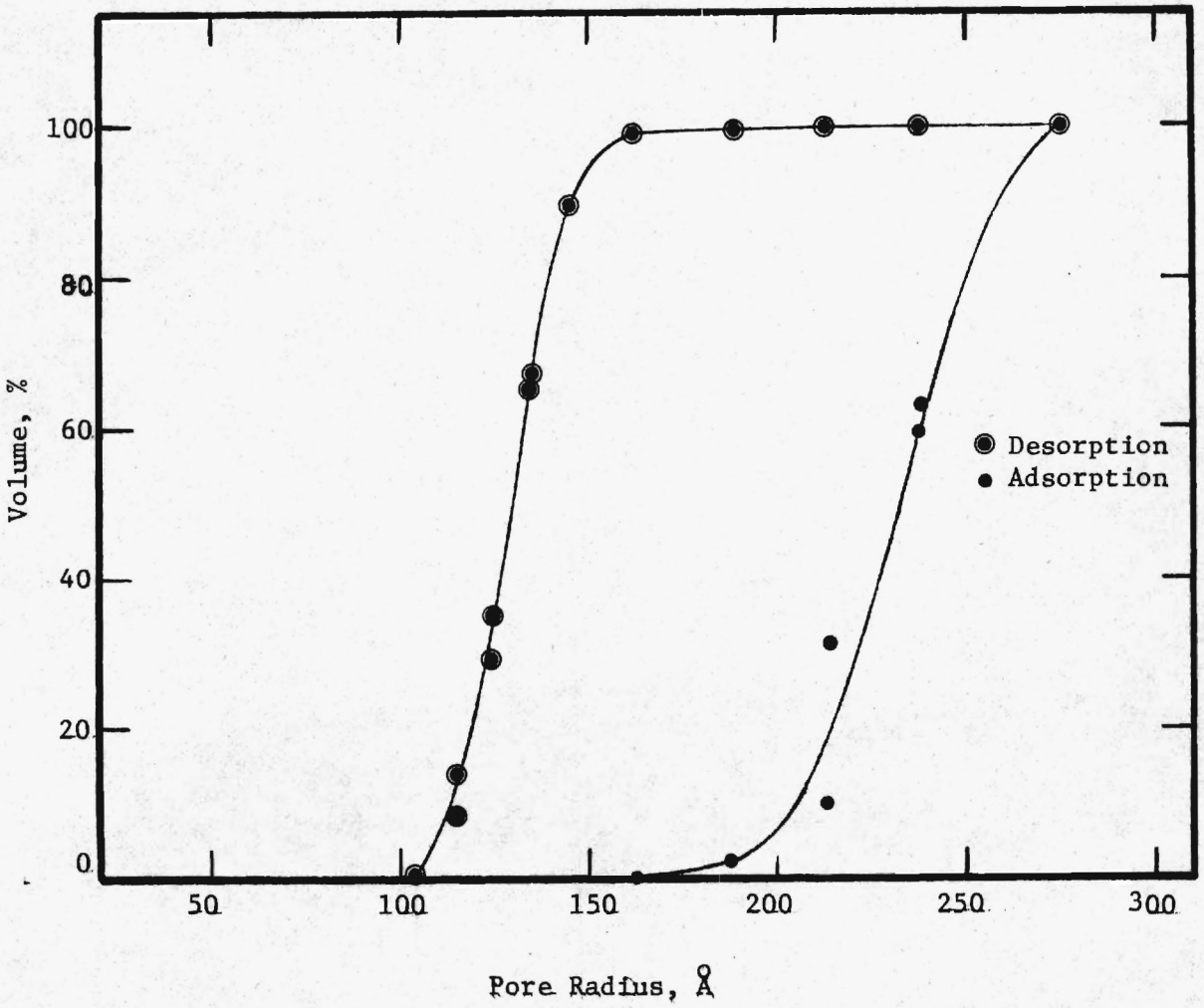

Figure 33. Pore Volume as a Function of Radius for Nominal 215 Å Porous Glass from Adsorption-Desorption .

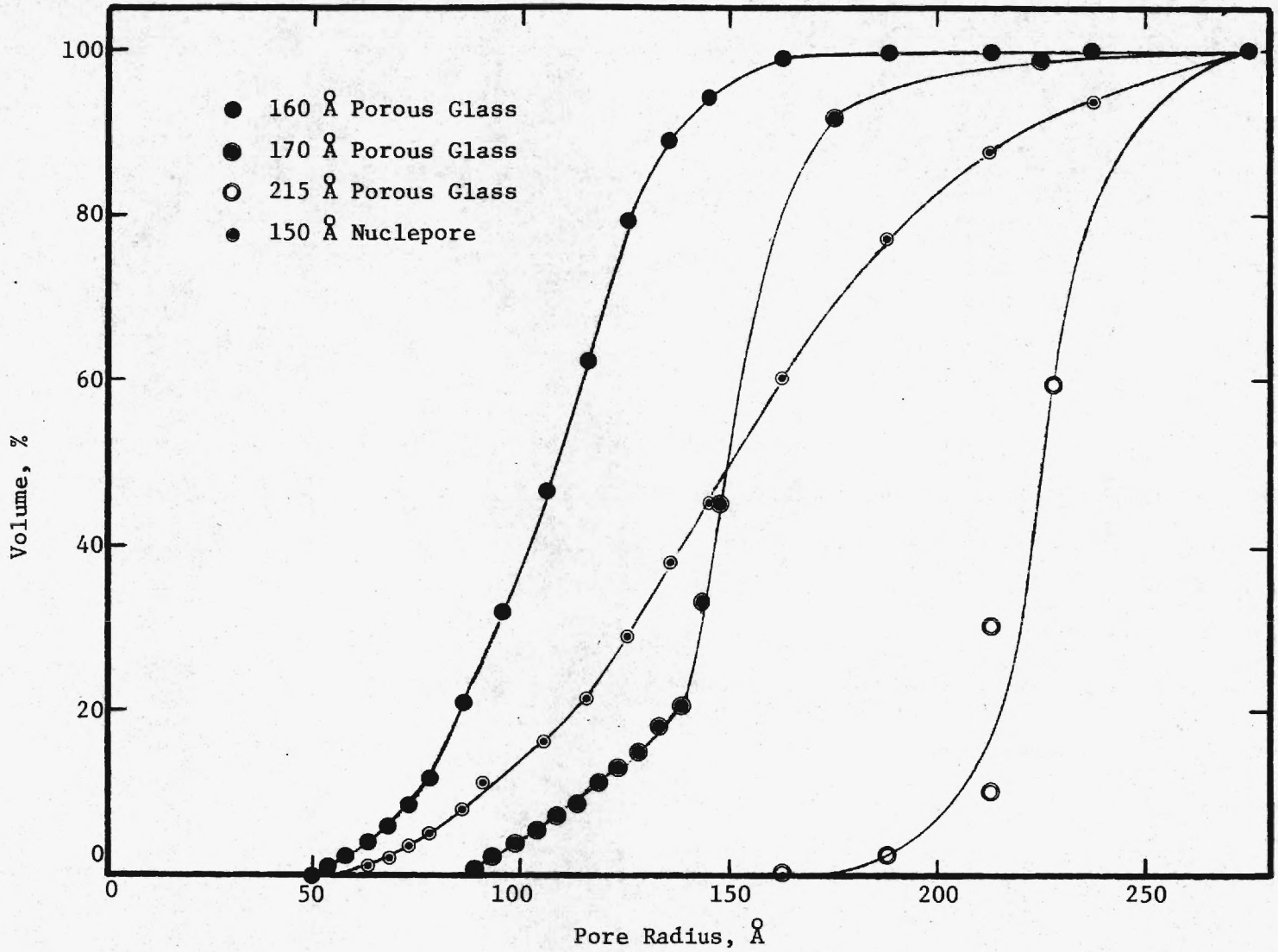

Figure 34. Pore Volume as a Function of Radius for all Materials from Gas Adsorption.

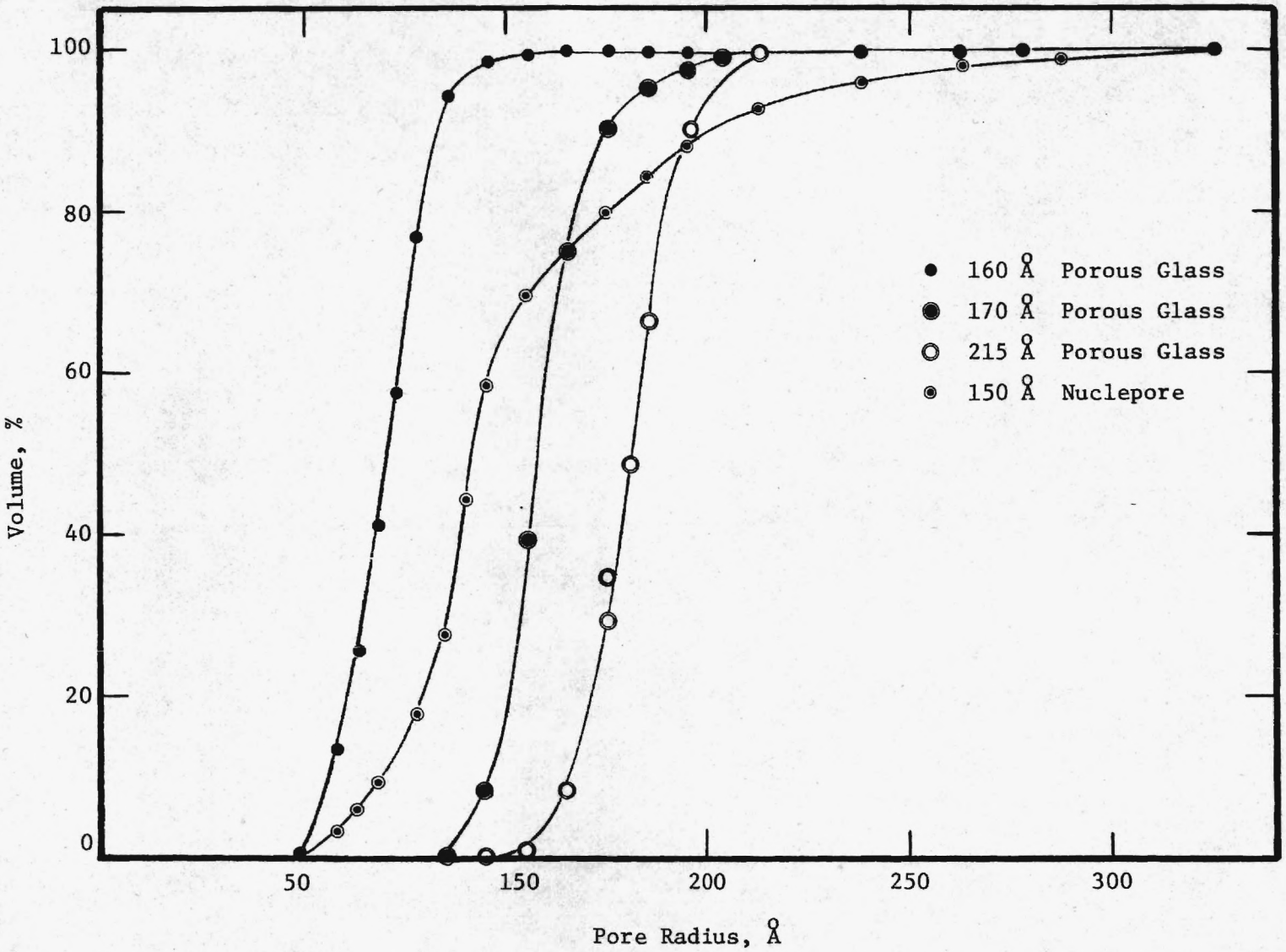

Figure 35. Pore Volume as a Function of Radius for all Materials from Gas Desorption.

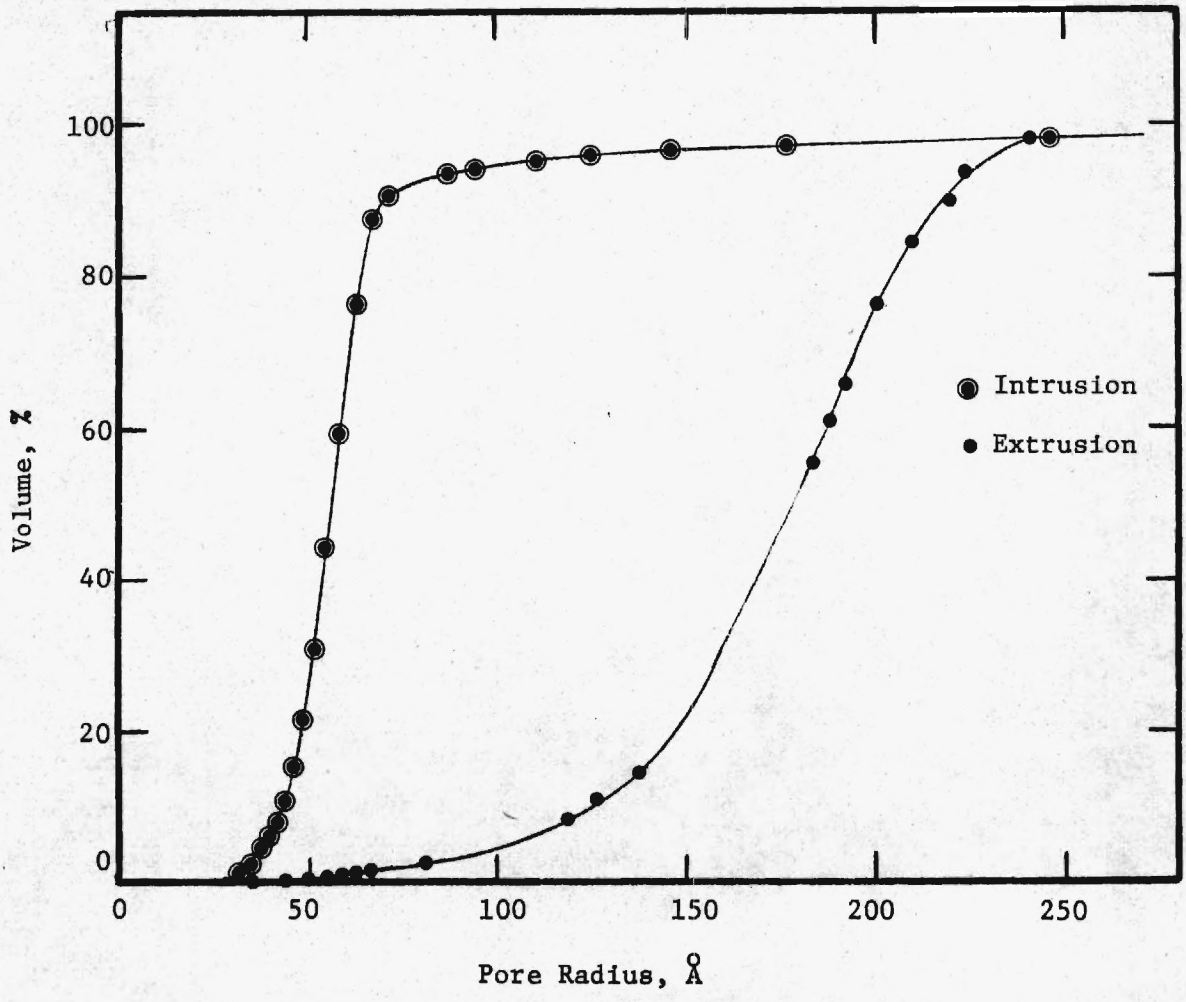

Figure 36. Pore Volume as a Function of Radius for Nominal 160 Å Porous Glass from Mercury Porosimetry.

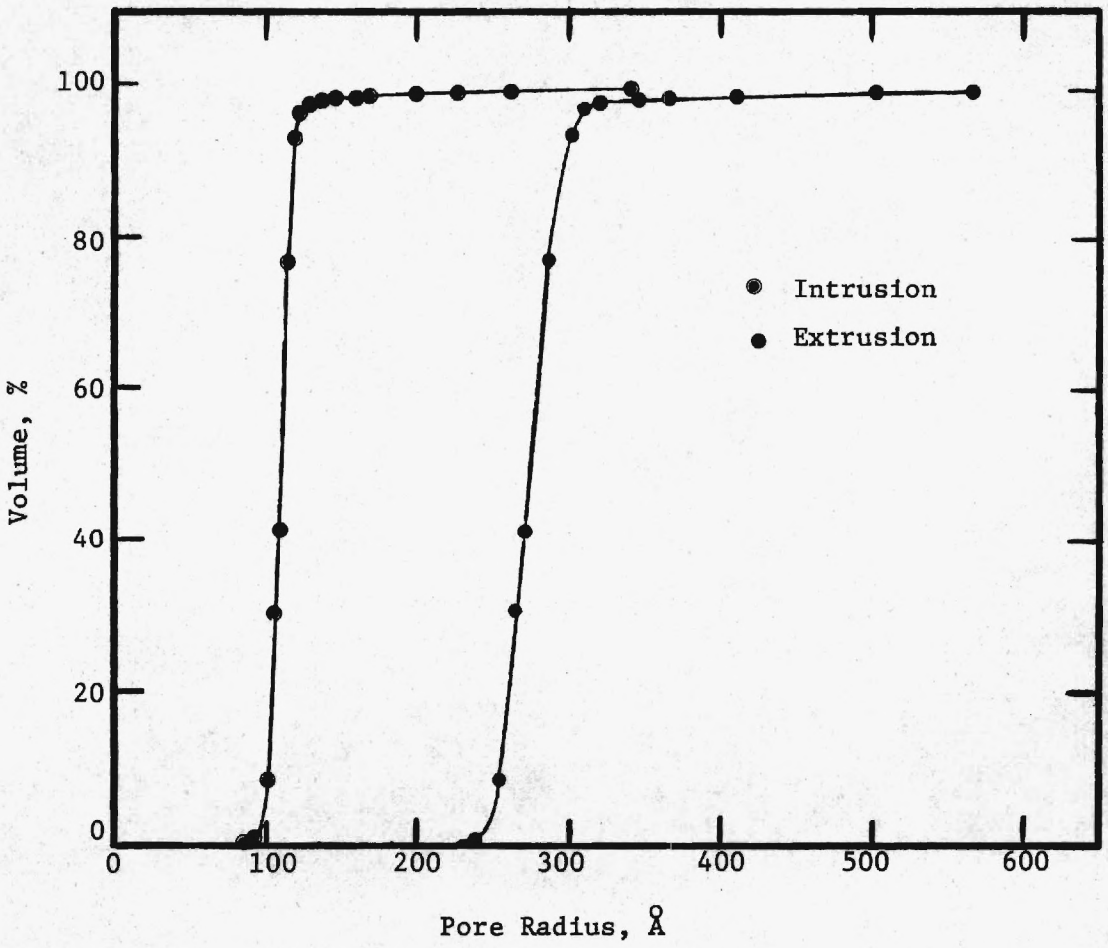

Figure 37. Pore Volume as a Function of Radius for Nominal 215 Å Porous Glass from Mercury Porosimetry.

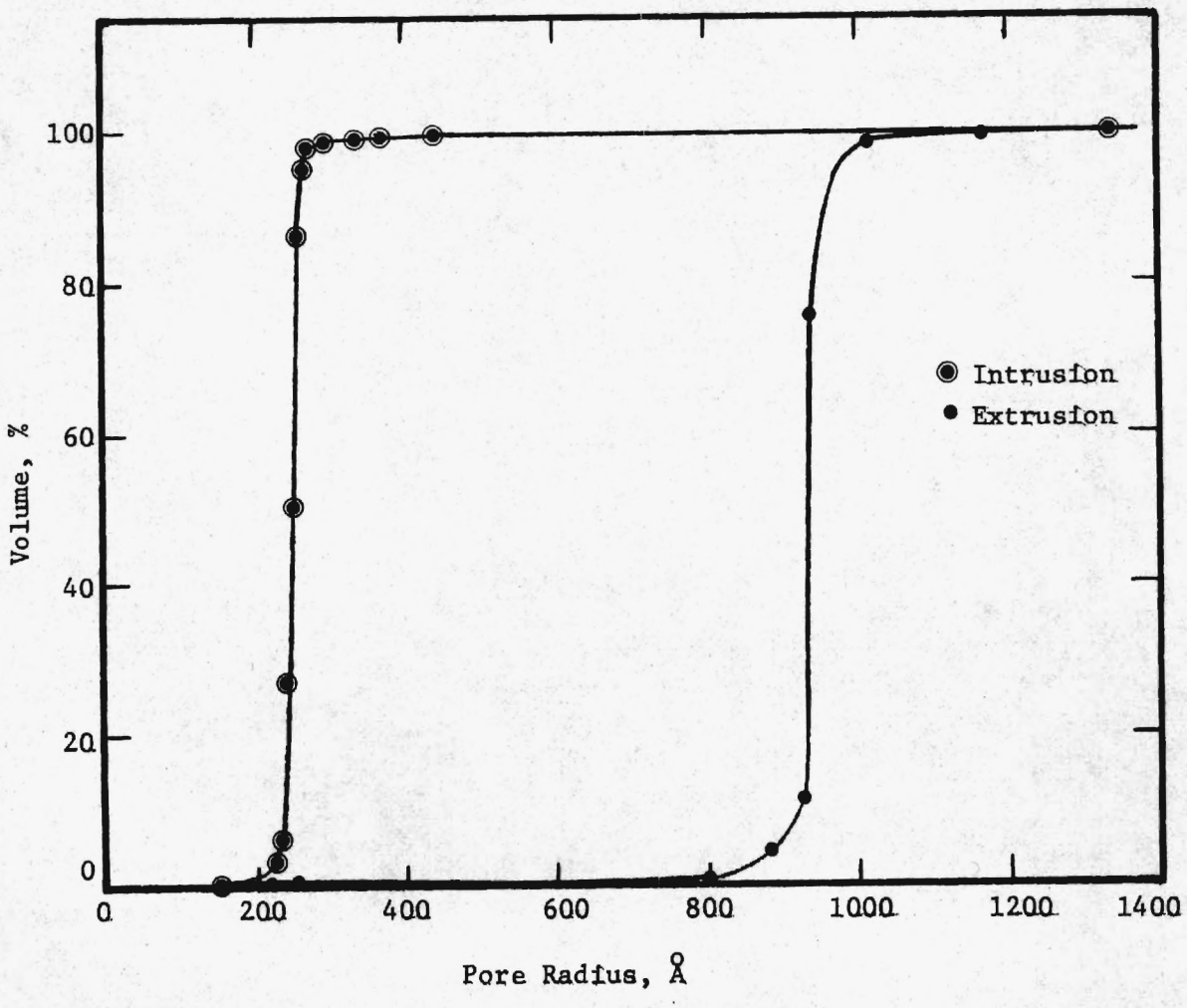

Figure 38. Pore Volume as a Function of Radius for Nominal 475 Å Porous Glass from Mercury Porosimetry.

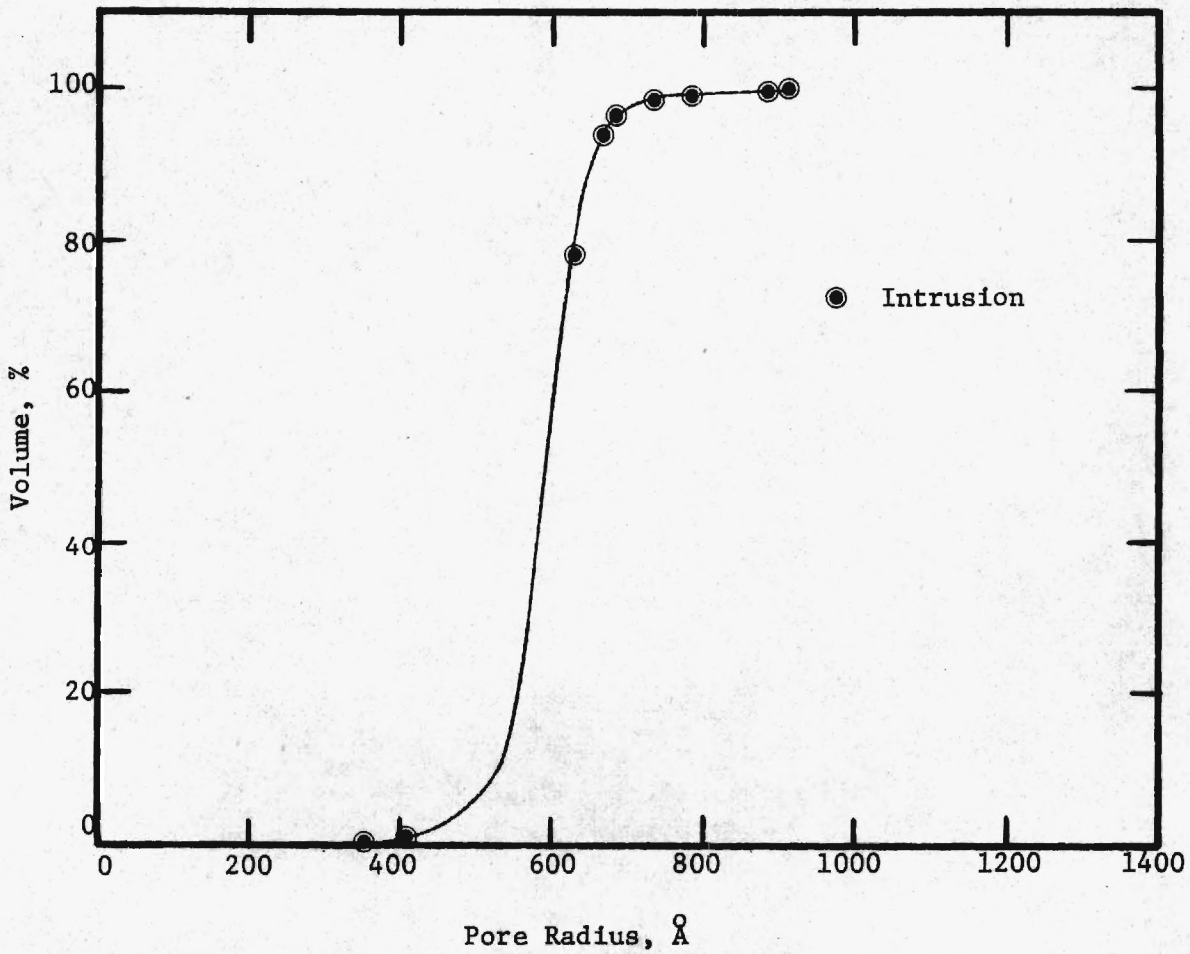

Figure 39. Pore Volume as a Function of Radius for Nominal 1093 Å Porous Glass from Mercury Porosimetry.

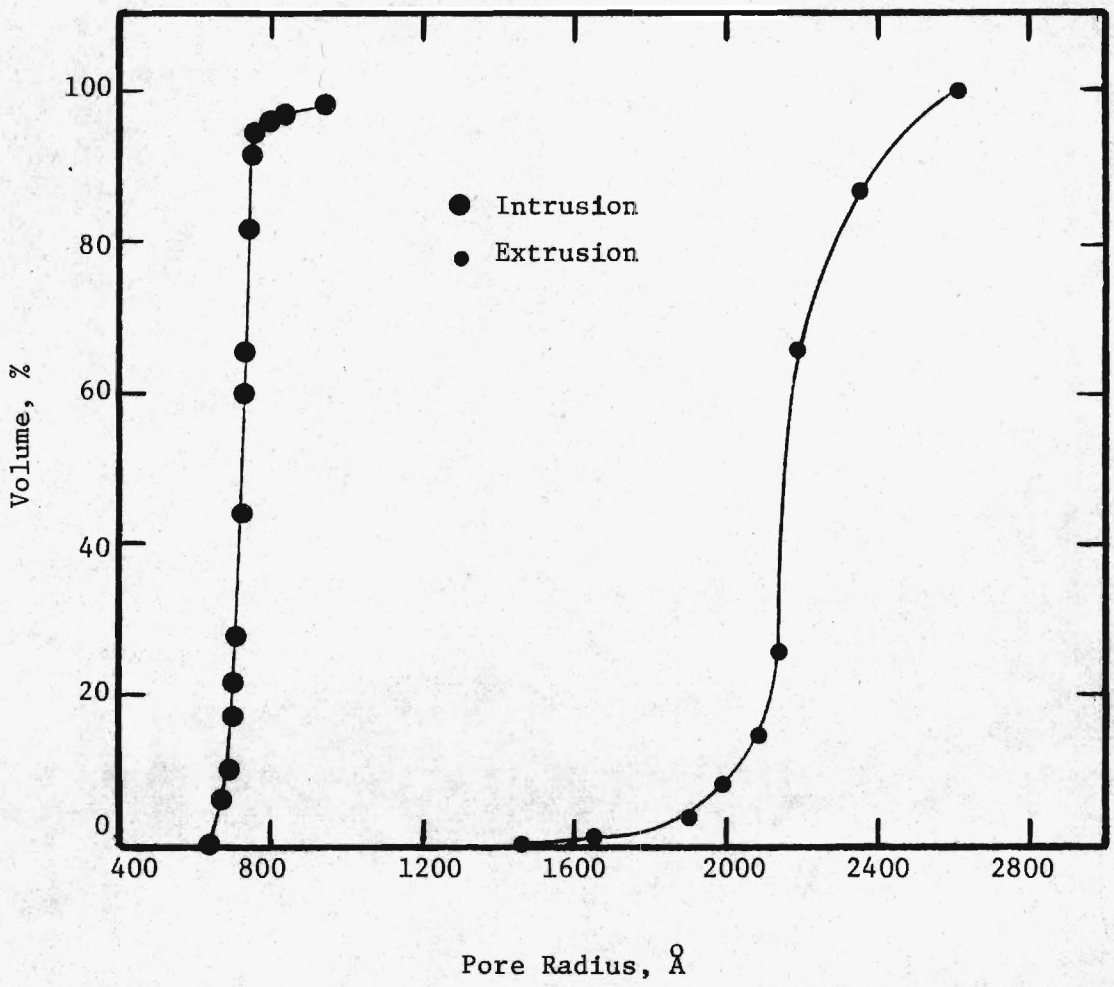

Figure 40. Pore Volume as a Function of Radius for Nominal 1223 Å Porous Glass from Mercury Porosimetry.

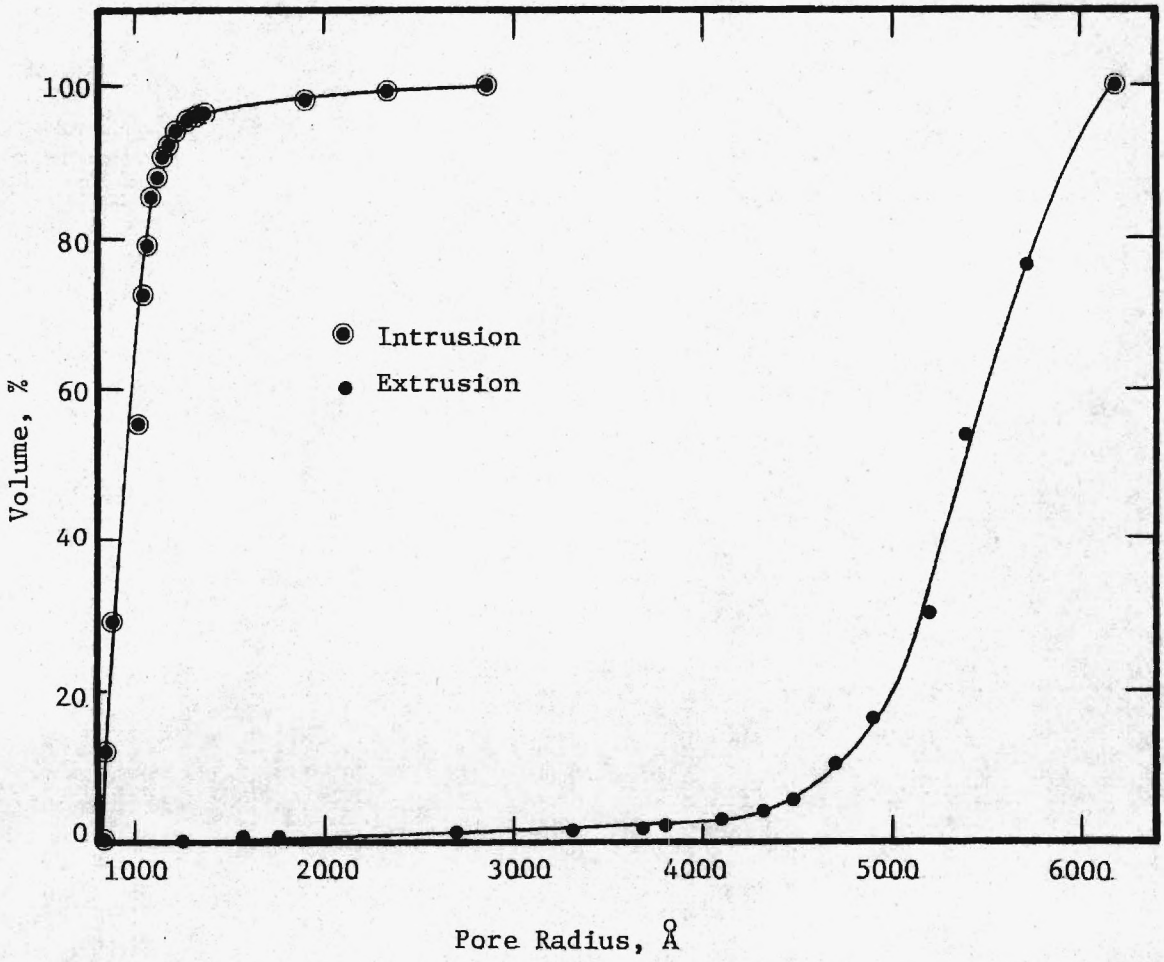

Figure 41. Pore Volume as a Function of Radius for Nominal 1933 Å Porous Glass from Mercury Porosimetry.

VII. BIBLIOGRAPHY

1. Rieger, R. A., The Selective Chemical Etching of CeO_2 Doped Gd_2O_3-Mo Composites, M. S. Thesis, Georgia Institute of Technology, December, 1973.

2. Barrall, E. M. and Cain, J. H., "Optical and Electron Microscopy of Bio-Glass Chromatography Substrates," J. Polymer Sci. 21, 253-65 (1968).

3. Watanabe, M., Noake, H., and Aiba, T., "Electron Micrographs of Some Borosilicate Glasses and Their Internal Structure," J. Am. Ceramic Soc. 42, 593-99 (1959).

4. Karmaukhov, A. P., "Combined Investigation of the Pore Structure of Catalysts. I. Some Problems in the Contemporary State of the Sorption Method," Kinetika in Kataliz 8, 172-81 (1967).

5. Svatá, M., "Determination of Pore Size and Shape Distribution from Porosimetric Hysteresis Curves," Powder Tech. 5, 345-9 (1971/72).

6. Linsen, B. G., and van der Heuvel, A. "Pore Structures" The Gas-Solid Interface, Vol. 2, (E. A. Flood, ed)., Marcel Dekker, New York, (1967),pp 1025-53.

7. deBoer, J. H., "The Shapes of Capillaries," The Structure and Properties of Porous Materials (D. H. Everett and F. S. Stone, eds.), Butterworths, London (1958), pp. 68-94.

8. Lippens, B. C. and deBoer, J. H., "Studies on Pore Systems in Catalysts. V. The t method. J. Catalysis 4, 319-23 (1965).

9. Sing, K. S. W., "Empirical Method for Analysis of Adsorption Isotherms," Chem. & Ind. (1968), pp 1520-1.

10. Sing, K. S. W., "Utilization of Adsorption Data in the BET Region," Surface Area Determination (D. H. Everett and R. H. Ottewill, R. H., eds.), Butterworths, London (1970), pp 25-42.

Final Physical E-19-625

NATIONAL SCIENCE FOUNDATION
Washington, D.C. 20550

RESEARCH GRANT BUDGET & FISCAL REPORT

Form Approved
OMB No. 99-R0013

INSTITUTION AND ADDRESS	NSF PROGRAM	GRANT PERIOD
Georgia Institute of Technology Atlanta, Georgia	Solid and Particulate Processing	*from* 5/1/74 *to* 10/31/76 REPORTING PERIOD *from* 5/1/74 *to* 2/21/77*

GRANT NUMBER	BUDGET DUR. (MOS.)	PRINCIPAL INVESTIGATOR(S)	GRANTEE ACCOUNT NUMBER
ENG74-02718 A01	6	Orr	E-19-625

	NSF Funded Man Months			NSF AWARD BUDGET	CUMULATIVE GRANT EXPENDITURES *Do Not Round*
	Cal.	Acad.	Summ.		
A. SALARIES AND WAGES					
1. Senior Personnel					
a. 1 (Co)Principal Investigator(s)	1			$ 813	
b. Faculty Associates					
Sub-Total				$ 813	$ 4,169.56
2. Other Personnel (Non-Faculty)					
a. 1 Research Associates–Postdoctoral	6			6,000	
b. Non-Faculty Professionals					
c. 1 Graduate Students				1,733	
d. Pre-Baccalaureate Students					
e. Secretarial–Clerical					
f. 2 Technical, Shop, and Other				425	
TOTAL SALARIES AND WAGES				$ 8,971	$ 27,228.00
B. STAFF BENEFITS IF CHARGED AS DIRECT COST				111	413.18
C. TOTAL SALARIES, WAGES, AND STAFF BENEFITS (A + B)				$ 9,082	$ 27,641.18
D. PERMANENT EQUIPMENT					-0-
E. EXPENDABLE EQUIPMENT AND SUPPLIES				190	7,430.76
F. TRAVEL 1. DOMESTIC (INCLUDING CANADA)					-0-
2. FOREIGN					-0-
G. PUBLICATION COSTS					178.46
H. COMPUTER COSTS IF CHARGED AS DIRECT COST					-0-
I. OTHER DIRECT COSTS Adsorption Analyses				400	871.15
J. TOTAL DIRECT COSTS (C through I)				$ 9,672	$ 36,121.55
K. INDIRECT COSTS 65% of Salaries and Wages				5,831	**18,225.49
L. TOTAL COSTS (J plus K)				$ 15,503	$ 54,347.04
M. AMOUNT OF THIS AWARD (ROUNDED)				$ 15,500	
N. CUMULATIVE GRANT AMOUNT				$ 54,400	
O. UNEXPENDED BALANCE (N. BUDGET MINUS L. EXPENDITURE)					$ 52.96

REMARKS: Use extra sheet if necessary

*No obligations were made outside the grant period of 5/1/74 through 10/31/76.

** 65% of $ 9,651.65 = $ 6,273.57
68% of $17,576.35 = $11,951.92
$27,228.00 $18,225.49

SIGNATURE OF PRINCIPAL INVESTIGATOR	TYPED OR PRINTED NAME	DATE
	Clyde Orr, Jr.	Feb. 24, 1977

I CERTIFY THAT ALL EXPENDITURES REPORTED ARE FOR APPROPRIATE PURPOSES AND IN ACCORDANCE WITH THE AGREEMENTS SET FORTH IN THE APPLICATION AND AWARD DOCUMENTS

SIGNATURE OF AUTHORIZED OFFICIAL	TYPED OR PRINTED NAME & TITLE	DATE
	C. Evan Crosby, Associate Director of Financial Affairs	3/1/77

FOR NSF USE ONLY

Organ. Code	F.Y.	Fund ID	Prog. Code	Ob. Class	O/Dres.	Award No.	Amd.	Inst. Code	Unexpended Balance	Trans.	Lot
									$		

NSF Form 98, May 1975 *SUPERSEDES JULY 1971 EDITION WHICH MAY BE USED UNTIL SUPPLY EXHAUSTED*

E-19-625

NATIONAL SCIENCE FOUNDATION
Washington, D.C. 20550

SUMMARY OF COMPLETED PROJECT

Form Approved
OMB No. 99R0013

Please read instructions on reverse carefully before completing this form.

INSTITUTION AND ADDRESS	2. NSF PROGRAM	3. GRANT PERIOD
Georgia Institute of Technology School of Chemical Engineering Atlanta, Ga. 30332	Solid and Particulate Processing	5/1/74 (from) 10/31/76 (to)

GRANT NUMBER	5. BUDGET DUR. (MOS)	6. PRINCIPAL INVESTIGATOR(S)	7. GRANTEE ACCOUNT NUMBER
ENG74-02718	16	C. Orr & A. A. Liabastre	

SUMMARY (Attach list of publications to form)

Porous solid materials are encountered widely in the chemical process industry, in pollution control, and in life support systems, and they are found in a great many items of commerce. Filters, adsorbents, and catalyst supports are prominent among commercial items. The size and shape of the pores are of primary concern in every instance, since they strongly influence the efficacy of the solid in its specific role. These size and shape parameters are generally evaluated by one of two analytical techniques, high-pressure mercury penetration or low-temperature gas adsorption and desorption. Both techniques rely on extrapolations of theoretical hypotheses and physical constants obtained under conditions far removed from those actually prevailing under application.

This research has examined the several assumptions of the techniques and attempted to correlate experimental results with carefully determined values from electron microscopy. Controlled pore glasses and Nuclepore membranes, both materials having pores with right-cylinder characteristics, were employed. The former was examined in a series of samples having a narrow distribution of pores with mean diameters from 7.5 to 193 nm while the latter had a somewhat wider pore diameter distribution with means from 15 to 5000 nm. The glasses were quite rigid while the membranes were flexible and compressible.

Mercury penetration was found to give very reliable values for the mean pore size, distribution of sizes, and pore volume when accurate values for the mercury contact angle and material compressibility were included. Standard methods for calculating pore size and pore distribution from gas adsorption and desorption data yielded results of the proper magnitude, but a re-evaluation of the contact angle and interfacial tension for liquid nitrogen is necessary to produce results comparable with those from mercury penetration and electron microscopy.

SIGNATURE OF PRINCIPAL INVESTIGATOR/ PROJECT DIRECTOR	TYPED OR PRINTED NAME	DATE
	Clyde Orr	5/1/77

List of Publications

1. Orr, C., "Surface Area Measurement--The Present Status", Dechema-Monographien 79B, 39-60 (1976).

2. Orr, C., "Der derzeitige Stand der Methoden zur Bestimmung von Pulver-Oberflachen," Chem.-Ing.-Tech. 48, 680-9 (1976).

3. Liabastre, A. A. and Orr, C., "An Evaluation of Pore Structure by Mercury Penetration", submitted to J. Coll. & Interface Sci.

BLIOGRAPHIC DATA EET	1. Report No.	2.	3. Recipient's Accession No.

Title and Subtitle An Evaluation of Pore Structure by Mercury Porosimetry	5. Report Date 4/77 (date of preparation) 6.
Author(s) A. A. Liabastre and C. Orr	8. Performing Organization Rept. No.
Performing Organization Name and Address Georgia Institute of Technology School of Chemical Engineering Atlanta, Ga. 30332	10. Project/Task/Work Unit No. E-19-649 11. Contract/Grant No. ENG74-02718
Sponsoring Organization Name and Address National Science Foundation Division of Engineering, Solid and Particulate Processing 1800 G Street, S.W. Washington, D.C. 20550	13. Type of Report & Period Covered Final 14.

Supplementary Notes

Abstracts

The validity of and the assumptions inherent in high-pressure mercury penetration and low-temperature gas adsorption or desorption techniques for assessing pore size and volume were critically examined by correlating experimental results from application of the techniques with values obtained by electron microscopy. Controlled pore glasses and Nuclepore membranes, both materials having pores with right-cylinder characteristics, were employed. Mean pore diameters ranged from 7.5 to 5000 nm.

Mercury penetration was found to give very reliable results when accurate values for the mercury contact angle and material compressibility were employed. Standard methods for calculating pore size and volume from gas adsorption or desorption data yielded values of the proper magnitude, but a further evaluation is necessary to produce results of comparable quality.

The study is continuing.

Key Words and Document Analysis. 17a. Descriptors

Pore size
Pore volume
Mercury penetration

Identifiers/Open-Ended Terms

Pore analysis
Porosimetry

COSATI Field/Group

Availability Statement	19. Security Class (This Report)	21. No. of Pages
Release unlimited	UNCLASSIFIED	34
	20. Security Class (This Page) UNCLASSIFIED	22. Price

Georgia Institute of Technology
School of Chemical Engineering
Atlanta, Georgia

Clyde Orr, Principal Investigator

NSF Grant No. ENG74-02718 (GK-43616)
May 1, 1974 - October 31, 1976

INVESTIGATION INTO THE PHYSICAL STRUCTURE OF POROUS CATALYSTS AND ADSORBENTS

Porous solid materials are encountered widely in the chemical process industry, in pollution control, and in life support systems, and they are found in a great many items of commerce. Filters, adsorbents, and catalyst supports are prominent among commercial items. The size and shape of the pores are of primary concern in every instance, since they strongly influence the efficacy of the solid in its specific role. These size and shape parameters are generally evaluated by one of two analytical techniques, high-pressure mercury penetration or low-temperature gas adsorption and desorption. Both techniques rely on extrapolations of theoretical hypotheses and physical constants obtained under conditions far removed from those actually prevailing under application.

This research has examined the several assumptions of the techniques and attempted to correlate experimental results with carefully determined values from electron microscopy. Controlled pore glasses and Nuclepore membranes, both materials having pores with right-cylinder characteristics, were employed. The former was examined in a series of samples having a narrow distribution of pores with mean diameters from 7.5 to 193 nm while the latter had a somewhat wider pore diameter distribution with means from 15 to 5000 nm. The glasses were quite rigid while the membranes were flexible and compressible.

Mercury penetration was found to give very reliable values for the mean pore size, distribution of sizes, and pore volume when accurate values for the mercury contact angle and material compressibility were included. Standard methods for calculating pore size and pore distribution from gas adsorption and desorption data yielded results of the proper magnitude, but a re-evaluation of the contact angle and interfacial tension for liquid nitrogen is necessary to produce results comparable with those from mercury penetration and electron microscopy.

Details of the mercury penetration portion of the study are included in the attached manuscript which has been submitted to the Journal of Colloid and Interfacial Science. The gas adsorption and desorption work is the subject of another article presently in preparation. The two attached reprints* relate to early phases of this research.

No theses have resulted from this work and nothing patentable has been uncovered.

* Orr, C., "Surface Area Measurement--The Present Status", Dechema-Monographien, 79B, 39-60 (1976).
Orr, C., "Der derzeitige Stand der Methoden zur Bestimmung von Pulver-Oberflächen", Chem.-Ing.-Tech. 48, 680-9 (1976).

Collaborators in the investigation include Dr. Albert A. Liabastre, research scientist, Mr. Marco Morales, graduate student in Chemical Engineering, and Mr. John L. Brown, Principal Research Scientist, of the Georgia Tech Engineering Experiment Station.

This research is continuing under NSF Grant No. ENG76-10057 wherein materials having cylindrical pores with one closed end and cavities of special shapes are receiving special attention.

Respectfully submitted,

Clyde Orr
Principal Investigator

CO/jc

Surface Area Measurement -- The Present Status

Orr, C.

Summary

Presently the surface area of powders cannot be determined reliably in every instance. Attention to structural features such as microcracks and pores within the particles is essential for determining the reliability of measurements. Acceptable methods are outlined for evaluating the surface area of nonporous particles and particles containing relatively large pores. With powders having microcracks only the outside surface area can be estimated by established methods. The contribution to surface area of moderate size pores is determinable when the shapes of the pores can be modeled; otherwise only estimates are obtained. The fraction of the surface attributable to a specific composition can be determined when particle surface regions differ considerably in chemical activity.

Kurzfassung

Bis heute läßt sich die Oberfläche disperser Feststoffe nur angenähert bestimmen. So wird die Zuverlässigkeit von Oberflächenmessungen im wesentlichen durch strukturelle Merkmale wie Mikrobrüche und Poren in den Partikeln bestimmt. Es werden brauchbare Methoden für die Messung der Oberfläche von nichtporösen Partikeln und von Partikeln mit relativ grossen Poren besprochen. Weist der Feststoff Mikrobrüche auf, so kann nur die äußere Oberfläche mit bekannten Methoden ermittelt werden. Der Beitrag mittlerer Porengrößen zur Oberfläche läßt sich bestimmen, wenn Annahmen über die Form der Poren gemacht werden. In allen anderen Fällen ist nur eine Schätzung möglich. Oberflächengebiete einer bestimmten spezifischen Zusammensetzung lassen sich nur bestimmen, wenn diese sich in ihrer chemischen Aktivität beträchtlich unterscheiden.

Résumé

Présentement, l'aire de la surface des poudres ne peut pas être déterminée de *facon* certaine dans tous les cas. Il est essentiel, pour déterminer la fiabilité des mesures, de porter attention aux caractéristiques structurales de la particule telles que les microfissures et les pores. Des méthodes acceptables, pour évaluer l'aire de la surface des particules non poreuses at des particules contenant des pores relativement importants, pont présentées dans leurs grandes lignes. Pour les poudres ne comportant que des microfissures, il n'est possible d'estimer, par des méthodes confirmées, que l'aire de la surface extérieure. On peut déterminer la contribution des pores de taille modéreé ă l'aire de la surface lorsque la forme géométrique des pores peut être represenutee par un modèle-Dans le cas contraire, on ne peut obtenir qu'une estimation. Il est possible de déterminer la fraction de la surface attribuable ă une composition donneé lorsqu'il existe des régions, sur la surface de la particule, qui ont des activités chimiques neetement différentes.

Introduction

In fine powders, a relatively great proportion of the atoms are at, or near, the surface, causing powders to exhibit properties distinctly different from the same material in bulk form and to do so in a manner strongly dependent on the magnitudes of their surface areas. A fine powder is more reactive than the same material in

bulk; it shows enhanced solubility; it sinters at a lower temperature; it has more adsorptive capacity; and it exhibits greater catalytic activity. The influence of surface area is so pronounced in some instances that surface appears almost as important as chemical composition. In the case of elastomer reinforcement, for example, the magnitude of specific surface area is nearly as significant as whether the particles are carbon, silica, or calcium carbonate.

Surface area magnitude alone is not the only important criterion, however. Individual fine particles may have a surface structure containing microcracks, and larger particles and agglomerates of particles are likely to contain pores and crevices of greater dimensions. Surface area assessment must take into account these general structural features and also consider the accessibility of the surface. A surface catalyst, as an example, is of little value if most of its area is accessible only by way of narrow passageways along which reacting species and reaction products must move by slow diffusional processes.

In addition, surfaces of particles composed of two or more chemical substances, such as a catalyst consisting of an active metal and an inert carrier substrate, may contain varying proportions of the active element. In this case it becomes quite important to know the relative magnitude of the surface represented by the active species only.

This evaluation of surface area measurement examines (1) the current status of technology for revealing total surface; (2) the capabilities for evaluating surface associated with micropores (here taken as having one dimension of 20 Å or less), mesopores (20 to 500 Å), and macropores* (>500 Å); and (3) the means for determining the surface area contribution of a particular component in a mixture of elements. No attempt is made to review in entirety the development of current ideas or to cite all major contributors to them. Rather, this approach is primarily directed toward practical problems of surface area evaluation and the significance of results and not toward the details of contending theories. Hopefully, enough reference information is included to facilitate further searching should the need arise. Instrumentation and methods are included only to the extent necessary to identify methods and to call attention to some of the newer developments and directions from which future advances are likely to proceed.

Gas Adsorption and Desorption

A fine particle revealing the major recognized structural characteristics is represented in Figure 1. It displays relatively large planar regions but also includes lattice distortions, dislocations, and a microcrack. Should a number of such

*Designations in accordance with Manual of Symbols and Terminology for Physicochemical Quantities and Units, Appendix II, Definitions, Terminology and Symbols in Colloid and Surface Chemistry, Adopted by International Union of Pure and Applied Chemistry, Washington, D. C., USA, 1971.

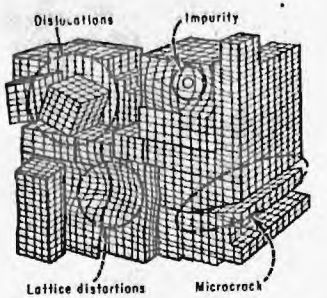

Figure 1. Particle Revealing Major Structural Characteristics

particles be joined, perhaps accompanied by partial fusion, it is easy to visualize a structure containing mesopores and macropores as well. Because surface area on the molecular level is the parameter in question, a logical "probe" with which it may be measured consists of gas molecules. Nitrogen gas is most frequently the vehicle used, although other gases may be employed as noted subsequently.

Total Surface

Nitrogen molecules are induced to attach, or adsorb, onto the exposed surface of a powder, especially when the powder temperature is reduced well below ambient. The process of attachment is conceived as one in which the molecules first cover the surface with a layer one molecule deep, then build to a second layer, and so on, as more and more gas is admitted. Actually, gas molecules do not behave quite so orderly. They may be expected to accumulate in somewhat less than representative amounts along exposed edges, in abnormally greater amounts along interior angles, and in either greater or lesser amounts where impurities protrude or where the lattice is otherwise distorted. Within a microcrack, gas molecules are exposed to attractive forces from several directions simultaneously and surely accumulate here in greater profusion than on a planar region. Excluding micropores for the present, the regions of abnormal adsorption are comparatively very small, and those surface portions having enhanced adsorptive activity are countered to a degree by regions of lower-than-average adsorptivity. The overall result is that adsorbing an inert gas, such as nitrogen, on a solid surface leads to the most widely employed and accepted measure of surface area available today.

Evidence that low temperature gas adsorption measurements yield surface areas upon which reliance can be placed comes from a number of sources. Confirmation is most directly obtained when particle area is calculated from electron microscopic size measurements on regular cubic or spherical particles. When this is done carefully and large numbers of particles are measured, the agreement of results is exceptionally good, many such determinations having been examined and tabulated /1,2/. Among other independent tests giving further confirmation may be mentioned, as

representive, those involving liquid phase adsorption /3/, surface energy /4/, and x-ray scattering /5/.

Total surface area determination by the gas adsorption method is most frequently accomplished according to a procedure generally referred to as the BET method, the designation deriving from the last names of its early proponents: Steven Brunauer, Paul Emmett, and Edward Teller. The powder to be evaluated is first subjected to heating and evacuation to remove gases and water vapor accumulated from atmospheric exposure. The cleaned material is then subjected in a stepwise manner to increasing pressures of nitrogen gas while held at the temperature of liquid nitrogen. Some of the gas effectively is removed from contributing to the pressure because of adsorption, or attachment to the solid surface. The volume V of this adsorbed gas per unit mass of powder at standard temperature and pressure conditions can be calculated from before- and after-exposure pressure measurements. Adsorbed volume plotted against the relative pressure P/P_s, where P is the measured equilibrium pressure following each stepwise addition of gas and P_s the saturation (or vapor) pressure of nitrogen, yields a BET adsorption isotherm. Reversing the procedure and removing gas from the powder surroundings in a stepwise manner while still at liquid nitrogen temperature yields a desorption isotherm. Figure 2 shows the development of a typical BET isotherm for a nonporous powder accompanied on the left by a pictorial representation of gas molecules (small circles) adsorbed on a solid surface. The isotherm on the right will be discussed subsequently.

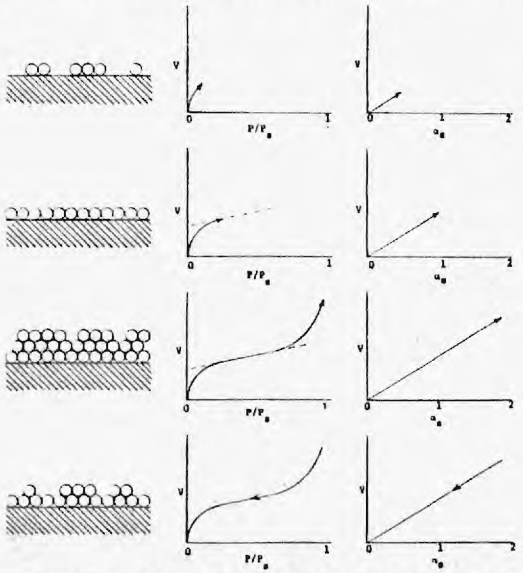

Figure 2. Low Temperature Nitrogen Adsorption and Desorption Isotherms on Nonporous Surface

The particular condition of interest at the moment is the second depiction of the BET adsorption isotherm where the surface is shown to be covered by a monomolecular layer of adsorbed gas. This condition is pictured as occurring just as a linear region of the isotherm begins forming. If the lowest asymptotic point to the linear region is taken as the condition of monolayer completion, the number of adsorbed gas molecules is readily calculated from the adsorbed volume V corresponding to the asymptote point. The specific surface of the solid, area per unit mass, can then be computed if a value is assigned to the area occupied by each gas molecule. For nitrogen the best evidence points to an average value of 16.2 $\AA^2$ per molecule /6/ as applicable to most powders.

Experimental evidence that the asymptotic point corresponded approximately to monolayer coverage was offered /7/ in the mid 1930's. Much effort since that time has been devoted to establishing this experimental observation on a sound theoretical basis. To date the two-constant adsorption isotherm equation /8/

$$\frac{P}{V\,(P_s - P)} = \frac{1}{V_m c} + \left(\frac{c - 1}{V_m c}\right) \frac{P}{P_s} \qquad (1)$$

is most widely accepted. Here V_m is the adsorbed gas monolayer volume, c a constant associated with the energy of adsorption, and other terms as previously defined. When data are plotted as $P/[V(P_s-P)]$ versus P/P_s a line having a linear region is obtained. From its slope and intercept the value of V_m (and c) is obtained which is more satisfactory than trying to locate the asymptote point.

Equation 1 was derived assuming, among other things, all adsorption sites energetically equal, no lateral interaction among adsorbed molecules, and an infinite number of adsorbed layers at a relative pressure of unity, none of which can be entirely accepted without reservation. Thus, questions remain about surface area evaluation because of these doubts and most likely will continue until theoretical difficulties are fully resolved. Nevertheless as noted above, a great many tests involving other lines of evidence confirm the results of BET surface area measurements. The theory may be less than satisfactory, but the practical result is one of the most reliable measurements in the entire field of particle technology.

As indicated on Figure 2, admitting additional gas beyond the monolayer condition gives rise to an adsorbed layer of increasing thickness. The statistical thickness of this layer on nonporous substances should be directly related to the available surface area if uniform stacking and packing of adsorbed molecules is assumed. From a number of measurements on different solids this appears to be approximately so, permitting the thickness of the layer t, in Angstrom units, to be described/9,10, 11/ by the relationship

$$t = 3.54 \left[\frac{5}{\ln (P_s/P)} \right]^{1/3} \qquad (2)$$

The fact that data involving different powders can be so represented with fair reliability has given rise to an empirical method of isotherm analysis known as the thickness method, or for short, the t-method/12/. Its use provides a simple and direct means for interpreting adsorption isotherms. If a plot of the volume of gas adsorbed by a powder versus the adsorbed layer thickness calculated from eq. 2 gives a straight line, the adsorbing powder is almost certainly nonporous. If, on the other hand, the line breaks or curves it is evidence there are pores or cracks in the sample which are filling as the relative pressure increases, and once filled, are removing a part of the surface from development of further layer thicknesses.

Another empirical approach giving insight into adsorption interpretation /13,14/ replaces thickness t by $V/V_{0.4}$, designated α_s, where $V_{0.4}$ is the volume of gas adsorbed at a relative pressure of 0.4, this being the condition near which monolayer coverage is usually complete. Values of α_s are established from data on a nonporous reference solid. Ideally, this solid should be identical, except for the absence of pores, to the powder with pores being investigated. This leads to the empirical adsorption isotherm equation /15/

$$S = 2.89 \frac{V}{\alpha_s} \qquad (3)$$

where S is the sample specific surface area in square meters per gram, V in units of cubic centimeters per gram at standard conditions, and the constant, 2.89, applies specifically to silica powders. Like the t-method of analysis, the α_s-method yields a linear plot of adsorbed gas volume versus α_s for nonporous materials and a plot with deviations from linearity when pores are present. The values of V and α_s plotted are at the same relative pressure, adsorbed volumes V being taken from experimental measurements and α_s values from previously established data for the non-porous reference solid. Equation 3 is the basis for the plots on the right of Figure 2; when a straight line results, as illustrated, the powder is not porous and its surface area is simply obtained as the product of the constant and the slope of the line. The utility of α_s plots will be explored further later.

Differing requirements in speed of analysis, absolute accuracy, particle pretreatment, and the like, have resulted in numerous modifications of the basic BET technique. Volumetric measurements, as outlined above, are most widely used because they generally give the best combination of accuracy, rapidity, and reliability. Gravimetric measurements on high surface powders where the weight of the adsorbed gas is comparatively large are most accurate, but making the measurements generally requires longer to accomplish and demands greater operator care and attention. Modified gas chromatographic systems using mixed gases, perhaps a few percent of

nitrogen in helium (assumed non-adsorbing at liquid nitrogen temperature), are relatively rapid but they require calibration. Commercialization is such that it is now possible to obtain a completely computer controlled instrument capable of directing the previously described tests, calculating surface areas, plotting isotherms, and making all of the other analyses as described later.

Gases other than nitrogen are also employed satisfactorily. Krypton and argon are used at liquid nitrogen temperature. Krypton gives more reliable results than nitrogen with low surface powders in volumetric systems because lesser quantities of it remain unadsorbed due to its low saturation pressure. Carbon dioxide adsorption at room temperature is being increasingly used. Butane at ice-water temperature and propane at 20°C are other possible combinations. At these latter temperatures chemical reactions, giving what is termed chemisorption, are increasingly likely, so checking of surface area values with low temperature tests is essential.

Micropore Surface

The preceding excluded from discussion powders with pores. Nitrogen adsorption isotherms for a microporous material, i.e., one with cracks less than 20 Å wide, typically appear as shown by Figure 3, which again attempts to depict a surface structure and to show the corresponding BET and α_s-isotherm development. The typical BET isotherm rises rapidly at low relative pressure and then rises little more even at high relative pressures. The α_s isotherm also rises rapidly at first and may go through one or more slope changes.

At one time it was thought surfaces containing micropores sufficiently wide to accommodate only one molecular layer on each wall accounted for the observed measurements, and surface areas could be calculated by taking the plateau of the BET isotherm as representing completion of monolayer formation. Once these cracks filled, less surface remained for subsequent layer development, hence the BET isotherm would be expected to rise rapidly at first and then more slowly later as it does. When this interpretation was applied to activated carbons, however, it led to such high specific surface areas that fully 90% of all the carbon atoms would have to have been exposed in the surface /1/, a requirement that cannot be reconciled with mechanical and other properties. The interpretation requiring single layer formation in cracks thus was revised /16/, and now the interpretation favored is a surface containing micropores which can be several molecular diameters wide and which readily fill with the adsorbing gas in a liquid-like state well before exterior regions complete monolayer formation. The isotherm plateau according to this picture cannot represent single layer formation since it includes micropore filling.

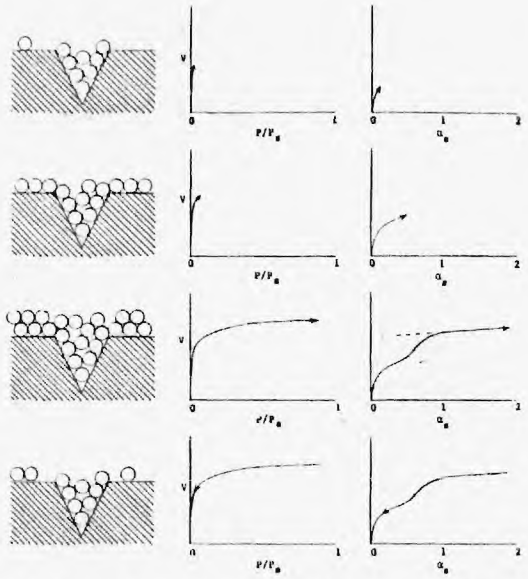

Figure 3. Low Temperature Nitrogen Adsorption and Desorption Isotherm on Microporous Surface

The term "liquid-like" is employed here to signify that considerable uncertainty exists regarding the true state of the micropore-adsorbed phase. It is unlikely to behave as a true liquid and exhibit a meniscus, for example, as does a liquid in a larger capillary tube because of the relatively small number of molecules in its exposed surface. It appears evident, however, that within a micropore the forces exerted on a gas molecule giving rise to adsorption are enhanced because of the nearness of the walls. Calculations of the magnitude of this enhancement are not precise in view of the obvious uncertainties, but the evidence /17/ indicates it must amount to a several fold increase in adsorption forces and overshadow the forces exerted by a plane surface.

At the present time there is no certainty as to where along an adsorption isotherm the walls of the micropores first become covered with adsorbed molecules, but it probably occurs while both isotherm curves of Figure 3 are nearly vertical. The first bends of the isotherms very likely represent the filling in of interior micropore spaces and, possibly, the beginning of significant external surface coverage. Subsequent, more nearly horizontal portions of the isotherms represent multilayer development on the surface external to the micropores. Once multilayer formation begins on the external surface, eq. 3 might be expected to apply. Thus the slope V/α_s of the line segment of the upper linear region of an α_s isotherm

multiplied by the equation constant may give as reliable a value for the external surface area of a microporous powder as is currently obtainable. The internal, or micropore, area is not presently determinable from gas adsorption measurements nor can the total surface area be reliably obtained. Accepting the plateau value from a BET isotherm as representing monolayer completion results in an excessive total surface area value, but just how excessive is uncertain, since this depends on the number and relative size of the micropores.

Values for the constant of eq. 3 of known applicability to specific types of material are presently limited. There needs to be more investigation with a variety of powders. The suggestion has been made /15/ that useful information relative to micropore size and area might be obtained from a series of adsorption tests using vapors with different molecular sizes. The apparent surface area registered would be expected to diminish as molecular size increased, ultimately attaining the external surface area when the adsorbing molecules could no longer penetrate any of the micropores. Low-angle x-ray scattering, as discussed later, may ultimately bring forth further information.

Mesopore Surface

Adsorption isotherms for powders having within their structure mesopores may reveal still different characteristics as shown on Figure 4. To a relative pressure of about 0.4 or an α_s of approximately unity nitrogen isotherms for nonporous, mesoporous, and macroporous (but not microporous) powders are essentially indistinguishable, so total surface areas are obtained as described above, viz., by eq. 1 or perhaps eq. 3.

The upper regions of the isotherms of Figure 4 showing hysteresis, or divergence in the adsorption and desorption branches, contain the information relating to mesopore surface area. Here the isotherm shape and position are related to pore geometry by condensation and evaporation phenomena as described generally by the Kelvin capillary condensation equation/18/

$$\ln (P/P_s) = \frac{-2\gamma V \cos \theta}{RT\, r_m} \qquad (4)$$

where γ is the liquid surface tension, V the molar volume of the condensed phase, θ the contact angle between liquid and solid surface (assumed zero in the case of condensed nitrogen), R the gas constant, T the absolute temperature, and r_m the mean radius of the liquid meniscus related to the two main radii of the liquid surface in a straight capillary r_1 and r_2 by

$$\frac{2}{r_m} = \frac{1}{r_1} + \frac{1}{r_2} \qquad (5)$$

These radii are indicated on Figure 4 for a straight cylindrical mesopore. As shown to the left of the figure, only one radius r_1 along the longitudinal axis is thought

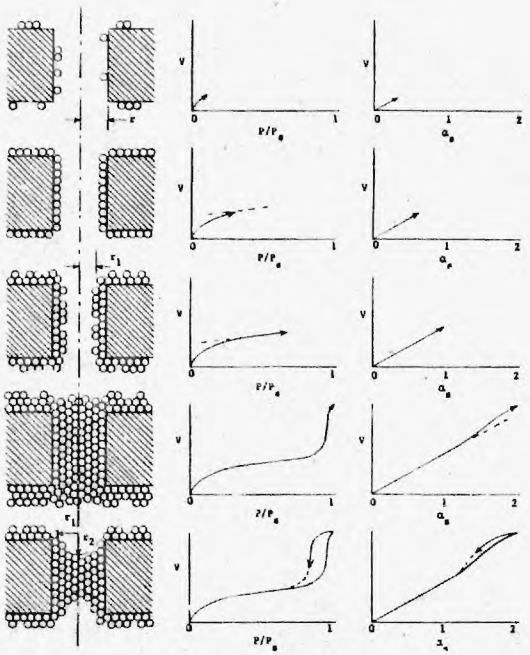

Figure 4. Low Temperature Nitrogen Adsorption and Desorption Isotherms on Mesoporous Surface

to control condensation (adsorption branch of isotherm) while the two radii r_1 and r_2 are equal and both operative in regulating evaporation (desorption branch). From this and from eq. 5 it can be seen that a cylindrical mesopore open at both ends should fill with condensate when $r_m = 2r_1$, since $r_2 = 0$, and empty when $r_m = r_1 = r_2$. No pore is completely empty when condensation begins nor entirely empty when its condensate is lost because of the layer of adsorbed molecules on its walls /19/, this adsorbed layer thickness t presumably being given by eq. 2. The mesopore radius r can thus be calculated using data from the adsorption branch of the isotherm if eq. 4 is rewritten

$$\ln (P/P_s)_a = - \frac{\gamma V}{RT(r - t)} \qquad (6)$$

or from desorption data by

$$\ln (P/P_s)_d = - \frac{2\gamma V}{RT(r - t)} \qquad (7)$$

if the pores indeed are open-ended and cylindrical.

A pore structure such as depicted in Figure 4 is quite unique although it is approximated by synthetic chrysotile /20/. Very recently Dr. Albert A. Liabastre and the writer have collaborated on an investigation* of adsorption phenomena using specially prepared polycarbonate film. Preliminary results indicate this film has 10^9 to 10^{10} holes/cm^2 in a rather narrow distribution centered at about 125 Å radius. With larger holes this film is marketed for filtration uses under the tradename Nuclepore.** Electron microscopic examination of hundreds of holes established the size, and microtomed cross-sections proved them to be essentially round, straight-walled, and about 200 times as long as wide. The low-temperature adsorption and desorption isotherms obtained*** with this film and nitrogen gas are presented as Figure 5. The same distribution of pore radii within experimental error is obtained from either branch of the isotherm using, as appropriate, eqs. 6 and 7, and this distribution corresponds very well with that obtained by electron microscopy. This is the most direct and convincing evidence of the correctness of the condensation-evaporation theory as outlined of which the writer is aware.

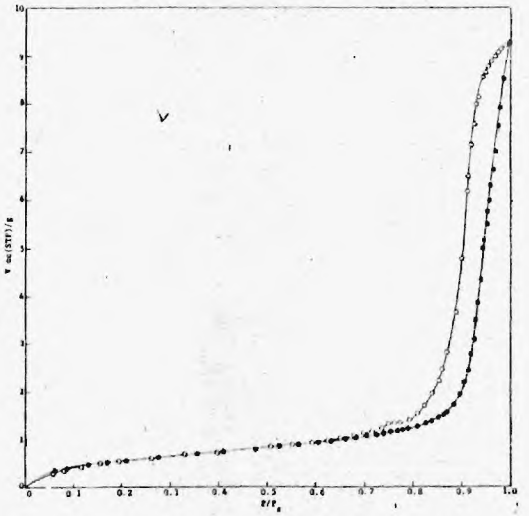

Figure 5. Low Temperature Nitrogen Adsorption and Desorption with Cylindrical Mesopores

Calculating mesopore sizes from adsorption and desorption data and from pore sizes their surface area is straightforward for a regular pore geometry. These computations as well as those for other pore geometries, actual or assumed, are conveniently performed in a stepwise manner, beginning at a high relative pressure. The volume of

*Support from NASA, grant No. NSG-2004, and NSF, grant No. GK-43616.

**Nuclepore Corp., Pleasanton, California, USA.

***Using Model 2500 DIGISORB, Micromeritics Instrument Corp., Norcross, Georgia, USA.

gas either adsorbed or desorbed within an increment of relative pressure on a BET isotherm is taken from the ordinate and either eqs. 6 or 7 is applied to find the corresponding mesopore radius using eq. 2 to establish adsorbed layer thicknesses. Details of the calculation can be found in a number of publications /11,21,22/. Once mesopore area is determined, the external area is, of course, the difference between that and the total surface area as obtained from the lower relative pressure region of the isotherm.

The presence of hysteresis on an isotherm plot is indicative of mesopores but, unfortunately, it alone is not sufficient evidence to prove their presence. If the pores of Figure 4 had been closed with one hemispherical end, the filling and emptying processes would be expected to be identical and no hysteresis would be evident. The pores would fill from the open end and empty the same way. The liquid meniscus would remain hemispherical with $r_m = r_1 = r_2$, meaning that eq. 7 would be applicable for calculating pore radii. Indiscriminate application of eq. 7 can lead to difficulties, however. It should be apparent that calculations giving pores sizes and surface areas can be carried out even when no pores exist, or, if hysteresis is demanded as evidence of mesopores, then a material with pores closed at one end might be characterized as nonporous. Conical, wedge, and certain other closed-end mesopore geometries also yield isotherms without hysteresis /23/. The only safe practice for establishing the presence or absences of pores in these cases is to resort to microscopic examination or to a mercury penetration test as described later.

Hysteresis is not confined only to pores open at two ends. It can also arise from mesopores having entry cross-sections smaller than cavities to which the entrances connect. Such mesopores are expected to fill at a relative pressure determined by their greatest radius and to empty at a lesser relative pressure established by the entry passageway. Obviously, many geometrical pore situations involving interconnections, convolutions, and twisted and turning passages can be envisioned that would produce hysteresis in this manner. In these cases, some evidence of mesopore structure may be gleaned from the particular shape and relative position of the adsorption and desorption branches of the isotherm by comparison with theoretical analyses applying to specific geometries /24/, but no such test can establish uniquely the actual structure or surface area.

Considerable debate has appeared in the technical literature over whether the adsorption or desorption branch is preferable for calculating mesopore sizes and surface areas for powders. Clearly, with unknown pore shapes the answer cannot be supplied until pore geometry is resolved. Then, if the shape can be adequately described mathematically in terms of the Kelvin equation, it makes no difference. Both adsorption and desorption data should give the same result as was the case for the polycarbonate material having right-cylinder mesopores.

While very good agreement between theory and experiment is possible for specific mesopore shapes, the necessity of a pore model in order to reduce to usefulness data relating to unknown pore geometrics poses a severe practical limitation. Also the range of pore sizes (approximately 20 to 500 Å) over which the technique can be applied is restrictive. Furthermore, obtaining the data and making the computations is tedious and time consuming unless automation and computer programming is available. The net result, presently, is that definitive mesopore surface area information is likely only to be obtained with considerable effort and a good bit of luck in finding, perhaps with the aid of microscopic examination, an appropriate pore model. If a cylindrical, slit, or other pore shape is unrealistically assumed, as is very often the case, the results may very well create more confusion that insight. For example, the mesopore surface area in such situations is frequently computed to exceed the total surface area, an obvious impossibility. Much remains to be resolved before mesoporous powder surface characteristics can be completely determined.

Pore Surface from Mercury Penetration

Mercury, a nonwetting liquid for most solids, penetrates into holes of 90 μm radius when driven by a pressure of about 3 kg/cm^2 and into 17 Å radius holes under a pressure of nearly 1.5×10^5 kg/cm^2. Thus, if a porous powder after evacuation, is inundated with mercury and pressure P is applied, the mercury will be forced into pores of radius r in accordance with/25/

$$Pr = -2\sigma\cos\theta \qquad (8)$$

where σ is the mercury surface tension and θ the advancing contact angle between mercury and solid. The technique, involving simultaneous measurements of the applied pressure and the intruded volume, is widely employed in assessing pore dimensions. It is recommended as one means for establishing whether or not a powder showing no adsorption-desorption hysteresis, as discussed above, actually has pores or is truly nonporous. It can also be employed for evaluating pore surface area. Again a pore model must be employed.

If the pores are assumed cylindrical, the product of the pressure P and the intruded mercury volume dV gives the work required to bring about intrusion which is related to the mercury surface area dS thereby created through /26/

$$P\,dV = -\sigma\cos\theta\,dS \qquad (9)$$

Taking σ and θ as invariant with pressure, eq. 9 becomes simply

$$S = B\int_{V_2}^{V_1} P\,dV \qquad (10)$$

where B is a constant with magnitude depending on the values of σ and θ. The quantity $\int PdV$ may be obtained by graphical integration of a porosimeter curve, the plot of P versus V. The surface area S is that of the mercury extending into pores of radius r as defined by eq. 8, which presumably, is equal to that of the pore walls. Pore surfaces attributable to various radii ranges can be obtained by selection of integration limits, and geometrical models other than the right-cylinder one may be applied through appropriate alteration of the above equations.

The technique as outlined is not appropriate when reentrant pores exist. In this case, porosimeter curves with both increasing and decreasing pressures can be obtained and a scanning analysis applied /27/. However, at the present time the influence of advancing and receding contact angles, which can be quite different, is not clear in such an analysis, and the scanning techniques has not been demonstrated rigorously to apply. Particle and pore distortion because of the high pressures involved is potentially a problem /28/, and restricts use of the method. Nevertheless, mercury penetration testing is recommended as an adjunct to gas adsorption-desorption in establishing conclusively the presence or absence of pores and in supplying information about probable pore surface area.

Liquid-Phase Adsorption

The adsorption (or sorption, as the phenomenon is sometimes termed) of a substance such as a dye or iodine dissolved in a liquid onto the surface of an immersed powder is frequently suggested as a simple means of surface measurement. In most instances this is not so. Unlike volumetric or gravimetric gas adsorption where only one molecular species is available for adsorption, there is in liquid adsorption competition between solvent and solute molecules for the surface with the result that monolayers composed largely of one molecular species are achieved only when the solute has a considerably greater affinity than the solvent for the surface. Also both the orientation upon adsorption and the area occupied by solute molecules are influenced by concentration and probably by other factors. There are situations, however, in which liquid-phase adsorption can be appropriate and useful.

One of these is in evaluating carbon black intended for rubber reinforcing, particularly in correlating the surface area of the carbon black with automobile tire treadwear. Many carbon black particles contain micropores too small for rubber molecules to penetrate, so gas adsorption results can be grossly misleading. In this case the appropriate parameter is the external surface only of the carbon black. This external surface might be determined by the α_s-method described previously, but the adsorption of certain surfactants from aqueous solution is faster and involves simpler equipment /29,30,31/. One such surfactant is cetyltriethylammonium bromide (CTAB). Its adsorption on carbon black yields an isotherm having a nearly horizontal plateau much like the BET one on Figure 3 when the amount of adsorbed solute is plotted versus relative concentration, the actual concentration divided by the

concentration at saturation. Here, however, the plateau region represents primarily monolayer coverage of the external surface because the CTAB molecules are larger than micropore widths and solute adsorption is much favored over solvent adsorption.

Carbon black is equilibrated with an aqueous solution of CTAB, the black is removed by centrifugation, and the equilibrium liquid is analyzed for unadsorbed surfactant. The difference in initial and final concentrations along with carbon black weight and CTAB molecule size information permits specific surface area to be calculated. Results so obtained agree reasonably well with surfaces calculated from electron microscopic sizes which do not bring micropores into consideration.

In general, liquid-phase methods are recommended only when dictated by other considerations such as temperature instability. The chemical p-nitrophenol might be suggested as the solute for beginning any liquid-phase adsorption exploration. This compound dissolves in both water and organic solvents, its concentration in solution is readily detected colorimetrically, and it has been shown to give fairly reliable surface areas with several powders /32,33/. For compounds not detectible by a simple colorimetric or a straightforward titration analysis, resort to microcalorimetry /34,35/ or a variety of infrared and ultraviolet analyses may be justified. It is possible with materials having a range of pore sizes that the surface contributions of the various pores can be estimated by a repetition of tests employing solute molecules of increasing dimensions, there having been instances/36/ where this procedure has yielded significant information. Small changes in both solvent and solute purity can drastically alter results, so composition needs to be carefully controlled in liquid-phase testing. Liquid-phase adsorption must be regarded as a secondary method for surface area evaluation at this time, and,when possible,results should be correlated with another method, preferably gas adsorption.

Surface Area by Permeametry

No review of surface area determination would be complete without mention of permeametry. In this technique a dry gas is caused to flow through a packing of compressed powder and surface area information is deduced from measurements of flow rate and pressure loss. When conditions are such that viscous flow prevails, the results, at best, are indicative of a surface corresponding to a hypothetical smooth envelope engulfing each particle, but, more likely, they indicate only a relative degree of fineness. Using a gas such as helium under reduced pressure conditions where Knudsen flow predominates, more influence is registered by the particle surface structure on the flow. Consequently, Knudsen-flow results correspond relatively closely to gas adsorption measures of surface area when the particles are nonporous /37,38/. Surface areas appear to be satisfactory with powders having some porosity /39,40/ but permeametry cannot be expected to indicate reliably powder areas under all circumstances.

Establishing Knudsen flow conditions requires a powder to be evacuated initially nearly as well as for a gas adsorption test, so making a complete permeametric measurement is at least as time consuming as a gas adsorption analysis. There seems to be no advantage to be gained by use of low-pressure permeametry.

Surface Area by X-ray Scattering

Low-angle x-ray scattering has been little used for surface area assessment, but its potential appears promising, especially when rapidity of analysis is important. X-rays are partially deflected through small angles when they encounter an electron density change as they do upon passage through powders. The resulting scatter is related theoretically to surface area/41,42/ through measurements of the intensity of the undeflected portion of the x-ray beam and the energy scattered out to approximately 5^{o} /5,43/. Such calculations require property data not readily available or easily acquired for many materials, however.

An alternate technique is to relate the deviated beam intensity for a powder of unknown surface area to that of another powder having had its surface area established by prior gas adsorption measurement. Plots of x-ray intensity versus angle for two chemically identical powders adjusted in quantity for identical main-beam absorption should appear as in Figure 6, with the two curves revealing a region where intensities bear a constant ratio to one another. This intensity ratio appears also to be the ratio of surface areas /44/. Once complete scanning curves establish both the angular region of constant ratio for a powder and the intensity curve for the reference sample, only the intensity at one angle within the region must be determined for the unknown powder to arrive at its surface area. Analyses may thereafter be accomplished routinely in a few minutes. This technique needs evaluation. It obviously will not be applicable where the chemical composition of a powder varies significantly from that of the standard to which it is referenced.

Chemisorption

Chemisorption is utilized when it is desired to identify that proportion of a powder surface having a particular characteristic or property. In contrast to adsorption where conditions are chosen to promote multimolecular layer formation and condensation, chemisorption is deliberately conducted to induce the formation of specific chemical bonds which restrict molecule attachment to a single molecular layer on particular reaction sites. Liquid-phase as well as gas-phase chemisorption might be employed, but practice is almost entirely restricted to gas chemisorption. The gases generally employed -- hydrogen, oxygen, carbon monoxide, ammonia, etc.-- are selected because they are very reactive rather than nearly inert like nitrogen, krypton, and argon.

Catalysts constitute the primary materials for which identifying the active surface area apart from the total surface is important. A typical example might be a silica

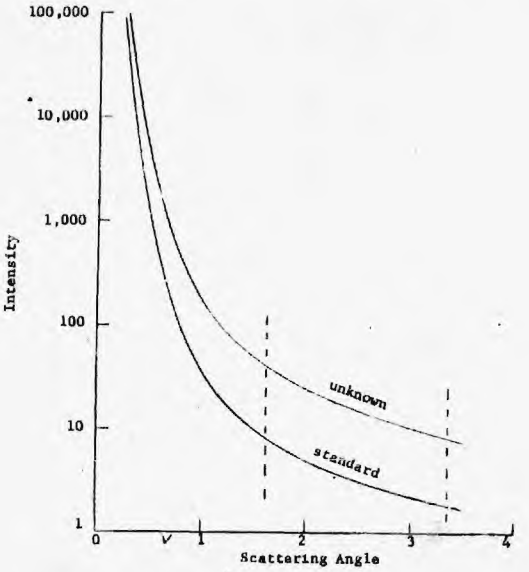

Figure 6. Low-Angle X-ray Scattering.

base incorporating a small percentage of platinum. Ideal partitioning of these components would place all the platinum in the exposed surface and have the silica serve only as a support. Practical catalysts exhibit both components in the surface, hence their proportion is of significance.

Conditions for a chemisorption evaluation are selected to maximize bonding of the reacting gas, e.g., carbon monoxide, wherever the active agent, perhaps platinum, is exposed and minimize its attachment at the inactive, say silica, regions. The fraction of the surface composed of platinum can then be established from the amount of carbon monoxide uptake since the total surface, consisting of both platinum and silica, can be determined by the low temperature adsorption of an inert gas, perhaps nitrogen.

Instrumentation as employed for previous adsorption analyses is basically applicable for chemisorption use provided it incorporates elevated temperature capability. In a typical experiment, the catalyst is first evacuated while being heated. Then hydrogen gas is usually passed over it for several hours with the catalyst at 400 to $450^{o}C$ to ensure the reduction of all exposed metal, after which the catalyst is again thoroughly evacuated. The temperature is now lowered, perhaps to $200^{o}C$, and a carbon monoxide isotherm is determined by admitting this gas in increments and

recording equilibrium pressures and gas uptakes. Until metallic surface atoms are completely reacted, there is little rise in equilibration pressure and a plot of gas volume chemisorbed versus equilibrium pressure is much like the adsorption isotherm of Figure 3 except the vertical portion of the curve is even steeper, the change of curvature more abrupt, and the plateau almost totally horizontal. There is little adsorption of gas at 200°C, and carbon monoxide and silica have little tendency to react. Thus the volume of carbon monoxide taken up is due almost entirely to monolayer chemisorption on the platinum. The surface contributed by platinum is computed from the carbon monoxide uptake volume. Basically the same general procedure is followed regardless of the active component and the particular gas; platinum and carbon monoxide are used here only as possible examples.

The bonding arrangement of gas to metal presents a complication, however. The effective area occupied by a chemisorbed gas may be one atom to one surface atom or there may be a sharing of each gas molecule through weak and strong bonds to surface atoms. Several types of bonding, for example, are possible for carbon monoxide on an alumina-supported nickel catalysts depending on the nickel content and the fractional coverage of the carbon monoxide /45/. By way of illustration, the area of platinum equivalent to one hydrogen molecule has been reported/46/ as 22.4 $Å^2$ but only 12.3 $Å^2$ for nickel /47/. Carbon monoxide coverage on platinum has been put at 17.8 $Å^2$ /48,49/.

Surface coverage values such as the above are determined by low-temperature BET measurements using a pure metal powder or thin metal film and following with chemisorption tests on the same powder or film. In this manner information such as 0.27 cm^3 (STP) of chemisorbed oxygen corresponds to 1 m^2 of silver surface has been developed /50/. Basic chemisorption background data are generally so reported and so used today. When the active component is itself a combination of elements, detailed studies may be needed to arrive at the effective coverage value.

Conclusions

The total surface area of a powder, except when the particles contain micropores, can be arrived at reliably by BET measurements even though a completely satisfactory theoretical explanation has not been achieved. Liquid-phase adsorption and Knudsen flow permeametry are sometimes applicable to total surface evaluation, but their reliability must be established by other testing, notably by BET, and usually then have little to recommend their use. Low angle x-ray scattering may offer a real saving of analysis time once the standard for comparison has been established. Potentially, x-ray scattering measurements can include the area contribution of micropores, but this capability is dependent on the availability of a chemically identical reference standard.

Micropore surface area is presently not determinable with any degree of certainty.

The low temperature adsorption of gases having differing molecule sizes remains to be demonstrated as applicable for resolving micropore surface contribution. The extremely high pressures required renders mercury penetration suspect where micropores are involved because of the possibility of pore distortions, and x-ray scattering has yet to be confirmed as a means for including micropores.

The Kelvin capillary condensation and evaporation equation provides a firm foundation for mesopore surface area measurement, and results are satisfactory when the pore geometry is known and rigorously describable. Under other circumstances, results are dependent on the applicability of the pore model. Mercury penetration surface evaluations are also limited to the reliability of model representation. Liquid-phase adsorption using solute molecules of differing sizes may occasionally permit obtaining information of value.

External surface area may be established apart from internal surface area when the internal surface is confined to micropores by the liquid-phase adsorption of solute molecules larger than micropores; at least this appears to be rather well established in the case of microporous carbon. The surface external to micropores can also be estimated with data from the multilayer region of an α_s isotherm. With larger pores, the external surface is best computed by subtracting the pore area determined by one or more of the other applicable techniques from the total surface area.

Specific-component surface representation is determinable by chemisorption if attention is given to the mode of attachment of the chemisorbed molecule to the active component, or components, of the surface.

References

/1/ S. J. Gregg
and K. S. W. Sing: Adsorption, Surface Area and Porosity, Academic Press, London, 1967.

/2/ C. Orr, Jr.
and J. M. DallaValle: Fine Particle Measurement, Macmillan, New York, 1959.

/3/ H. A. Smith
and J. F.Fuzek: J. Am. Chem.Soc. 68 (1946) 229.

/4/ W. D. Harkins,
and G. Jura: J. Chem. Phys. 11 (1943) 431.

/5/ A. Reynouprez: Surface Area Determination (D. H. Everett and R. H. Ottewill, eds.), Butterworths, London (1970) 361.

/6/ A. L. McClellan
and H. F. Harnsberger: J. Coll. & Interface. Sci. 23 (1967) 577.

/7/ S. Brunauer
and P. H. Emmett: J. Am. Chem. Soc. 59 (1937) 2682.

/8/ S. Brunauer
P. H. Emmett and E. Taller: J. Am. Chem. Soc. 60 (1938) 309.

/9/ J. H. DeBoer,
B. C. Lippens and B. G. Linsen: J. Catalysis 3 (1964) 36.

/10/ J. H. DeBoer,
B. G. Linsen and Th. J. Osinga: J. Catalysis 4 (1965) 643.

/11/ D. Dollimore
and G. R. Heal: J. Coll & Interface Sci. 33 (1970) 508.

/12/ B. C. Lippens
and J. H. deBoer: J. Catalysis 4 (1965) 319.

/13/ K.S.W. Sing: Chem. & Ind. (1968) 1520.

/14/ K.S.W. Sing: Surface Area Determination (D. H. Everett and R. H. Ottewill, eds.), Butterworths, London (1970) 25.

/15/ M. R. Bhambhani,
P. A. Cutting, K.S.W. Sing and D. H. Turk: J. Coll. & Interface Sci. 38, (1972) 109.

/16/ C. Pierce
J. W. Wiley and R. N. Smith, J. Phys. Chem. 53, (1949) 669.

/17/ P. J. Anderson
and R. F. Horlock: Trans. Faraday Soc. 65 (1969) 251.

/18/ B. G. Linsen
and A. van den Heuvel: The Solid Gas Interface, 2 (E. A. Flood, ed.) Dekker, New York (1970) 1025.

/19/ D. H. Everett
and J. M. Haynes: Colloid Science 1 (1973) 123.

/20/ J. J. F. Scholten
A. M. Beers, and A. M. Kiel: J. Catalysis 36 (1975) 23.

/21/ D. Dollimore
and G. R. Heal: J. Appl. Chem. 14 (1964) 109.

/22/ B. F. Roberts: J. Coll. & Interface Sci. 23 (1967) 266.

/23/ R. M. Barrer,
N. McKenzie and J.S.S. Reay: J. Coll. Sci. 11 (1956) 479.

/24/ D. H. Everett: The Structure and Properties of Porous Materials (D. H. Everett and F. S. Stone eds.) Butterworths, London (1958) 95.

/25/ H. L. Ritter
and L. C. Drake: Ind. Eng. Chem., Anal. Ed. 17 (1945) 782.

/26/ H. M. Rootare
and C. F. Prenzlow: J. Phys. Chem. 71 (1967) 2733.

/27/ M. Svatá: Powder Tech. 5 (1971/72)345.

/28/ D. J. Baker
and J. B. Morris: Carbon 9 (1971) 687.

/29/ T. G. Lamond
and C. R. Price: Rubber J. 152 (1970) 49.

/30/ H. Arai
and K. Yoshizaki: J. Coll. & Interface Sci. 35 (1971) 149.

/31/ J. Janzen
and G. Kraus: Rubber Chem. Tech. 44 (1971) 1287.

/32/ C. H. Giles
T. H. MacEwan, S. N. Nakhawa and D. Smith" J. Chem. Soc. (London) (1960) 3973.

/33/ C. H. Giles
and S. N. Nakhwa: J. Appl. Chem. 12 (1962) 266.

/34/ C. E. Templer: Particle Size Analysis (M. J. Groves and J. L. Wyatt-Sargent eds.), The Society for Analytical Chemistry, London (1972) 301.

/35/ T. Allen
and R. M. Patel: Particle Size Analysis (1970)(M. J. Groves and J. L. Wyatt-Sargent eds.), The Society for Analytical Chemistry, London (1972) 311.

/36/ C. H. Giles
A. P. D'Silva and A. Cameron: Chem. & Ind. (1969) 239.

/37/ G. Kraus
and J. W. Ross: J. Phys. Chem. 57 (1953) 334.

/38/ C. Orr, Jr.: Anal. Chem. 39 (1967) 834.

/39/ J. F. Brock
and C. Orr, Jr.: Anal. Chem. '44 (1972) 1534.

/40/ N. C. Stanley Wood
and A. Chatterjee: Powder Tech. 9 (1974) 7.

/41/ G. Porod: Kolloid Zeit. 124 (1951) 83.

/42/ E. D. Eanes
and A. S. Posner: The Solid-Gas Interface 2 (E. A. Flood, ed.) Dekker, New York (1967) 975.

/43/ D. N. Winslow
and S. Diamond: J. Am. Chem. Soc. 57 (1974) 193.
/44/ R. A. Van Nordstrand
and K. M. Hack: Presented, Division of Petroleum Chemistry, American Chemical Society, Chicago, Illinois, USA, Sept. 9-11 (1953).
/45/ J.T. Yates
and C. W. Garland: J. Phys. Chem. 65 (1961) 617.
/46/ C. R. Adams,
H. A. Bonesi, R. M. Curtis and R. G. Mersenheimer: J. Catalysis 1 (1962) 336.
/47/ O. Beeck: Advances in Catalysis 2, Academic Press, New York (1950) 151.
/48/ O. Beeck
and A. W. Ritchie: Disc. Faraday Soc. 8 (1950) 159.
/49/ J. R. Anderson
and B. G. Baker, J. Phys. Chem. 66 (1962) 482.
/50/ J. J. F. Scholten,
J. A. Konvalinka and F. W. Beekman: J. Catalysis 28 (1973) 209.

Der derzeitige Stand der Methoden zur Bestimmung von Pulver-Oberflächen*

Clyde Orr**

Bis heute läßt sich die Oberfläche disperser Feststoffe nur angenähert bestimmen. So wird die Zuverlässigkeit von Oberflächenmessungen im wesentlichen durch strukturelle Merkmale wie Mikrobrüche und Poren in den Partikeln bestimmt. Es werden brauchbare Methoden für die Messung der Oberfläche von nichtporösen Partikeln und von Partikeln mit relativ großen Poren besprochen. Weist der Feststoff Mikrobrüche auf, so kann nur die äußere Oberfläche mit bekannten Methoden ermittelt werden. Der Beitrag von Poren mittlerer Größe zur Oberfläche läßt sich bestimmen, wenn Annahmen über die Form der Poren gemacht werden. In allen anderen Fällen ist nur eine Schätzung möglich. Oberflächengebiete einer bestimmten spezifischen Zusammensetzung lassen sich nur bestimmen, wenn diese sich in ihrer chemischen Aktivität beträchtlich unterscheiden.

In Pulvern befindet sich ein relativ großer Teil der Atome an der oder nahe der Oberfläche. Dies führt dazu, daß sich die Eigenschaften von Pulvern erheblich von den Eigenschaften des gleichen Materials in kompakter Form unterscheiden, und zwar in Abhängigkeit von der Größe der Oberfläche. Feinverteilte Stoffe sind erheblich reaktiver als dasselbe Material in kompakter Form. Sie zeigen eine verbesserte Löslichkeit und sintern bei niedrigeren Temperaturen. Weiterhin weisen sie eine größere Adsorptionskapazität auf und eine größere katalytische Aktivität. Der Einfluß der Oberflächengröße ist in manchen Fällen so ausgeprägt, daß sie beinahe ebenso wichtig ist wie die chemische Zusammensetzung. Bei der Verstärkung von Elastomeren ist z. B. die Größe der spezifischen Oberfläche in erster Näherung genauso wichtig wie die Art des verwendeten Füllstoffs (Kohlenstoff, Siliciumdioxid, Calciumcarbonat).

Die Größe der Oberfläche ist jedoch nicht das einzige wichtige Kriterium. In der Oberfläche der einzelnen Partikeln können sich z. B. Mikrorisse befinden. Größere Partikeln und Partikelagglomerate weisen häufig Poren und größere Spalten auf. Bei der Bestimmung der Oberflächengröße müssen diese strukturellen Merkmale berücksichtigt werden und weiterhin auch die Zugänglichkeit der Oberfläche. Ein Oberflächen-Katalysator ist z. B. nur wenig leistungsfähig, wenn ein großer Teil seiner Oberfläche nur über enge Passagen zugänglich ist, durch die die reagierenden Species und Reaktionsprodukte diffundieren müssen.

Weiterhin kann die Oberfläche von Partikeln, die aus zwei oder mehr chemischen Substanzen, wie z. B. ein Träger-Katalysator (reaktives Metall und inerte Trägersubstanz) bestehen, wechselnde Anteile des aktiven Elements enthalten. In diesem Fall ist es außerordentlich wichtig, den Oberflächen-Anteil der aktiven Komponente zu kennen.

Im folgenden werden die nachstehenden Gesichtspunkte behandelt: 1) der derzeitige Stand der Methoden zur Bestimmung der Gesamtoberfläche; 2) die Möglichkeiten zur Bestimmung von Oberflächen mit Mikroporen (Durchmesser $\leqslant 20$ Å), Mesoporen (20 bis 500 Å) und Makroporen[1] (>500 Å); und 3) die Verfahren zur Bestimmung des Oberflächen-Anteils einer speziellen Komponente. Es wird nicht versucht, sämtliche Methoden umfassend und ins Detail gehend zu behandeln. Im Mittelpunkt der Überlegungen stehen die praktischen Probleme bei der Bestimmung und Abschätzung der Oberflächen-Größe und die Bewertung der Ergebnisse, keinesfalls jedoch Details von miteinander konkurrierenden Theorien. Der Aufsatz enthält zahlreiche Literaturhinweise für die Untersuchung weitergehender Fragen. Geräte und Methoden werden nur soweit behandelt, wie es nötig ist, um die Methoden zu verstehen und die Aufmerksamkeit auf einige neuere Entwicklungen zu lenken, die in Zukunft vermutlich an Bedeutung gewinnen werden.

Gas-Adsorption und -Desorption

Ein Teilchen mit mehreren charakteristischen Strukturfehlern ist in Abb. 1 abgebildet. Es zeigt relativ große ebene Bereiche, weiterhin Gitter-Deformationen, Versetzungen und Mikrorisse. Wenn sich mehrere derartige Partikel zusammenlagern, gegebenenfalls unter teilweisem Verschmelzen, kann man sich leicht vorstellen, daß eine Struktur mit Mesoporen

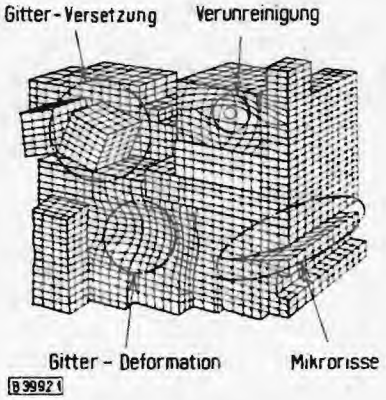

Abb. 1. Ein Teilchen mit den wichtigsten Strukturmerkmalen.

* Vortrag auf dem Symposium „Partikelmeßtechnik", 17./19. September 1975 in Nürnberg.

** Prof. Dr. C. Orr, Georgia Institute of Technology, School of Chemical Engineering, Atlanta, Georgia 30332/USA.

1) Größeneinteilung in Übereinstimmung mit dem Manual of Symbols and Terminology for Physico-chemical Quantities and Units, Appendix II, Definitions, Terminology and Symbols in Colloid and Surface Chemistry, übernommen von der International Union of Pure and Applied Chemistry, Washington D.C., USA, 1971.

und Makroporen entsteht. Da es sich bei der Oberflächen-Bestimmung um den molekularen Bereich handelt, ergibt sich zwangsläufig, daß für die Messung vor allem Gasmoleküle in Frage kommen. Am häufigsten wird Stickstoff verwendet, obwohl sich – wie weiter unten ausgeführt – auch andere Gase eignen.

Gesamtoberfläche

Die Stickstoff-Moleküle bedecken die Pulver-Oberfläche bzw. werden von der Oberfläche adsorbiert, besonders dann, wenn die Pulvertemperatur sehr niedrig ist. Bei der Adsorption bedecken die Moleküle die Oberfläche zunächst mit einer monomolekularen Schicht; dann wird eine zweite Schicht aufgebaut usw., wenn mehr Stickstoff zugegeben wird. In der Praxis verläuft die Anlagerung der Gasmoleküle nicht so schematisch. Sie lagern sich etwas weniger stark an exponierten Kanten an, dagegen in erheblich stärkerem Maße in Winkeln und in größeren oder kleineren Mengen an Stellen mit Verunreinigungen oder Gitterstörungen. In Mikrorissen sind die Moleküle den Anziehungskräften von verschiedenen Seiten gleichzeitig ausgesetzt. Darum ist hier die Adsorption erheblich stärker als in ebenen Bereichen. Wenn man zunächst einmal von den Mikroporen absieht, sind die Bereiche mit anormaler Adsorption relativ klein. Die Oberflächenbereiche mit verstärkter Adsorptionsaktivität werden in ihrer Wirkung durch Bereiche mit geringer Aktivität kompensiert. Dieser Ausgleich ist der Grund dafür, daß die Adsorption eines inerten Gases, z. B. Stickstoff, auf der Oberfläche eines Feststoffs die heute am meisten angewandte Methode zur Oberflächen-Bestimmung ist.

Die Zuverlässigkeit von Oberflächen-Bestimmungen durch Gas-Adsorption bei niedrigen Temperaturen läßt sich mit Hilfe mehrerer unterschiedlicher Methoden nachweisen. Auf direktem Wege ist dies möglich, wenn die Partikel-Oberfläche bei kubischen oder kugelförmigen Teilchen mit Hilfe der Elektronenmikroskopie bestimmt wird. Bei sorgfältiger Durchführung und Ausmessung einer größeren Anzahl von Teilchen ist die Übereinstimmung der Ergebnisse außerordentlich gut [1, 2]. Unter den weiteren unabhängigen Prüfmethoden sollen an dieser Stelle nur noch die Flüssigphasen-Adsorption [3], die Bestimmung der Oberflächen-Energie [4] und die Röntgen-Streuung [5] erwähnt werden.

Zur Bestimmung der gesamten Oberfläche mit Hilfe der Gas-Adsorption wird meist die BET-Methode von *Brunauer, Emmett* und *Teller* verwendet. Das zu untersuchende Pulver wird zunächst erhitzt und evakuiert, um Gase und Wasser von der Oberfläche zu entfernen. Das gereinigte Material wird dann bei der Temperatur von flüssigem Stickstoff mit Stickstoff-Gas beaufschlagt, wobei der Druck stufenweise erhöht wird. Ein Teil des Stickstoffs wird durch Adsorption oder Bedeckung der Feststoff-Oberfläche der Gasphase entzogen und trägt dann nicht mehr zum Druck bei. Das Volumen V des adsorbierten Gases, bezogen auf eine bestimmte Menge Pulver bei Standard-Temperatur und -Druck, läßt sich aus den Druckmessungen vor und nach der Stickstoff-Zugabe bestimmen. Wenn man das adsorbierte Volumen gegen den rel. Druck P/P_s aufträgt, wobei P der gemessene Gleichgewichtsdruck nach der stufenweisen Zugabe von Gas und P_s der Sättigungsdruck des Stickstoffs ist, erhält man eine BET-Adsorptionsisotherme. Durch Umkehren des Vorganges und Entfernen des Gases in mehreren Stufen – ebenfalls bei der Temperatur von flüssigem Stickstoff – erhält man eine Desorptionsisotherme. Abb. 2 zeigt den Verlauf einer BET-Isotherme für ein nichtporöses Pulver, wobei auf der linken Seite die Anordnung der Gasmoleküle (kleine Kreise), die auf der Feststoff-Oberfläche adsorbiert sind, dargestellt ist. Die Isothermen auf der rechten Seite der Abbildung werden nachstehend diskutiert.

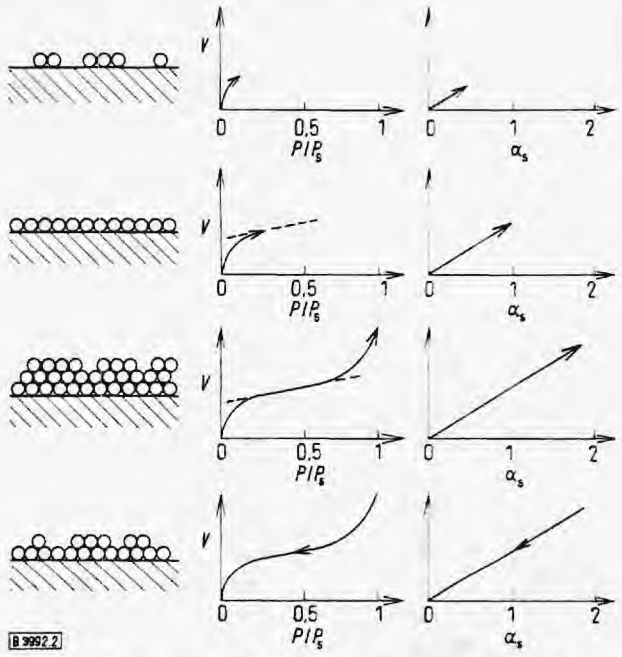

Abb. 2. Adsorptions- und Desorptionsisothermen von Stickstoff an einem nichtporösen Material bei niedriger Temperatur.

Von besonderem Interesse ist die zweite Darstellung der Adsorptions-Isotherme, bei der die Oberfläche mit einer monomolekuren Schicht von adsorbiertem Gas bedeckt ist. Hierbei geht die Isotherme in eine Gerade über. Wenn man den niedrigsten asymptotischen Punkt des linearen Bereichs als Anzeichen für eine vollständige monomolekulare Schicht betrachtet, läßt sich die Anzahl der adsorbierten Gasmoleküle ohne weiteres aus dem adsorbierten Volumen V, das zu diesem asymptotischen Punkt gehört, berechnen. Die spezifische Oberfläche des Feststoffs (m^2/g) läßt sich ermitteln, wenn bekannt ist, wie groß der Flächenbedarf pro Molekül ist. Für Stickstoff beträgt dieser Wert etwa 16,2 $Å^2$ pro Molekül [6]. Er läßt sich für die meisten Pulver benutzen.

Der experimentelle Nachweis dafür, daß der asymptotische Punkt in etwa einer monomolekularen Bedeckung entspricht [7], gelang etwa Mitte der dreißiger Jahre. Seitdem wurden viele Versuche gemacht, um diesen experimentellen Befund auf eine gesicherte theoretische Basis zu stellen. Meist wird eine Adsorptionsisothermen-Gleichung mit zwei Konstanten verwendet [8]:

$$\frac{P}{V(P_s - P)} = \frac{1}{V_m c} + \left(\frac{c-1}{V_m c}\right)\frac{P}{P_s} \quad . \tag{1}$$

Hierin ist V_m das Volumen der adsorbierten Gas-Monoschicht und c eine Konstante, die mit der Adsorptionsenergie zusammenhängt. Wenn man $P/(V[P_s - P]$ gegen P/P_s aufträgt, erhält man eine Kurve mit einem linearen Bereich.

Aus ihrer Steigung und dem Ordinaten-Abschnitt erhält man den Wert für V_m (und c). Dieses Verfahren ist einfacher als die Bestimmung des asymptotischen Punktes im $V, P/P_s$-Diagramm.

Gl. (1) wurde unter anderem unter der Annahme abgeleitet, daß alle Adsorptionsplätze energetisch gleichwertig sind, daß keine seitlichen Wechselwirkungen der adsorbierten Moleküle vorliegen und daß eine unbegrenzt große Zahl von adsorbierten Schichten bei einem rel. Druck von 1 vorliegt. Keine dieser Bedingungen kann ohne Einschränkungen akzeptiert werden. Deswegen bleiben noch einige Fragen bei der Bestimmung der Oberflächengröße offen und werden es vermutlich auch bleiben, bis die theoretischen Fragen umfassend geklärt sind. Nichtsdestoweniger soll noch einmal darauf hingewiesen werden, daß die mit Hilfe der BET-Methode erhaltenen Werte mit den entsprechenden Werten nach anderen Verfahren übereinstimmen. Wenn auch noch keine zufriedenstellende Theorie zur Verfügung steht, so handelt es sich doch bei den Meßergebnissen um zuverlässige Werte, und zwar für das gesamte Gebiet der Partikel-Technologie.

Abb. 2 zeigt, daß die weitere Zugabe von Gas über die Monoschicht-Bedeckung hinaus zu einer größeren Schichtdicke führt. Die mittlere Dicke dieser Schicht sollte bei nichtporösen Substanzen in einer direkten Beziehung zu der Oberflächengröße stehen, falls die adsorbierten Moleküle regelmäßig angeordnet sind. Zahlreiche Messungen mit unterschiedlichen Feststoffen haben ergeben, daß die vorliegenden Verhältnisse in etwa diesen Vorstellungen entsprechen. Man kann deshalb die Dicke der Schicht t (Å) mit folgender Beziehung [9–11] beschreiben:

$$t = 3{,}54 \left(\frac{5}{\ln (P_s/P)} \right)^{1/3} . \qquad (2)$$

Die Beobachtung, daß Gl. (2) für unterschiedliche Pulver zuverlässige Werte liefert, führte zur Entwicklung einer empirischen Methode bei der Isothermen-Analyse, die als Dicken-Methode (t-Methode) bekannt ist [12]. Mit ihr lassen sich die Adsorptionsisothermen ohne größere Mühe interpretieren. Wenn man das durch ein Pulver adsorbierte Gasvolumen gegen die Dicke der adsorbierten Schicht, berechnet nach Gl. (2), aufträgt und eine Gerade erhält, dann weist das adsorbierende Pulver mit einiger Sicherheit keine Poren auf. Wenn andererseits diese Kurve einen Knick zeigt oder gekrümmt ist, so deutet dies auf Poren oder Risse hin, die mit zunehmendem rel. Druck aufgefüllt werden und, einmal gefüllt, für die weitere Entwicklung der Schichtdicke auf der Oberfläche nicht mehr zur Verfügung stehen.

Bei einer weiteren empirischen Methode zur Interpretation der Adsorption [13,14] wird die Schichtdicke t durch $V/V_{0,4}$, abgekürzt α_s, ersetzt, wobei $V_{0,4}$ das adsorbierte Gasvolumen bei einem rel. Druck von 0,4 darstellt. Bei diesem Druck ist die Entwicklung der monomolekularen Bedeckung nahezu vollständig. Werte für α_s stehen aus Daten für nichtporöse Referenzstoffe zur Verfügung. Im Idealfall ist dieses Referenzpulver mit Ausnahme der fehlenden Poren identisch mit dem zu untersuchenden Stoff. Dies führt zu folgender empirischen Gleichung für die Adsorptionsisotherme [15]:

$$S = 2{,}89\, V/\alpha_s , \qquad (3)$$

wobei S die spezifische Oberfläche der Probe in m^2/g und V das Gasvoloumen in ml/g bei Standardbedingungen ist. Die Konstante 2,89 gilt speziell für SiO_2-Pulver. Wie bei der t-Methode erhält man auch bei der α_s-Methode bei der Auftragung des adsorbierten Gasvolumens gegen α_s bei porenfreien Material eine Gerade und eine gekrümmte Kurve, falls Poren vorliegen. Die für V und α_s aufgetragenen Werte gelten für den gleichen rel. Druck. Das adsorbierte Volumen V erhält man aus experimentellen Bestimmungen und Werte für α_s aus den bereits früher erwähnten Angaben für ein porenfreies Referenzpulver. Gl. (3) ist die Grundlage für die Auftragung der Kurven auf der rechten Seite von Abb. 2. Wenn man eine Gerade erhält, so ist dies ein Zeichen dafür, daß das Pulver nicht porös ist. Die spezifische Oberfläche läßt sich dann ohne weiteres als Produkt aus der Konstanten und der Neigung der Geraden bestimmen. Die Zweckmäßigkeit der α_s-Darstellung wird später noch näher erläutert.

Die unterschiedlichen Anforderungen an die Analysengeschwindigkeit, die Genauigkeit, die Partikel-Vorbehandlung usw. haben zu zahlreichen Abänderungen der grundlegenden BET-Technik geführt. Die oben beschriebenen volumetrischen Bestimmungen werden häufig angewandt, da sie eine hervorragende Kombination von Genauigkeit, Schnelligkeit und Zuverlässigkeit bieten. Die gravimetrische Bestimmung von Pulvern mit großer Oberfläche, bei denen das Gewicht des adsorbierten Gases relativ große ist, sind sehr genau, jedoch dauern die Messungen länger und erfordern mehr Sorgfalt. Modifizierte gaschromatografische Systeme, bei denen Gasmischungen verwendet werden, ggf. einige Prozent Stickstoff in Helium (dabei wird angenommen, daß Helium bei der Temperatur des flüssigen Stickstoffs nicht adsorbiert wird), sind relativ schnell durchzuführen, erfordern jedoch eine Kalibrierung. Es stehen inzwischen handelsübliche Geräte mit Computer-Auswertung für die oben beschriebenen Methoden zur Verfügung, die auch die Oberfläche berechnen, die Isothermen aufzeichnen und alle diejenigen Analysen durchführen, die später beschrieben werden.

Außer Stickstoff lassen sich auch andere Gase mit zufriedenstellenden Ergebnissen einsetzen. Krypton und Argon werden bei der Temperatur von flüssigem Stickstoff benutzt. Bei Pulvern mit geringer Oberfläche erhält man bei Krypton bei volumetrischen Bestimmungen zuverlässigere Resultate als bei Stickstoff, da ein geringerer Anteil des Gases wegen des niedrigeren Sättigungsdruckes unadsorbiert bleibt. In zunehmendem Maße wird auch die Adsorption von Kohlendioxid bei Raumtemperatur angewendet. Weitere geeignete Gase sind Propan bei der Temperatur von Eis/Wasser-Mischungen und Butan bei 20 °C. Bei diesen höheren Temperaturen muß man damit rechnen, daß eine Chemisorption stattfindet. Deshalb ist eine Kontrolle der erhaltenen Oberflächen-Werte durch Bestimmung bei niedrigeren Temperaturen unbedingt zu empfehlen.

Oberflächen mit Mikroporen

In den vorangehenden Abschnitten wurden porenfreie Pulver behandelt. In Abb. 3 ist die Stickstoff-Adsorptionsisotherme für ein mikroporöses Material dargestellt. Unter Mikroporen versteht man Poren mit einer Weite unter 20 Å. Im linken Teil der Abbildung wird der Verlauf der Adsorption durch ein schematisches Modell wiedergegeben, der rechte Teil enthält die BET- und α_s-Adsorptionsisothermen.

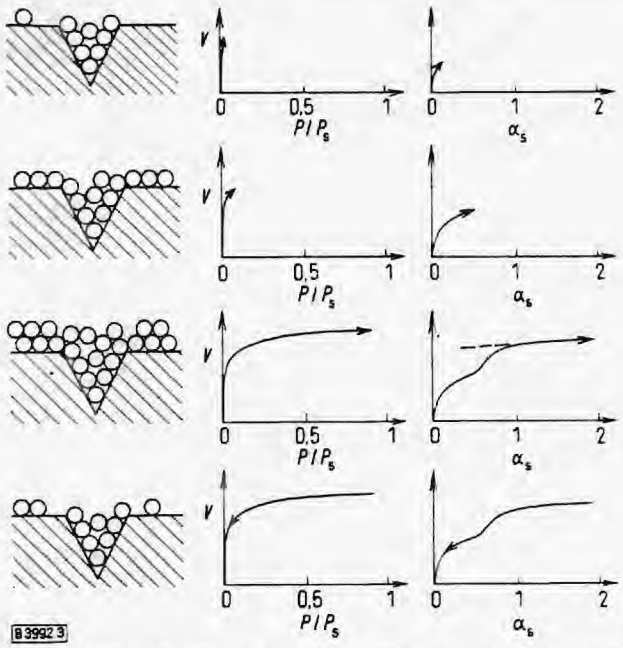

Abb. 3. Stickstoff-Adsorptions- und -Desorptionsisothermen bei mikroporösem Material und niedrigen Temperaturen.

Die typische BET-Isotherme steigt bei niedrigem rel. Druck steil an und dann nur noch wenig, selbst bei hohem rel. Druck. Die α_s-Isotherme steigt ebenfalls zunächst steil an und kann dabei mehrere Wendepunkte aufweisen.

Eine Zeit lang nahm man an, daß Oberflächen mit Mikroporen, die genügend weit sind zur Ausbildung einer einzigen monomolekularen Schicht auf jeder Wandseite, der Grund für die beobachteten Messungen sind. Die Oberflächengröße ließe sich dann mit Hilfe des Plateaus der BET-Isotherme als Nachweis für die Bildung einer vollständigen Monoschicht bestimmen. Wenn die Poren erst einmal gefüllt sind, dann steht eine geringere Oberfläche für den anschließenden Aufbau von Mehrfach-Schichten zur Verfügung. Bei Anwendung dieser Vorstellungen auf die Adsorption an Aktivkohle erhielt man eine so große spezifische Oberfläche, daß 90 % aller Kohlenstoff-Atome sich an der Oberfläche befinden müßten [1]. Dieses Ergebnis läßt sich nicht mit den mechanischen und anderen Eigenschaften des verwendeten Kohlenstoffs in Einklang bringen. Deshalb mußte die Annahme der Monoschicht-Bildung in den Spalten revidiert werden [16]. Man nimmt nun an, daß die Mikroporen eine Weite von mehreren Molekül-Durchmessern aufweisen und schnell mit adsorbiertem Gas gefüllt werden, wobei sich ein flüssigkeitsähnlicher Zustand einstellt, bevor auf der äußeren Oberfläche die Monoschicht-Bildung abgeschlossen ist. In Übereinstimmung mit diesen Vorstellungen repräsentiert das Isothermen-Plateau nicht mehr die Monoschicht-Bildung, da die Auffüllung der Mikroporen mit eingeschlossen ist.

Die Bezeichnung „flüssigkeitsähnlich" wird verwendet, um auf die erhebliche Unsicherheit hinzuweisen, die in bezug auf den realen Zustand der adsorbierten Phase in den Mikroporen besteht. Diese Phase verhält sich mit einiger Wahrscheinlichkeit nicht wie eine echte Flüssigkeit und bildet z. B. auch keinen Meniskus aus, wie z. B. eine Flüssigkeit in einem Kapillarrohr, da sich nur eine relativ geringe Anzahl von Molekülen an der exponierten Oberfläche befindet. Es ist einleuchtend, daß die Kräfte innerhalb der Mikroporen, die zu der Adsorption der Gasmoleküle führen, wegen der Nähe der Wände verstärkt sind. Es gibt wegen zahlreicher Unsicherheiten noch keine genauen Berechnungen dieser Verstärkung, aber es ist damit zu rechnen [17], daß man es mit um ein mehrfaches größeren Adsorptionskräften als an ebenen Oberflächen zu tun hat.

Zur Zeit besteht noch keine Klarheit darüber, wo sich die Wände der Mikroporen im Verlauf der Adsorptionsisotherme zunächst mit adsorbierten Molekülen bedecken, jedoch kann man annehmen, daß dies der Fall ist, wenn die Isothermen in Abb. 3 nahezu vertikal verlaufen. Die erste Krümmung der Isotherme repräsentiert wahrscheinlich die Auffüllung der Mikroporen und evtl. den Beginn der Bedeckung der freien Oberfläche. Der annähernd horizontale Bereich der Isothermen zeigt die Mehrschichten-Bedeckung der freien Oberfläche an. Bei Beginn der Mehrschichten-Bedeckung der externen Oberfläche sollte sich Gl (3) anwenden lassen. Man erhält so aus der Neigung V/α_s der Kurve im oberen linearen Bereich einer α_s-Isotherme multipliziert mit der Konstanten einen zuverlässigen Wert für die externe Oberfläche von mikroporösen Pulvern. Die Oberfläche der Mikroporen selbst läßt sich aus Gasadsorptionsmessungen z. Z. nicht bestimmen. Auch läßt sich die Gesamtoberfläche nicht zuverlässig ermitteln. Die Annahme, daß der Plateau-Wert der BET-Isotherme die Vervollständigung der Monoschicht-Bedeckung angibt, führt zu einem viel zu großen Wert für die Gesamtoberfläche. Es läßt sich jedoch nicht genau sagen, um wieviel zu groß dieser Wert ist, da dies von der Zahl und der Größe der Mikroporen abhängt.

Zur Zeit ist nur eine begrenzte Zahl von Konstanten (für Gl.-(3)) für verschiedene Materialien bekannt. Es ist unbedingt erforderlich, Untersuchungen mit einer Vielzahl von Pulvern anzustellen. Es wurde vorgeschlagen [15], Informationen über die Größe und die Fläche von Mikroporen durch eine Reihe von Adsorptionsversuchen zu erhalten, bei denen Dämpfe unterschiedlicher Molekülgröße verwendet werden. Die ermittelte scheinbare Oberflächen-Größe sollte dann mit zunehmender Molekülgröße abnehmen, bis man schließlich die äußere Oberfläche erhält, wenn die Moleküle nicht mehr in die Mikroporen eindringen können. Mit Hilfe der später behandelten Kleinwinkel-Röntgenstreuung lassen sich weitere Informationen erhalten.

Die Oberflächengröße von Mesoporen

Die Adsorptionsisothermen von Pulvern mit Mesoporen können eine recht unterschiedliche Charakteristik aufweisen, s. Abb. 4. Bis zu einem rel. Druck von etwa 0,4 bzw. einem α_s-Wert von ca. 1 lassen sich die Stickstoff-Isothermen von porenfreien Stoffen und Pulvern mit Meso- und Makroporen (aber nicht Mikroporen) normalerweise nicht unterscheiden, so daß sich die Gesamtoberfläche wie bereits beschrieben erhalten läßt, d. h. nach Gl. (1) bzw. (3). Der obere Bereich der Isothermen in Abb. 4 zeigt eine Hysterese, d. h. eine Aufspaltung in einen Adsorptions- und einen Desorptionszweig. Diese Hysterese beinhaltet eine Information über die Mesoporen-Oberfläche. Es besteht eine Beziehung zwischen dem Isothermen-Verlauf und der Isothermen-Lage zur Porengeometrie auf Grund von Kondensations- und Verdamp-

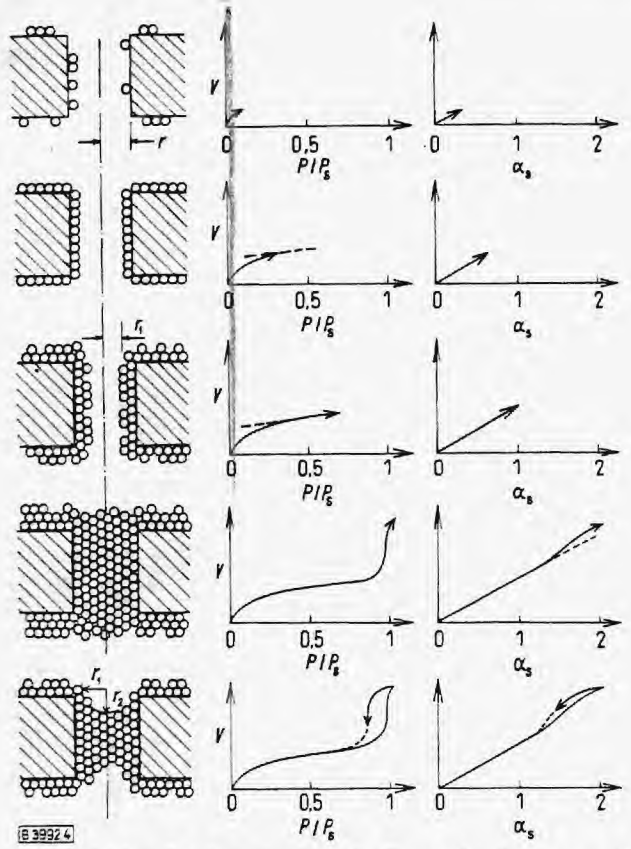

Abb. 4. Stickstoff-Adsorptions- und -Desorptionsisothermen bei einem Pulver mit Mesoporen und niedriger Temperatur.

fungserscheinungen, die sich durch die Kapillarkondensationsgleichung von *Kelvin* [18] beschreiben lassen:

$$\ln (P/P_s) = \frac{-2\gamma V \cos\Theta}{R T r_m} \quad . \tag{4}$$

γ ist dabei die Oberflächen-Spannung der Flüssigkeit, V das molare Volumen der kondensierten Phase, Θ der Kontaktwinkel zwischen der flüssigen und der festen Oberfläche (0 im Fall von kondensiertem Stickstoff), R die Allgemeine Gaskonstante, T die absolute Temperatur und r_m der mittlere Radius des Flüssigkeitsmeniskus, der sich aus den beiden Hauptradien der Flüssigkeits-Oberfläche in einer geraden Kapillare, r_1 und r_2, nach folgender Gleichung ermitteln läßt:

$$\frac{2}{r_m} = \frac{1}{r_1} + \frac{1}{r_2} \quad . \tag{5}$$

Diese beiden Radien sind in Abb. 4 für eine gerade, zylindrische Mesopore, die an beiden Enden offen ist, eingezeichnet. Wie aus dem linken Teil der Abb. 4 zu ersehen ist, ist nur der Radius r_1 für die Kondensation (Adsorptionszweig der Isotherme) von Bedeutung, wogegen die beiden Radien r_1 und r_2 bei der Verdampfung (Desorptionszweig) einen Einfluß ausüben. Hieraus und aus Gl. (5) läßt sich erkennen, daß sich eine zylindrische Mesopore, die an beiden Seiten offen ist, mit Kondensat füllt, wenn $r_m = 2\,r_1$ ist, da $r_2 = 0$, und sich leert, wenn $r_m = r_1 = r_2$. Keine Pore ist vollständig zu Beginn der Kondensation leer, noch ist sie nach dem Verdampfen des Kondensats vollständig leer, da sich an ihren Wänden eine Schicht von adsorbierten Molekülen [19] befindet. Die Dicke t der adsorbierten Schicht läßt sich vermutlich nach Gl. (2) bestimmen. Der Mesoporen-Radius r läßt sich mit Hilfe der Daten aus dem Adsorptionszweig der Isotherme bestimmen, wenn man Gl. (4) in folgender Form schreibt:

$$\ln (P/P_s)_a = -\frac{\gamma V}{R T (r - t)} \tag{6}$$

oder aus dem Desorptionszweig mit Hilfe folgender Gleichung:

$$\ln (P/P_s)_d = -\frac{2\gamma V}{R T (r - t)} \quad . \tag{7}$$

Voraussetzung ist auf jeden Fall das Vorliegen von Poren, die an beiden Enden offen sind und eine zylindrische Gestalt aufweisen.

Eine Porenstruktur wie in Abb. 4 ist ungewöhnlich, obwohl der synthetische Chrysotil [20] annähernd diese Porenform aufweist. Vor kurzem haben *Liabastre* und der Autor dieses Aufsatzes Adsorptionsuntersuchungen mit einem speziell präparierten Polycarbonat-Film durchgeführt[1]. Auf Grund vorläufiger Ergebnisse läßt sich sagen, daß dieser Film 10^9 bis 10^{10} Poren/cm² in ziemlich enger Verteilung um einen Radius von ca. 125 Å aufweist. Dieser Film wird mit größeren Poren kommerziell für Filtrationszwecke unter dem Handelsnamen Nuclepore[2] vertrieben. Abb. 5 zeigt Mikro-

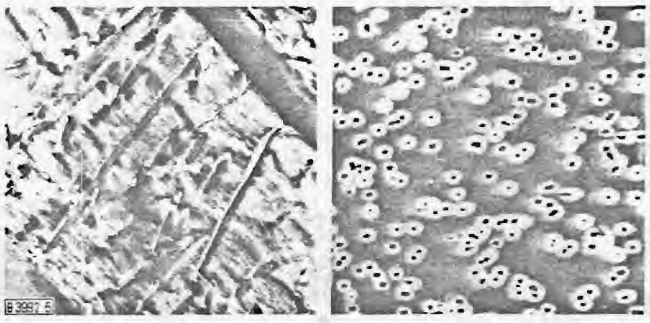

Abb. 6. Stickstoff-Adsorption und -Desorption bei einem Pulver mit zylindrischen Mesoporen bei niedriger Temperatur.

fotografien derartiger Poren, und zwar sowohl einen Querschnitt als auch einen Längsschnitt. Bei dem Längsschnitt werden nur wenige Poren erfaßt. Sie wurden durch Bestrahlen und anschließendes Auslaugen erhalten. Auf elektronenmikroskopischem Wege wurde die Größe von mehreren hundert Poren bestimmt. Die Querschnitte sind im wesentlichen rund. Die Poren verlaufen gerade und sind etwa 200mal so lang wie breit. Abb. 6 zeigt Adsorptions- und Desorptionsisothermen, die mit diesem Film mit Stickstoff bei niedrigen Temperaturen erhalten wurden[3]. Aus jedem der beiden Isothermen-Zweige wurde innerhalb des experimentellen Fehlers die gleiche Porenradien-Verteilung erhalten, Gln. (6) und (7); diese Verteilung stimmt sehr gut mit der mit Hilfe der Elektronenmikroskopie ermittelten überein. Dies ist der direkteste und überzeugendste Nachweis für die Richtigkeit der Kondensations/Verdampfungs-Theorie, die dem Autor dieser Arbeit bekannt ist. Es ist noch

1) Mit Unterstützung der NASA, Beihilfe Nr. NSG-2004, und der NSF, Beihilfe KG-43616.

2) Nuclepore Corporation, Pleasanton/Cal. (USA).

3) Verwendet wurde das Modell 2500 Digisorb, Micromeritics Instruments Corporation, Norcross/Georgia (USA).

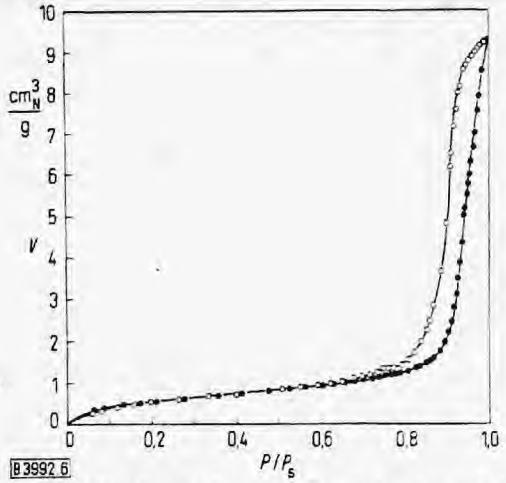

Abb. 5. SEM-Mikrofotografien von Poren in einem Polycarbonat-Film.

zu erwähnen, daß die Theorie in diesem Fall auf ein nahezu ideales Material angewandt wurde.

Die Berechnung der Mesoporen-Größe aus Adsorptions- und Desorptionsdaten ermöglicht eine einfache Oberflächenbestimmung bei symmetrischer Porengeometrie. Diese Berechnungen und auch Berechnungen für andere bekannte oder angenommene Porengeometrien lassen sich in einem schrittweisen Verfahren durchführen, wobei man bei einem hohen rel. Druck beginnt. Das bei der Änderung des rel. Druckes adsorbierte oder desorbierte Gasvolumen bei der BET-Isotherme entnimmt man der Ordinate und wendet dann Gl. (6) oder Gl. (7) an, um den entsprechenden Mesoporen-Radius zu bestimmen, wobei Gl. (2) verwendet wird, um die Dicke der adsorbierten Schicht zu erhalten. Einzelheiten dieser Berechnung wurden bereits in mehreren Arbeiten veröffentlicht [11, 21, 22]. Wenn man erst einmal die Mesoporen-Oberfläche ermittelt hat, läßt sich die äußere Oberfläche als Differenz zwischen der Gesamtoberfläche, ermittelt aus dem Bereich der Isotherme bei relativ niedrigem Druck, und der Mesoporen-Oberfläche berechnen.

Das Vorliegen einer Hysterese deutet bei Isothermen auf Mesoporen hin, jedoch ist dies leider kein hinreichender Nachweis für Mesoporen. Falls die Poren in Abb. 4 an einem Ende halbkugelig verschlossen sind, würden das Auffüllen und das Entleeren identisch verlaufen und keine Hysterese zu beobachten sein. Die Poren würden dann vom offenen Ende her gefüllt und auf dem gleichen Weg geleert werden. Der Flüssigkeitsmeniskus würde dann halbkugelig bleiben mit $r_m = r_1 = r_2$. Dies bedeutet, daß sich Gl. (7) für die Berechnung der Porenradien anwenden ließe. Die kritiklose Anwendung von Gl. (7) kann offensichtlich zu Schwierigkeiten führen. Es ist einleuchtend, daß sich die Berechnung von Porengrößen und -oberflächen auch dann durchführen läßt, wenn keine Poren vorliegen bzw. falls eine Hysterese als Nachweis für Mesoporen gefordert wird, dann wird eine Substanz, deren Poren an einem Ende geschlossen sind, als nichtporös charakterisiert. Auch kegelförmige und keilförmige Poren und bestimmte andere Mesoporen-Geometrien mit einem verschlossenen Ende ergeben Isothermen ohne Hysterese [23]. Der einzige sichere Weg zum Nachweis des Vorliegens oder Fehlens von Poren ist in derartigen Fällen die mikroskopische Untersuchung bzw. die später beschriebene Quecksilber-Penetrationsmethode.

Hysterese tritt nicht nur bei Poren auf, die an beiden Enden offen sind, sondern auch bei Mesoporen, bei denen der Eingangsquerschnitt kleiner ist als der Querschnitt im Inneren. Derartige Mesoporen werden bei einem relativen Druck aufgefüllt, der durch den größten Radius bestimmt wird, und leeren sich bei einem geringeren relativen Druck, der durch den Eingangsradius bestimmt wird. Bei zahlreichen anderen Porenverläufen, z. B. bei Querverbindungen, Windungen und gekrümmten Bereichen, ist mit einer Hysterese zu rechnen. In diesen Fällen kann man Aufschlüsse über die Mesoporen-Struktur auf Grund der speziellen Form und der relativen Lage des Adsorptions- und Desorptionszweigs der Isotherme erhalten, und zwar durch Vergleich mit einer theoretischen Analyse für spezielle Geometrien [24]. Jedoch kann keine derartige Untersuchung die exakte Bestimmung einer gegebenen Struktur oder Oberfläche liefern.

In zahlreichen Arbeiten wurde untersucht, ob sich der Adsorptions- oder der Desorptionszweig besonders gut für die Berechnung der Mesoporengröße und -oberfläche von Pulvern eignet. Selbstverständlich läßt sich diese Frage nur dann exakt beantworten, wenn die Geometrie der Pore bekannt ist. Falls sich die Porenform in geeigneter Weise mathematisch mit Hilfe der Kelvin-Gleichung beschreiben läßt, gibt es keine Unterschiede in der Genauigkeit. Adsorptions- und Desorptionsdaten müssen dann zu den gleichen Ergebnissen führen, wie sich auch bei den weiter oben beschriebenen Versuchen mit Polycarbonat-Material mit zylindrischen Mesoporen nachweisen ließ.

Während eine gute Übereinstimmung zwischen Theorie und Experiment bei speziellen Mesoporen-Strukturen möglich ist, ist die Verfügbarkeit eines geeigneten Porenmodells in der Praxis eine erhebliche Einschränkung. Auch der Porengrößen-Bereich (etwa 20 bis 500 Å), für den sich diese Technik eignet, stellt eine Restriktion dar. Weiterhin sind die Ermittlung der Daten und die Berechnung recht eintönig und zeitraubend, falls nicht ein automatisch arbeitendes Gerät und ein Computer-Programm zur Verfügung stehen. Insgesamt gesehen läßt sich sagen, daß sich eine Bestimmung der Mesoporen-Oberfläche meist nur mit erheblichem Aufwand durchführen läßt und weiterhin auch mit einer guten Portion Glück beim Ermitteln eines geeigneten Porenmodells. Falls fälschlicherweise zylindrische oder schlitzartige Poren angenommen werden, wie dies sehr häufig vorkommt, haben die Ergebnisse mehr Konfusion als Einblicke zur Folge. So wird z. B. bei der Bestimmung der Mesoporen-Oberfläche häufig ein Wert erhalten, der die Gesamtoberfläche erheblich übertrifft, was ganz offensichtlich nicht möglich ist. Es bleibt noch viel zu tun, bis Pulver mit Mesoporen-Oberflächen zweifelfrei und exakt untersucht werden können.

Bestimmung der Porenoberfläche mit Hilfe der Quecksilber-Penetrationsmethode

Das die meisten Feststoffe nicht benetzende Quecksilber dringt bei einem Druck von 3 bar in Poren mit einem Radius von 90 µm ein, in Poren mit 17 Å Radius bei einem Druck von etwa $1{,}5 \cdot 10^5$ bar. Wenn man auf ein poröses Pulver nach dem Evakuieren Quecksilber bei einem Druck P gibt, füllt das Quecksilber die Poren mit dem Radius r [25],

wobei sich der Vorgang mathematisch mit folgender Gleichung beschreiben läßt:

$$P r = -2\sigma\cos\Theta \ . \qquad (8)$$

Dabei ist σ die Oberflächenspannung des Quecksilbers, und Θ der Kontaktwinkel zwischen Quecksilber und Feststoff. Dieses Verfahren, bei dem simultan der angewandte Druck und das eingedrungene Quecksilber-Volumen bestimmt werden, wird häufig zur Porengrößen-Bestimmung benutzt. Es eignet sich auch dazu, um festzustellen, ob ein Pulver ohne Adsorptions/Desorptions-Hysterese wirklich keine Poren aufweist oder evtl. doch porös ist. Es eignet sich auch zur Bestimmung der Poren-Oberfläche. Hierfür muß wieder ein Porenmodell benutzt werden.

Wenn man zylindrische Poren annimmt, dann erhält man über das Produkt aus dem Druck P und dem eingedrungenen Quecksilber-Volumen dV die Arbeit, die erforderlich ist, um in die Poren einzudringen. Zwischen dieser Arbeit und der neugebildeten Quecksilber-Oberfläche besteht folgende Beziehung [26]:

$$P\,dV = -\sigma\cos\Theta\,dS \ .$$

Wenn man annimmt, daß sich σ und Θ mit dem Druck nicht ändern, erhält man aus Gl. (9)

$$S = B\int_{V_2}^{V_1} P\,dV \ .$$

B ist darin eine Konstante, deren Größe von σ und Θ abhängt. Die Größe $\int P\,dV$ läßt sich durch grafische Integration einer Porosimeter-Kurve erhalten (Auftragung von P gegen V). Als Oberflächengröße S erhält man die Oberfläche des Quecksilbers, das sich in den Poren mit dem Radius r, definiert nach Gl. (8), ausbreitet. Diese Oberfläche entspricht vermutlich der der Mesoporen-Wände. Die Zuordnung von Poren-Oberflächen zu verschiedenen Radiusbereichen ist durch die Auswahl entsprechender Integrationsgrenzen möglich. Außer dem Zylinder-Modell lassen sich auch andere geometrische Modelle für die Poren durch geeignete Abwandlung der obigen Gleichungen anwenden.

Tabelle 1. Ergebnisse bei zylindrischen Poren (Nucleopore, $d = 0{,}6$ µm).

Analysenmethode	Durchmesser-Verteilung [Vol.-%]			Poren-Größe [m²/g]	Poren-Vol. [ml/g]
	10 % kleiner [µm]	50 % [µm]	10 % größer [µm]		
Quecksilber-Penetration	0,47	0,62	0,81	1,05	0,155
Elektronen-Mikroskopie	0,51	0,63	0,73	0,89	0,142

Tab. 1 enthält einen Vergleich der Ergebnisse mit Hilfe der Quecksilber-Penetrationsmethode[4] mit den Resultaten, die mit Hilfe der Elektronenmikroskopie erhalten wurden. Verwendet wurde ein Polycarbonat-Filter mit einem mittleren Porendurchmesser von 0,6 µm. Die so erhaltenen Durchmesser-Verteilungen und auch die Oberflächengrößen und Porenvolumina weichen etwas voneinander ab. Die Übereinstimmung ist jedoch zufriedenstellend, wenn man berücksichtigt, daß es sich um zwei sehr verschiedenartige Methoden handelt, die mit gewissen Unsicherheiten behaftet sind.

Diese Technik läßt sich nicht bei einspringenden Poren anwenden. In diesem Fall kann man Porosimeter-Kurven mit zunehmendem und abnehmendem Druck erhalten und eine Scanning-Analyse anwenden [27]. Zur Zeit ist allerdings der Einfluß der vorrückenden und zurückgehenden Kontaktwinkel, die sich sehr stark unterscheiden können, in einer derartigen Analyse nicht überschaubar. Die Brauchbarkeit der Scanning-Methode wurde bisher noch nicht überzeugend nachgewiesen. Eventuell ergeben sich Probleme auf Grund von Teilchen- und Porenverformungen wegen des hohen Drucks [28] und schränken die Anwendung dieser Methode ein. Nichtsdestoweniger wird die Quecksilber-Penetrationsmethode als Ergänzung zu Gasadsorptions- und -desorptions-Messungen empfohlen, wenn es darum geht, exakt das Vorliegen oder Fehlen von Poren festzustellen und nähere Angaben über die gegebenenfalls vorliegende Poren-Oberfläche zu erhalten.

Adsorption aus flüssiger Phase

Die Adsorption (oder Sorption, wie dieser Effekt gelegentlich genannt wird) einer Substanz wie z. B. eines Farbstoffes oder von Jod, gelöst in einer Flüssigkeit, an der Oberfläche eines mit Flüssigkeit bedeckten Pulvers wird häufig als unproblematische Methode zur Oberflächen-Bestimmung empfohlen. In den meisten Fällen ist dies jedoch nicht so. Im Gegensatz zur volumetrischen und gravimetrischen Gasadsorption, bei der nur eine Molekülart für die Adsorption zur Verfügung steht, gibt es bei der Adsorption aus flüssiger Phase einen Verdrängungswettbewerb zwischen den Lösemittel-Molekülen und den gelösten Molekülen. Monomolekulare Schichten aus nur einer Molekülart erhält man nur dann, wenn der gelöste Stoff eine wesentlich größere Affinität zu der Oberfläche aufweist als das Lösemittel. Auch hängen die Ausrichtung bei der Adsorption und der Oberflächen-Bedarf der adsorbierten Moleküle von der Konzentration und ggf. auch von anderen Faktoren ab.

Es kommen jedoch auch Fälle vor, bei denen die Flüssigphasen-Adsorption mit Vorteil angewandt werden kann. Einer dieser Fälle ist die Beurteilung der Eignung von Ruß für die Gummi-Herstellung, wobei eine Beziehung zwischen der Oberflächengröße des Rußes und der Abriebfestigkeit der Automobil-Reifen besteht. Zahlreiche Ruß-Teilchen enthalten Mikroporen, die so klein sind, daß Kautschuk-Moleküle nicht eindringen können. Deshalb führen Gasadsorptionsmethoden zu grob irreführenden Ergebnissen. In diesem Fall ist die externe Oberfläche des Rußes der geeignete Parameter für die Beurteilung. Diese externe Oberfläche läßt sich mit Hilfe der bereits beschriebenen α_s-Methode ermitteln, jedoch ist die Adsorption von bestimmten oberflächenaktiven Stoffen in wäßriger Lösung schneller durchzuführen und erfordert eine einfachere Ausrüstung [29–31]. Ein derartiges Surfactant ist Cetyltriäthylammoniumbromid (CTAB). Bei seiner Adsorption an Ruß erhält man eine Isotherme mit einem nahezu horizontalen Plateau, sehr ähnlich der BET-Isotherme in Abb. 3, wenn man die Menge des gelösten

4) Verwendet wurde das Modell 905-1 Mercury Penetration Porosimeter, Micromeritics Instrument Corp., Norcross/Georgia (USA).

Adsorbens gegen die relative Konzentration aufträgt. Unter der relativen Konzentration versteht man die jeweils vorliegende Konzentration, dividiert durch die Sättigungskonzentration. Im Plateau-Bereich liegt eine monomolekulare Bedeckung der externen Oberfläche vor, da die CTAB-Moleküle größer sind als der Mikroporen-Durchmesser und weiterhin auch die Adsorption des gelösten Stoffes gegenüber der Adsorption von Lösemittel-Molekülen begünstigt ist.

Man wartet die Gleichgewichtseinstellung zwischen Aktivkohle und der wäßrigen CTAB-Lösung ab, entfernt den Ruß durch Zentrifugieren und bestimmt dann die Konzentration von nichtadsorbiertem Detergens in der Gleichgewichtslösung. Aus der Differenz zwischen Anfangs- und Endkonzentration, dem Ruß-Gewicht und der Größe der CTAB-Moleküle läßt sich die Oberfläche berechnen. Die so erhaltenen Ergebnisse stimmen ziemlich gut mit den Oberflächengrößen überein, die man mit Hilfe der Elektronenmikroskopie erhält, wobei die Mikroporen nicht erfaßt werden.

Ganz generell gesehen werden Methoden zur Adsorption aus flüssiger Phase dann empfohlen, wenn sie durch spezielle Gegebenheiten naheliegen, z. B. bei temperaturempfindlichen Stoffen. Für orientierende Versuche bei der Flüssigphasen-Adsorption eignet sich besonders p-Nitrophenol. Diese Verbindung löst sich sowohl im Wasser als auch in organischen Lösemitteln. Ihre Konzentration in Lösung läßt sich leicht colorimetrisch bestimmen. Mit verschiedenen Pulvern [32, 33] wurden ziemlich exakte Oberflächen-Größen bestimmt. Für Verbindungen, die sich nicht mit Hilfe einer einfachen colorimetrischen Methode oder einer einfach durchzuführenden Titration quantitativ nachweisen lassen, ist die Anwendung der Mikrocalorimetrie [34, 35] oder einer der zahlreichen Infrarot- oder Ultraviolett-Analysen möglich. Bei Stoffen mit Poren unterschiedlicher Größe kann der Oberflächen-Anteil der verschiedenen Porengrößen durch mehrfache Durchführung der Bestimmung bei Anwendung von gelösten Molekülen unterschiedlicher Größe erhalten werden. In mehreren Fällen [36] hat dieses Verfahren zufriedenstellende Ergebnisse geliefert.

Durch eine geringfügige Änderung der Reinheit sowohl des Lösemittels als auch des gelösten Stoffes erhält man stark verfälschte Ergebnisse. Deshalb muß die Reinheit der benutzten Substanzen bei der Flüssigphasen-Adsorption sorgfältig kontrolliert werden. Die Flüssigphasen-Adsorption ist z. Z. als ergänzende Methode zur Bestimmung der Oberflächen zu betrachten. Die Ergebnisse sollten möglichst mit einer anderen Methode, vorzugsweise der Gasadsorption, überprüft werden.

Oberflächen-Bestimmung mit Hilfe der Permeatrie

Ohne Erwähnung der Permeatrie wäre ein Überblick über die Methoden zur Oberflächen-Bestimmung nicht vollständig. Bei dieser Technik wird trockenes Gas durch komprimiertes Pulver geleitet. Eine Information über die Oberflächen-Größe erhält man durch Bestimmen der Durchströmungsgeschwindigkeit und des Druckverlustes. Bei zähflüssiger Strömung zeigen die Ergebnisse im günstigsten Fall eine Oberfläche an, die einer hypothetischen glatten Hülle um jedes einzelne Teilchen entspricht. Wahrscheinlich wird jedoch nur der relative Feinheitsgrad bestimmt. Bei Anwenden von Gas wie z. B. Helium unter vermindertem Druck, wobei Knudsen-Strömung vorherrscht, ist der Einfluß der Teilchen-Oberflächenstruktur auf die Strömung erheblich größer. Deshalb korrespondieren die Ergebnisse bei Knudsen-Strömung relativ gut mit den Oberflächen-Bestimmungen mit Hilfe der Gasadsorptions-Methode, falls die Teilchen nicht porös sind [37, 38]. Bei Pulvern mit geringer Porosität erhält man brauchbare Oberflächenwerte [39, 40]. Jedoch kann man nicht erwarten, daß die Permeatrie unter allen Umständen zuverlässige Resultate liefert. Zur Einstellung der Bedingungen für die Knudsen-Strömung muß das Pulver zu Beginn nahezu so gut wie bei Gasadsorptionsmessungen evakuiert werden. Eine vollständige Permeationsbestimmung ist deshalb nahezu so zeitraubend wie die Oberflächen-Bestimmung mit Hilfe der Gasadsorption. Durch Anwendung der Permeatrie bei niedrigem Druck wird somit kein Vorteil erreicht.

Oberflächen-Bestimmung durch Röntgen-Streuung

Die Kleinwinkel-Röntgenstreuung wird bisher nur wenig zur Bestimmung von Oberflächen-Größen benutzt, doch weist dieses Verfahren vielversprechende Möglichkeiten auf, besonders dann, wenn es auf eine schnelle Analyse ankommt. Röntgen-Strahlen werden bei Änderung der Elektronendichte, wie sie beim Durchgang durch ein Pulver vorliegt, z. T. in einem kleinen Winkel abgelenkt. Es besteht eine theoretische Beziehung zwischen der sich ergebenden Streuung und der Oberflächengröße [41, 42]. Nötig sind Messungen der Intensität des nicht abgelenkten Anteils des Röntgen-Strahls und der Energie der im Winkel von annähernd 5° gestreuten Strahlung [5, 43]. Derartige Berechnungen erfordern Werte für verschiedene Eigenschaften, die für zahlreiche Stoffe nicht leicht erhältlich bzw. nicht ohne weiteres zu bestimmen sind.

Diese Schwierigkeiten lassen sich durch ein anderes Vorgehen vermeiden. Die Intensität der Streustrahlung eines Pulvers mit unbekannter Oberfläche wird dabei auf die Intensität bei einem Referenzpulver mit bekannter Oberfläche bezogen. Eine Auftragung der Intensität der Streustrahlung gegen den Streuwinkel bei chemisch identischen Pulvern mit gleicher Adsorption des Hauptstrahles zeigt Abb. 7. In einem be-

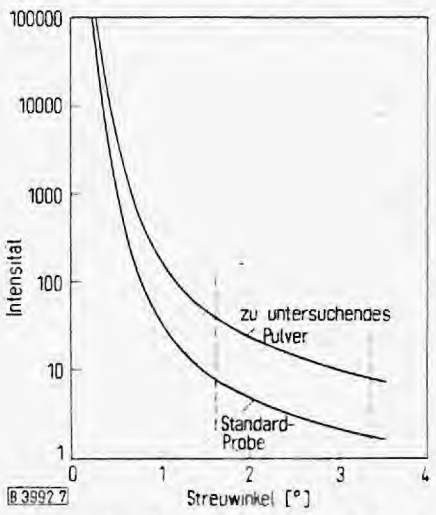

Abb. 7. Intensität der Streustrahlung als Funktion des Streuwinkels bei zwei chemisch identischen Proben mit unterschiedlicher Korngröße.

stimmten Winkel-Bereich ist das Intensitätsverhältnis für beide Proben konstant. Das Verhältnis der Intensitäten ist genauso groß wie das Verhältnis der Oberflächen [44]. Wenn man erst einmal den betreffenden Winkelbereich kennt und weiterhin eine Kurve für das Referenzpulver zur Verfügung steht, muß nur noch die Intensität bei einem einzigen Streuwinkel in diesem Bereich für das zu untersuchende Pulver bestimmt werden, um die Oberfläche zu erhalten. Die Analyse läßt sich routinemäßig in wenigen Minuten durchführen. Diese Technik läßt sich nicht anwenden, wenn sich die chemische Zusammensetzung des zu untersuchenden Pulvers erheblich von der der Standardprobe unterscheidet.

Chemisorption

Die Chemisorption wird vor allem dann angewendet, wenn man denjenigen Anteil einer Pulver-Oberfläche bestimmen will, der spezielle Eigenschaften aufweist. Im Gegensatz zur Adsorption, bei der die Bedingungen für eine Mehrfachbedeckung bzw. Kondensation eingestellt werden, wird die Chemisorption so geführt, daß bestimmte chemische Bindungen auftreten, so daß spezielle Reaktionsbereiche mit einer monomolekularen Schicht bedeckt werden. Es läßt sich sowohl eine Flüssigphasen- als auch eine Gasphasen-Chemisorption durchführen. In der Praxis wird fast ausschließlich die Gas-Chemisorption angewendet. Üblicherweise werden Gase wie Wasserstoff, Sauerstoff, Kohlenmonoxid, Ammoniak usw. gewählt, da sie sehr reaktiv im Vergleich zu inerten Gasen wie Stickstoff, Krypton und Argon sind.

Vor allem bei Katalysatoren ist es wichtig, den aktiven Anteil im Verhältnis zur Gesamtoberfläche zu kennen. Ein typisches Beispiel ist ein Kieselsäure-Katalysator mit einer geringen Menge Platin als aktiver Komponente. Bei einer idealen Verteilung dieser beiden Komponenten würde das Platin die äußere Oberfläche gleichmäßig bedecken, wobei die Kieselsäure nur als Träger dient. Technische Katalysatoren weisen jedoch beide Komponenten an der Oberfläche auf. Deshalb ist die Kenntnis ihrer Verteilung wichtig.

Die Bedingungen für die Chemisorption werden so gewählt, daß ein Maximum der Bindung des reagierenden Gases, z. B. Kohlenmonoxid, dort stattfindet, wo sich die aktive Komponente, z. B. Platin, befindet. Bei der inaktiven Komponente, z. B. Kieselsäure, soll keine Bindung auftreten. Der Anteil der mit Platin bedeckten Oberfläche kann dann aus der Kohlenmonoxid-Aufnahme ermittelt werden, wogegen sich die gesamte Oberfläche durch Adsorption eines inerten Gases, z. B. Stickstoff, bei niedriger Temperatur ermitteln läßt.

Im Prinzip lassen sich für die Chemisorption dieselben Geräte wie für die Adsorptionsanalyse verwenden, falls diese sich auch für höhere Temperaturen eignen. Bei einem typischen Versuch wird der Katalysator zunächst erhitzt und dabei evakuiert. Dann leitet man einige Stunden lang bei einer Katalysator-Temperatur von 400 bis 450 °C Wasserstoff über die Probe, um eine vollständige Reduktion zu erreichen. Anschließend wird wieder gründlich evakuiert. Die Temperatur wird dann auf ggf. 200 °C erniedrigt. Dann nimmt man eine Kohlenmonoxid-Isotherme auf, wobei das Gas in kleinen Anteilen zugegeben und jeweils Gleichgewichtsdruck und Gasaufnahme gemessen werden. Bis zur vollständigen Bedeckung der Metall-Atome an der Oberfläche steigt der Gleichgewichtsdruck nur wenig an. Bei der Auftragung des chemisorbierten Gasvolumens gegen den Gleichgewichtsdruck erhält man einen Kurvenverlauf wie in Abb. 3, jedoch mit dem Unterschied, daß der vertikal ansteigende Teil der Kurve noch steiler, der Wechsel der Krümmung noch ausgeprägter und das Plateau fast vollständig horizontal ist. Bei 200 °C findet kaum eine Adsorption des Gases statt, und das Kohlenmonoxid neigt nicht zur Umsetzung mit der Kieselsäure. Das aufgenommene Kohlenmonoxid-Volumen ist deshalb praktisch vollständig auf eine monomolekulare Bedeckung durch Chemisorption zurückzuführen. Der Oberflächen-Anteil des Platins läßt sich aus der Kohlenmonoxid-Aufnahme berechnen.

Bei der Bindung des Gases an das Metall bestehen mehrere Möglichkeiten. Es kann ein Gasatom auf ein Oberflächenatom entfallen, es ist jedoch auch eine Zuordnung des Gasmoleküls durch schwache und starke Bindungen zu mehreren Oberflächen-Atomen möglich. Diese verschiedenen Bindungstypen können z. B. vorkommen bei der Chemisorption von Kohlenmonoxid an einem Nickel-Katalysator auf Aluminiumoxid als Trägermaterial in Abhängigkeit vom Nickel-Gehalt und dem Bedeckungsgrad des Kohlenmonoxids [45]. So beträgt z. B. die von einem Wasserstoff-Molekül beanspruchte Äquivalentfläche bei Platin 22,4 $Å^2$ [46], jedoch nur 12,3 $Å^2$ bei Nickel [47]. Für die Chemisorption von Kohlenmonoxid an Platin wurden 17,8 $Å^2$ erhalten [48, 49].

Diese Werte für die Oberflächen-Bedeckung erhält man, indem man zuerst die gesamte Oberfläche mit Hilfe einer BET-Messung bei niedriger Temperatur bestimmt, wobei ein Pulver aus reinem Metall oder ein dünner Metall-Film verwendet wird, und dann Chemisorptions-Untersuchungen mit demselben Pulver oder Film durchführt. Auf diese Weise wurde z. B. gefunden, daß 0,27 cm^3 chemisorbierter Sauerstoff bei Normaldruck 1 m^2 Silber-Oberfläche bedeckt [50]. Grundlegende Daten über die Chemisorption werden normalerweise in dieser Art angegeben und verwendet. Wenn sich die aktive Komponente aus mehreren Elementen zusammensetzt, sind ins Detail gehende Untersuchungen nötig, um den betreffenden Bedeckungswert zu ermitteln.

Zusammenfassung

Die Gesamtoberfläche eines Pulvers, mit Ausnahme von Stoffen mit Mikroporen, läßt sich zuverlässig mit Hilfe von BET-Messungen bestimmen, obwohl eine zufriedenstellende theoretische Beschreibung bisher noch nicht zur Verfügung steht. Die Flüssigphasen-Adsorption und die Permeatrie bei Knudsen-Strömung lassen sich manchmal zur Bestimmung der Gesamtoberfläche anwenden. Die Zuverlässigkeit der erhaltenen Werte muß jedoch mit Hilfe anderer Untersuchungsmethoden, üblicherweise der BET-Methode, festgestellt werden. Deshalb sind diese Verfahren im allgemeinen kaum zu empfehlen. Mit Hilfe der Kleinwinkel-Röntgenstreuung sind sehr kurze Analysenzeiten möglich, wenn erst einmal eine Eichkurve mit einer Referenzprobe zur Verfügung steht. Im Prinzip schließt die Bestimmung der Röntgen-Streuung den Oberflächen-Anteil von Mikroporen ein. Eine chemisch identische Referenzprobe ist auf jeden Fall nötig.

Die Oberflächengröße von Mikroporen läßt sich zur Zeit nicht mit völliger Sicherheit bestimmen. Zur Bestimmung des Mikroporen-Anteils der Oberfläche läßt sich die Adsorption von Gasen mit unterschiedlicher Molekülgröße bei niedriger Temperatur anwenden. Wegen der erforderlichen außerordentlich hohen Drücke ist die Quecksilber-Penetrationsmethode in Gegenwart von Mikroporen problematisch, da dabei Mikroporen verformt werden können.

Die Kelvin-Gleichung für die Kapillarkondensation und -verdampfung dient als gesicherte Grundlage zur Bestimmung der Mesoporen-Oberfläche. Man erhält zufriedenstellende Werte, wenn sich die Poren-Geometrie genau beschreiben läßt. Anderenfalls hängen die Ergebnisse von der Anwendbarkeit eines Porenmodells ab. Die Bewertung der mit Hilfe der Quecksilber-Penetrationsmethode erhaltenen Oberflächengrößen hängt ebenfalls von der Zuverlässigkeit des Poren-Modells ab. Mit Hilfe der Flüssigphasen-Adsorption kann man gelegentlich wertvolle Informationen erhalten.

Die äußere Oberfläche läßt sich getrennt von der Mikroporen-Oberfläche bestimmen, wenn man bei der Flüssigphasen-Adsorption Moleküle verwendet, die größer als die Mikroporen sind. Dies Verfahren wird vor allem bei mikroporösem Kohlenstoff angewendet. Die Oberfläche läßt sich ohne Erfassung der Mikroporen auch mit Hilfe von Angaben aus dem Mehrschichten-Bedeckungsbereich der α_s-Isotherme ermitteln. Bei größeren Poren kann man die externe Oberfläche bestimmen, indem man von der Gesamtoberfläche die Porenoberfläche abzieht. Die durch aktive Komponenten bedeckte Oberfläche kann man mit Hilfe der Chemisorption bestimmen.

Eingegangen am 16. Dezember 1975 [B 3992]

Literatur

[1] *Gregg, S. J.; Sing, K. S. W.:* Adsorption, Surface Area and Porosity, Academic Press, London 1967.

[2] *Orr, Jr., C.; Dalla Valle, J. M.:* Fine Particle Measurement, Macmillan, New York 1959.

[3] *Smith, H. A.; Fuzek, J. F.:* J. Am. Chem. Soc. *68* (1946) S. 229.

[4] *Harkins, W. D.; Jura, G.:* J. Chem. Phys. *11* (1943) S. 431.

[5] *Reynouprez, A.:* Surface Area Determination (*D. H. Everett* and *R. H. Ottewill*, eds.), Butterworths, London 1970, S. 361.

[6] *McClellan, A. L.; Harnsberger, H. F.:* J. Colloid Interface Sci. *23* (1967) S. 577.

[7] *Brunauer, S.; Emmett, P. H.:* J. Am. Chem. Soc. *59* (1937) S. 2682.

[8] *Brunauer, S; Emmett, P. H.; Teller, E.:* J. Am. Chem. Soc. *60* (1938) S. 309.

[9] *De Boer, J. H.; Lippens, B. C.; Linsen, B. G.:* J. Catalysis *3* (1964) S. 36.

[10] *De Boer, J. H.; Linsen, B. G.; Osinga, Th. J.:* J. Catalysis *4* (1965) S. 643.

[11] *Dollimore, D.; Heal, G. R.:* J. Colloid Interface Sci. *33* (1970) S. 508.

[12] *Lippens, B. C.; De Boer, J. H.:* J. Catalysis *4* (1965) S. 319.

[13] *Sing, K. S. W.:* Chem. Ind. (1968) S. 1520.

[14] *Sing, K. S. W.:* Surface Area Determination (*D. H. Everett* and *R. H. Ottewill*, eds.), Butterworths, London 1970, S. 25.

[15] *Bhambhani, M. R.; Cutting, P. A.; Sing, K. S. W.; Turk, D. H.:* J. Colloid Interface Sci. *38* (1972) S. 109.

[16] *Pierce, C.; Wiley, J. W.; Smith, R. N.:* J. Phys. Chem. *53* (1949) S. 669.

[17] *Anderson, P. J.; Horlock, R. F.:* Trans. Faraday Soc. *65* (1969) S. 251.

[18] *Linsen, B. G.; Van den Heuvel, A.:* The Solid Gas Interface, Vol. *2* (*E. A. Flood*, ed.) Dekker, New York 1970, S. 1025.

[19] *Everett, D. H.; Haynes, J. M.:* Colloid Sci. *1* (1973) S. 123.

[20] *Scholten, J. J. F.; Beers, A. M.; Kiel, A. M.:* J. Catalysis *36* (1975) S. 23.

[21] *Dollimore, D.; Heal, G. R.:* J. Appl. Chem. *14* (1964) S. 109.

[22] *Roberts, B. F.:* J. Colloid Interface Sci. *23* (1967) S. 266.

[23] *Barrer, R. M.; McKenzie, N.; Reay, J. S. S.:* J. Colloid Sci. *11* (1956) S. 479.

[24] *Everett, D. H.:* The Structure and Properties of Porous Materials (*D. H. Everett* and *F. S. Stone*, eds.), Butterworths, London 1958, S. 95.

[25] *Ritter, H. L.; Drake, L. C.:* Ind. Eng. Chem., Anal. Ed. *17* (1945) S. 782.

[26] *Rootare, H. M.; Prenzlow, C. F.:* J. Phys. Chem. *71* (1967) S. 2733.

[27] *Svatá, M.:* Powder Tech. *5* (1971/72) S. 345.

[28] *Baker, D. J.; Morris, J. B.:* Carbon *9* (1971) S. 687.

[29] *Lamond, T. G.; Price, C. R.:* Rubber J. *152* (1970) S. 49.

[30] *Arai, H.; Yoshizaki, K.:* J. Colloid Interface Sci. *35* (1971) S. 149.

[31] *Janzen, J.; Kraus, G.:* Rubber Chem. Tech. *44* (1971) S. 1287.

[32] *Giles, C. H.; MacEwan, T. H.; Nakhawa, S. N.; Smith, D.:* J. Chem. Soc. (London) (1960) S. 3973.

[33] *Giles, C. H.; Nakhawa, S. N.:* J. Appl. Chem. *12* (1962) S. 266.

[34] *Templer, C. E.:* Particle Size Analysis (*M. J. Groves* and *J. L. Wyatt-Sargent* eds.), The Society for Analytical Chemistry, London 1972, S. 301.

[35] *Allen, T.; Patel, R. M.:* Particle Size Analysis (1970) (*M. J. Groves* and *J. L. Wyatt-Sargent* eds.), The Society for Analytical Chemistry, London 1972, S. 311.

[36] *Giles, C. H.; D'Silva, A. P.; Cameron, A.:* Chem. Ind. (1969) S. 239.

[37] *Kraus, G.; Ross, J. W.:* J. Phys. Chem. *57* (1953) S. 334.

[38] *Orr, C., Jr.:* Anal. Chem. *39* (1967) S. 834.

[39] *Brock, J. F.; Orr, C., Jr.:* Anal. Chem. *44* (1972) S. 1534.

[40] *Stanley Wood, N. G.; Chatterjee, A.:* Powder Tech. *9* (1974) S. 7.

[41] *Porod, G.:* Kolloid-Z. *124* (1951) S. 83.

[42] *Eanes, E. D.; Posner, A. S.:* The Solid-Gas Interface Vol. *2* (*E. A. Flood*, ed.) Dekker, New York 1967, S. 975.

[43] *Winslow, D. N.; Diamond, S.:* J. Am. Chem. Soc. *57* (1974) S. 193.

[44] *Van Nordstrand, R. A.; Hack, K. M.:* Presented, Division of Petroleum Chemistry, American Chemical Society, Chicago/Illinois (USA), 9./11. Sept. 1953.

[45] *Yates, J. T.; Garland, C. W.:* J. Phys. Chem. *65* (1961) S. 617.

[46] *Adams, C. R.; Bonesi, H. A.; Curtis, R. M.; Mersenheimer, R. G.:* J. Catalysis *1* (1962) S. 336.

[47] *Beeck, O.:* Adv. Catalysis *2* (1950) S. 151.

[48] *Beeck, O.; Ritchie, A. W.:* Disc. Faraday Soc. *8* (1950) S. 159.

[49] *Anderson, J. R.; Baker, B. G.:* J. Phys. Chem. *66* (1962) S. 482.

[50] *Scholten, J. J. F.; Konvalinka, J. A.; Beekman, F. W.:* J. Catalysis *28* (1973) S. 209.

AN EVALUATION OF PORE STRUCTURE BY MERCURY PENETRATION

by

Albert A. Liabastre and Clyde Orr
School of Chemical Engineering
Georgia Institute of Technology, Atlanta

SUMMARY

The pore structure of graded series of controlled pore glasses and Nuclepore membranes--both materials having pores with right-cylinder characteristics--were assessed by electron microscopy and mercury penetration. From comparisons of results, parameters in mercury penetration theory were evaluated, the correction for compressibility was examined, the cause of hysteresis was explored, and the general accuracy of the technique was appraised.

INTRODUCTION

Porous solid materials play important roles in technology having many ramifications throughout the economy. They are encountered widely in the chemical process industry, in pollution control, in life support systems, and in chemical research, to name only a few. Among the specific applications of porous solids are filters, adsorbents, chromatographic column packings, and catalyst supports. In every instances the size and shape of the

---

The work reported herein was made possible by National Science Foundation Grants Nos. ENG74-02718 and ENG76-10057.

pores are a primary concern, since these parameters influence the efficacy of the solid in its specific role. The size and shape features of porous solids are usually determined by one of two analytical techniques, mercury penetration or low temperature gas adsorption-desorption. Both techniques rely on extrapolations of theoretical hypotheses and physical constants obtained under conditions far removed from those actually prevailing under application. As a result they give information based on various assumptions having practical limitations and do not give unambiguous results. In cases where both analytical techniques are applied they sometimes give very different results.

This report examines the several assumptions in mercury penetration analysis and correlates experimental and microscopically determined values. A future report using the same experimental approach will consider the low temperature gas adsorption technique. The present problem was attacked by carefully examining and comparing results from selected materials having nearly cylindrical pores of relatively uniform diameter.

EXPERIMENTAL WORK

Two materials with pores in a variety of sizes were chosed for investigation. The first is known as controlled pore glass and was obtained* with nominal** pore diameters from 7.5 nm (=75 Å) to 193.3 nm (=1933 Å). It was chosen because its pores are relatively uniform, glass is very nearly incompressible, and it is widely employed in a number of applications. The other was Nuclepore membrane filters,*** which are polycarbonate sheets having holes

---

* Electro-Nucleonics, Inc., Fairfield, New Jersey.

** The nominal diameter as supplied by the manufacturer is used throughout for identification purposes.

*** Nuclepore Corporation, Pleasanton, California.

produced in them by a process consisting first of exposure to penetrating radiation followed by activated-track etching [1], hole size being controlled by the amount of etching. This material was chosen because its pores are essentially straight cylinders. It was commercially available at the time of initial purchase with nominal pore diameters from 30 to 8000 nm; by special arrangement membranes were obtained with nominal pores of 15 and 30 nm diameters having greater than normal pore densities.

Following material selection, the experimental effort consisted basically of electron microscopic examination to establish actual pore sizes and mercury penetration testing.

Electron Microscopic Examination: Considerable experimentation was necessary to elucidate both the glass and membrane pores sizes. For the glass, the procedure finally selected was first to crush it to a powder, heat the powder under vacuum to 180°C for one hour, raise the temperature to 250°C for 15 minutes, then cool to room temperature while still under vacuum. Powder samples were then placed in polyethylene mounting block forms which had previously been dried; Spurr resin* was poured over them; and the blocks were evacuated for 15 min. to aid pore penetration. Then the system was filled with nitrogen gas and set aside overnight. The next day the samples were cured at room temperature for 12 hours. Finally the cured samples were sectioned by microtome using a diamond knife into sections between 60 and 100 nm thick, and electron micrographs were made at microscope potentials of 80 and 100 kv. Figure 1 shows a typical electron micrograph obtained in this work. The lighter regions were interpreted as the pores in this study.

---

* Polyscience Inc., Warrington, Pennsylvania

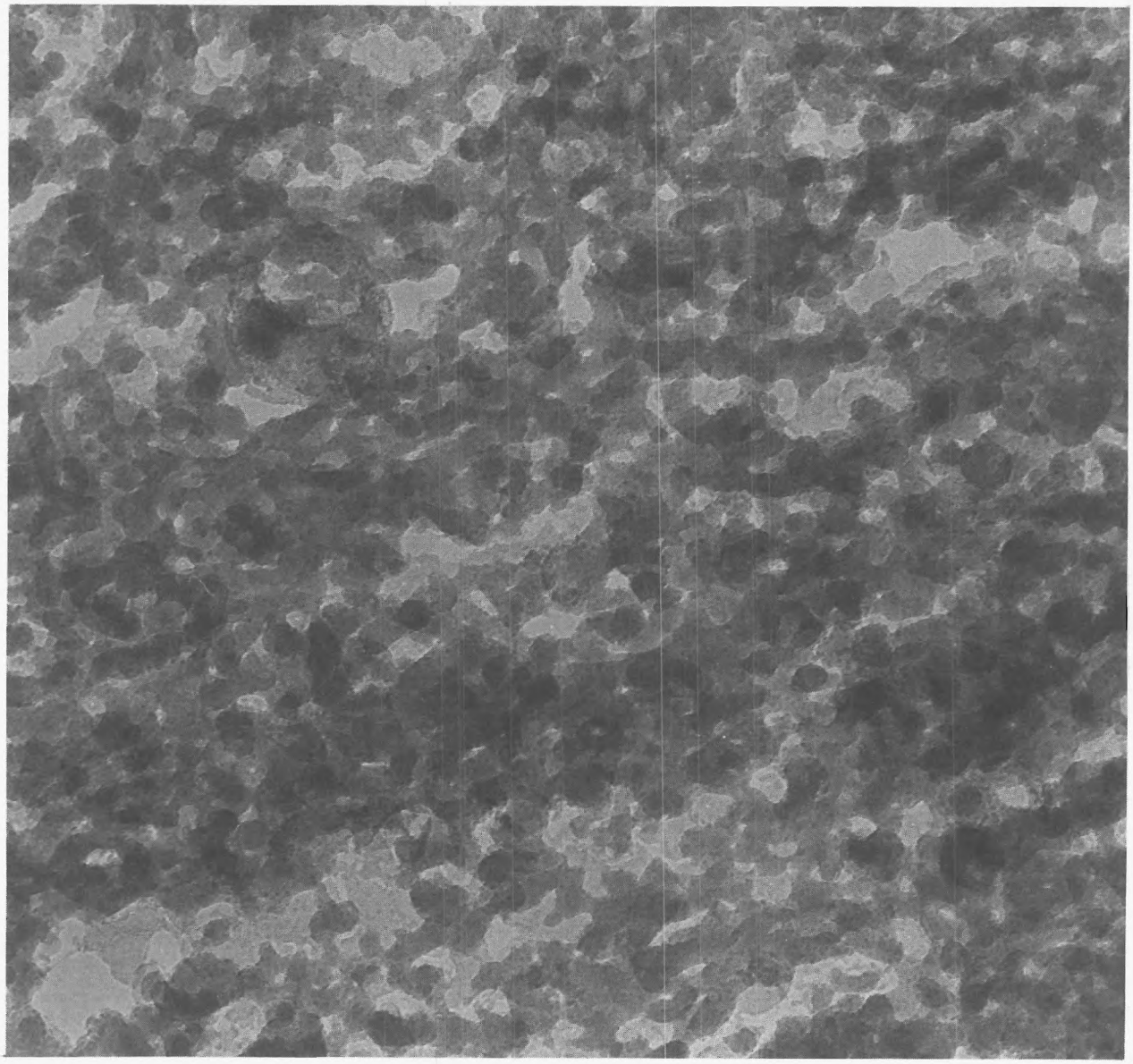

100 nm 192,000x

Figure 1. Transmission Electron Micrograph of Nominal 16 nm Controlled Pore Glass Using Ultramicrotomy.

It should be noted that the subsequent analysis of the micrographs can not be unambigous since the structure of the glass is quite complex. Wantanabe, Noake, and Aiba[2] suggested that porous glass has a honeycomb structure, i.e., linked cavities, while Karnaukhov[3] suggested that its structure was composed of cylindrical or close-to-cylindrical pores, closed and open-ended pores, and ink-bottle shaped pores. The only other known detailed evaluation of pore sizes from micrographs is that of Barrall and Cain[4], this work indicating the pores to be irregular, interconnected channels penetrating the entire glass structure. These latter investigators measured the widths of channels along lines oriented as nearly perpendicular as possible to one edge of each micro-channel, their resulting modal pore dimensions comparing quite well with their mercury porosimetry results. The micrograph analyses of this study were conducted along lines similar to those of Barrall and Cain[4] with much effort being made to determine the size distribution of the pores. In the case of the nominal 16 nm glass, for example, this method and the method of Barrall and Cain[4] were compared and yielded basically the same modal diameter.

For Nuclepore membranes containing nominal 15 and 30 nm diameter pores one technique involved first embedding the membranes in a suitable resin and then sectioning by microtome. Three types of resin were tried: Spurr, methylmethacrylate, and Araldite*. The Spurr resin and methlmethacrylate formed unsuitable bonds with the membrane while the Araldite resin formed a weak but usable bond. A typical sample preparation was as follows: The membrane was cut into approximately 6-mm diameter discs and soaked for 1 minute in water to remove the static charge. The discs were then soaked 1 hr in a 1% uranyl acetate in methanol solution in order to dye the pores for viewing

---

* Cargille Scientific, Inc., Cedar Grove, New Jersey.

in an electron microscope. After drying at room temperature, the discs were placed one at a time in a 20-mm diameter pool of Araldite, exercising caution not to entrap air. The Araldite-disc composite was next sandwiched between two pieces of tetrafluroethylene and cured overnight at 70°C. The composite was re-embedded in a capsule of Araldite and again cured overnight at 70°C. The capsule was finally microtomed using a diamond knife into 60 to 100 nm thick sections. Figure 2 shows a typical electron micrograph obtained by this method.

The carbon replica method was also employed in examining the 15 and 30 nm pores. This involved coating the membrane surface with a layer of carbon and then dissolving away the membrane using chloroform; this method avoided the possibility of pore distortion due to microtoming. A typical transmission electron micrograph is shown as Figure 3.

All larger pores were examined using standard scanning electron microscope techniques; typical micrographs are shown in Figures 4 and 5. The accuracy of this latter method is about $\pm$ 20 nm; the accuracy of the methods utilizing transmission electron microscopy is believed to be $\pm$ 2.0 nm.

All micrographs were analyzed using a Carl Ziess Particle Size Analyzer, Model TGZ3. A minimum of 1000 pores was measured for each nominal size material. The micrographs were obtained from at least five different sample sections and at several different magnifications. The results of these analyses were obtained as numbers of pores greater than specific diameters. Figures 6 and 7 show these "true" pore size distributions obtained from electron microscopy. The length of the bars indicates the error estimate.

Electron microscopic analysis also included cross-sectioning of Nuclepore membranes and examining pore shapes. Cross sections are shown in Figures 8 and 9. It was concluded from examining many such micrographs that the pores

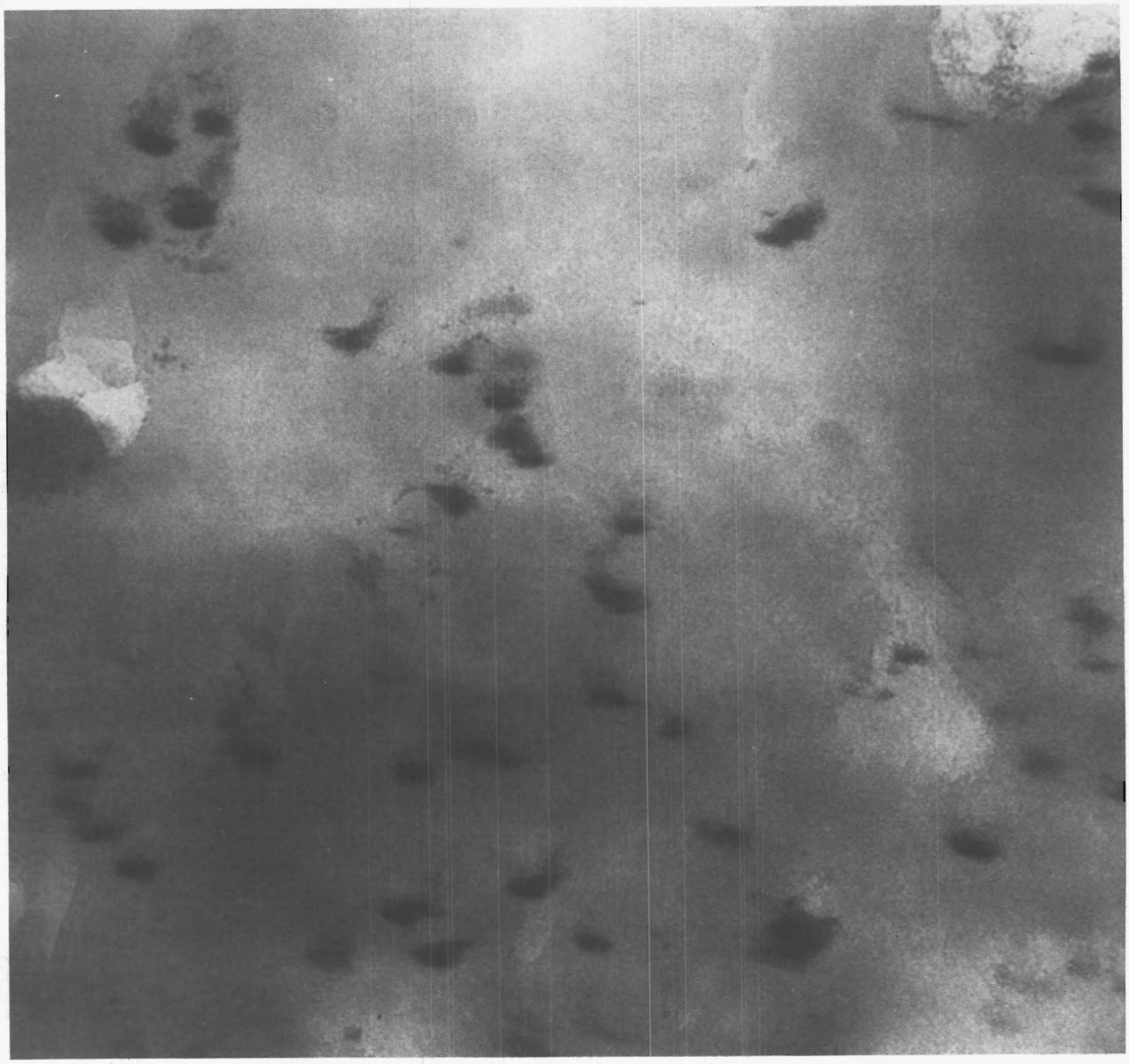

100 nm 192,000x

Figure 2. Transmission Electron Micrograph of Nominal 15 nm Nuclepore Membrane Using Ultramicrotomy.

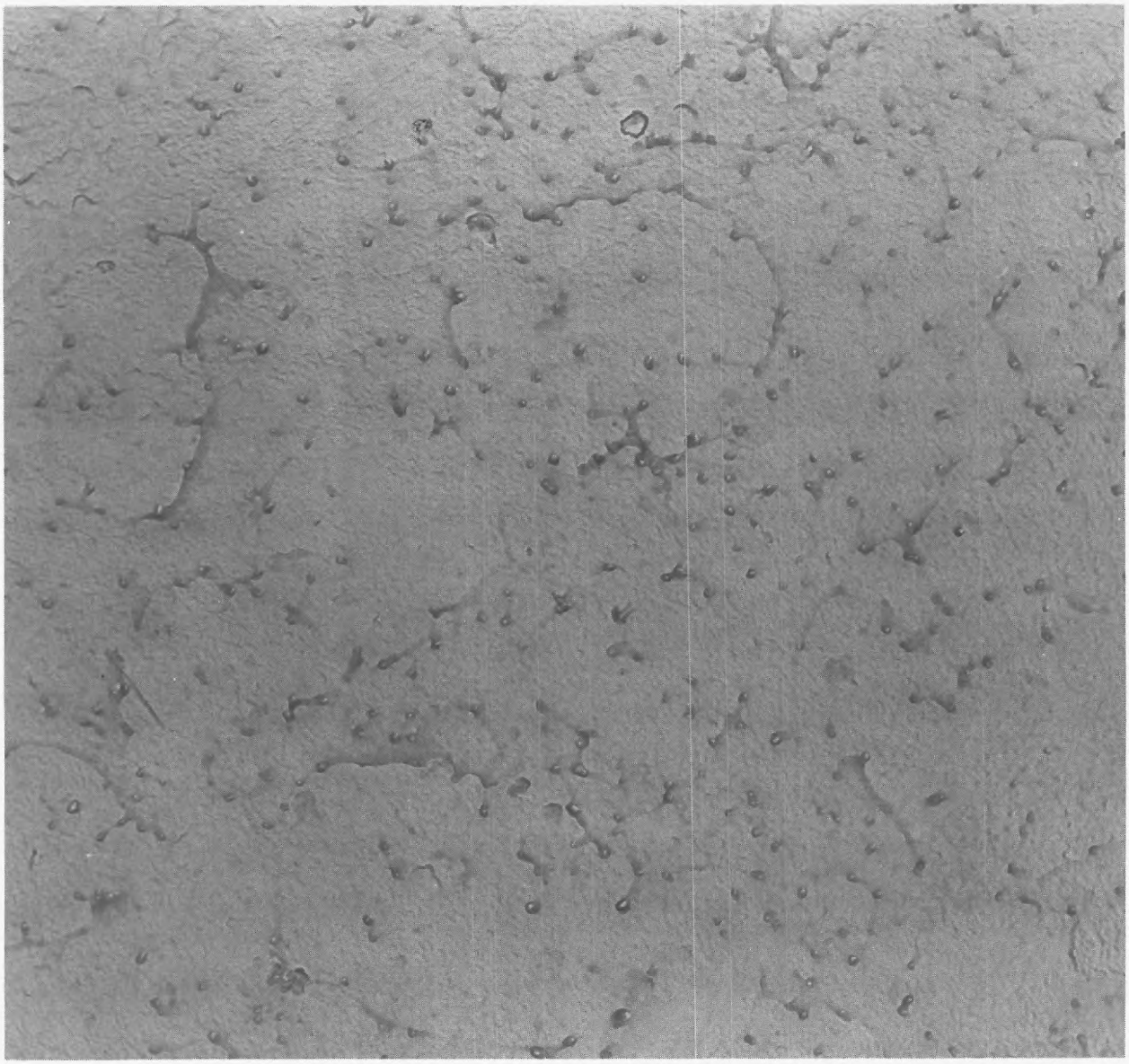

1,000 nm 46,700x

Figure 3. Transmission Electron Micrograph of Nominal 15 nm Nuclepore Membrane Using Carbon Replica, Smooth Side.

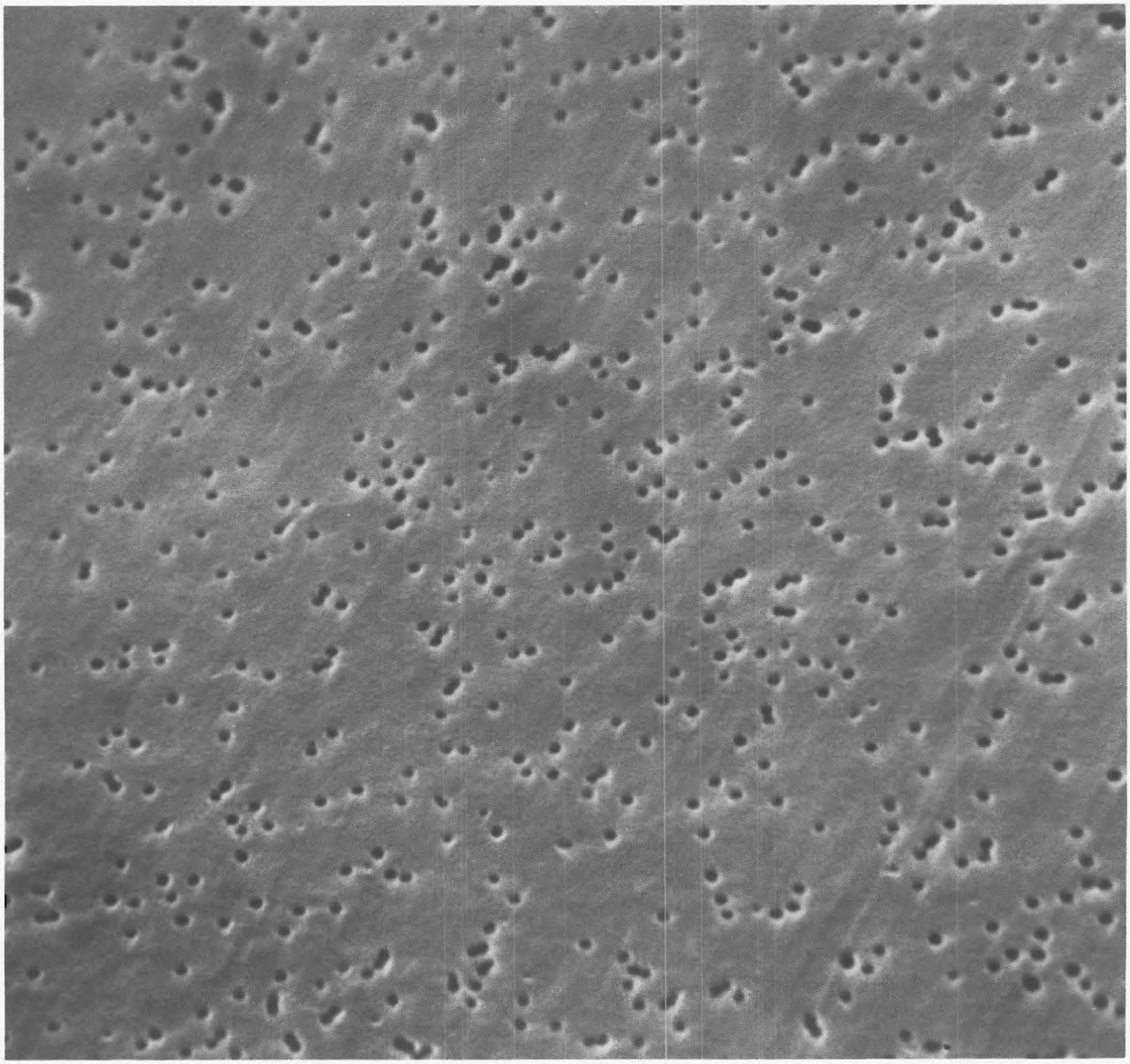

1,000 nm 13,200x

Figure 4. Scanning Electron Micrograph of Nominal 200 nm Nuclepore Membrane, Smooth Side.

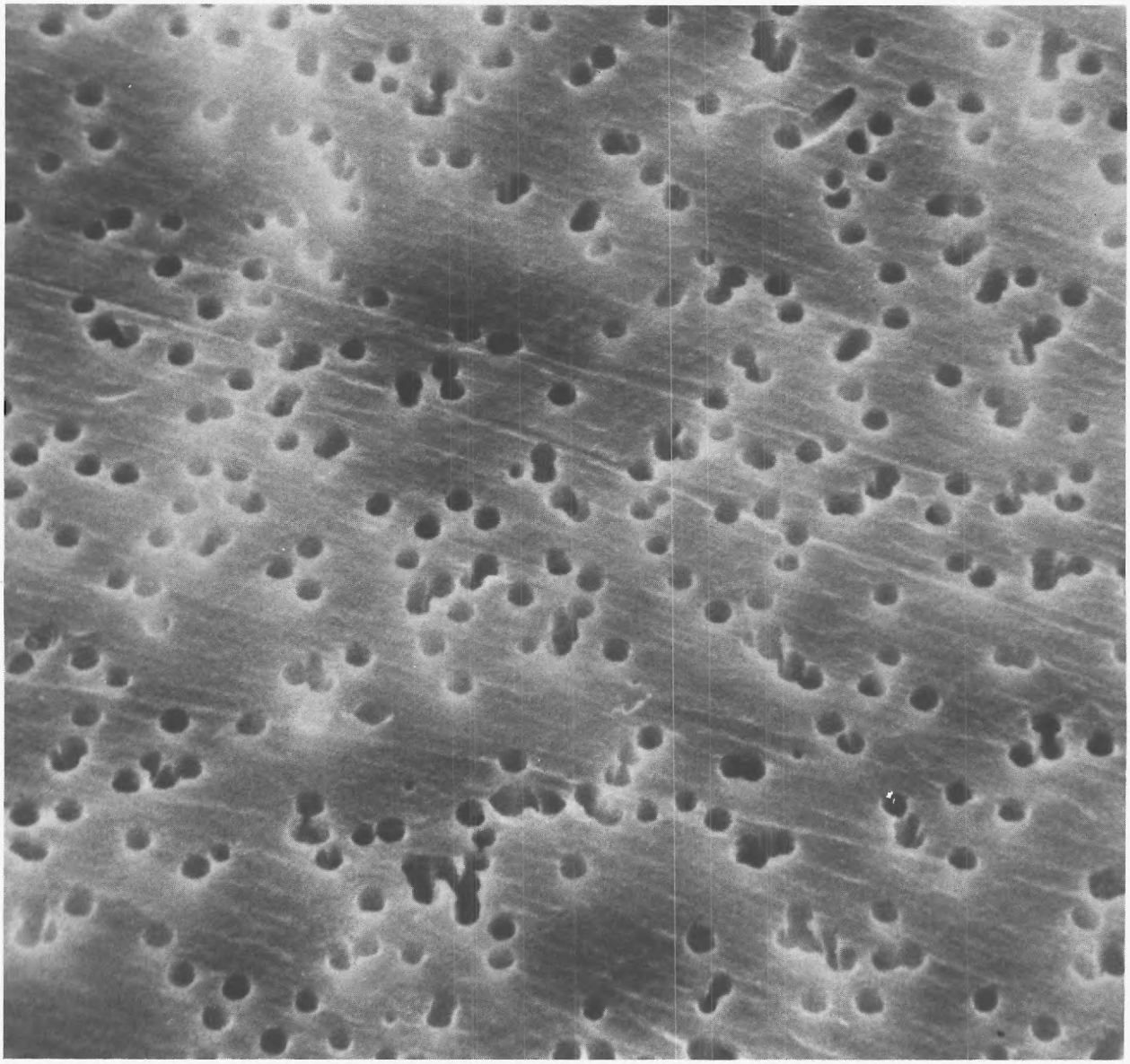

1,000 nm 4,158x

Figure 5. Scanning Electron Micrograph of Nominal 1,000 nm Nuclepore Membrane, Smooth Side.

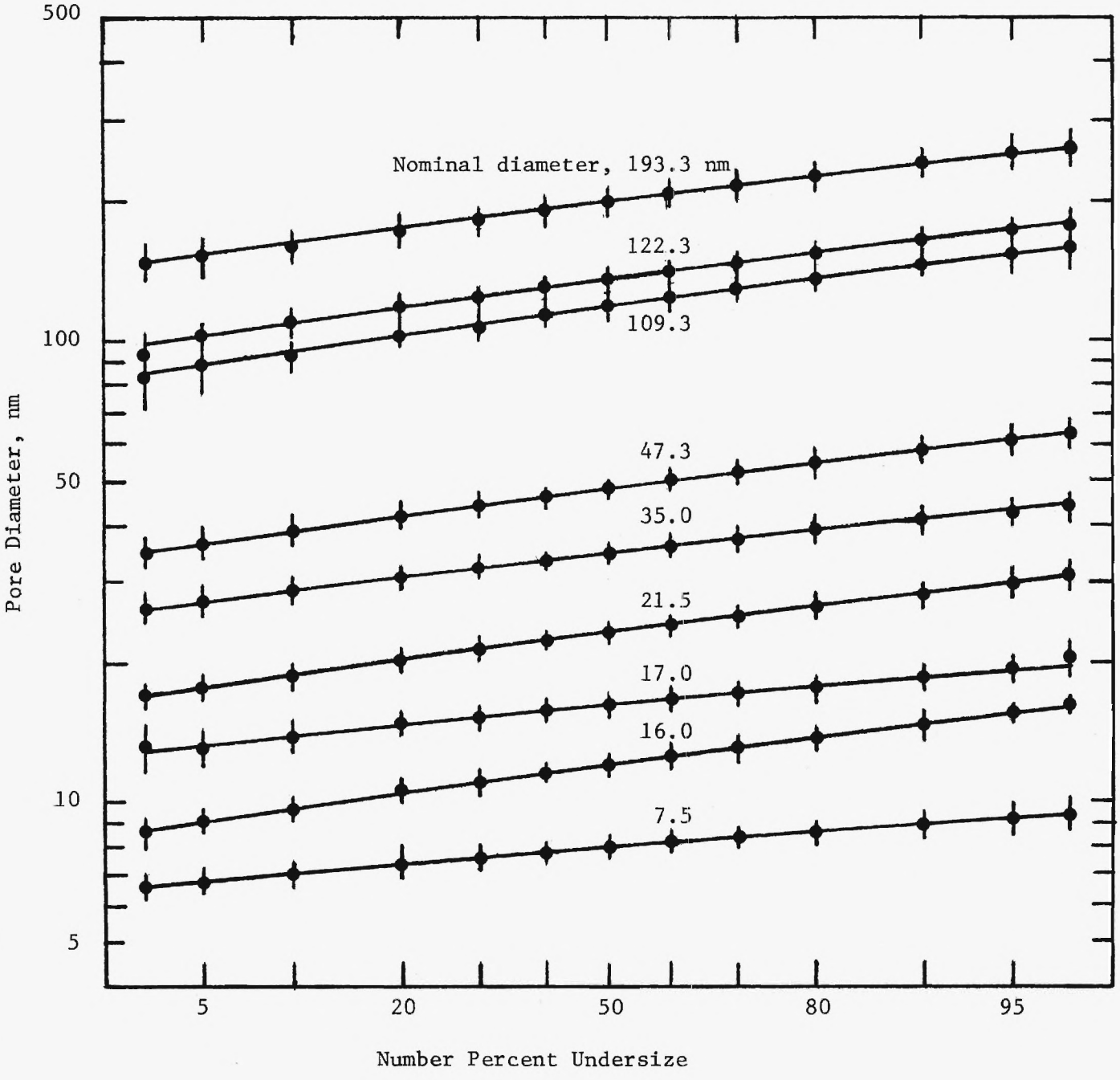

Figure 6. Pore Distribution for Controlled Pore Glass from Electron Microscopy.

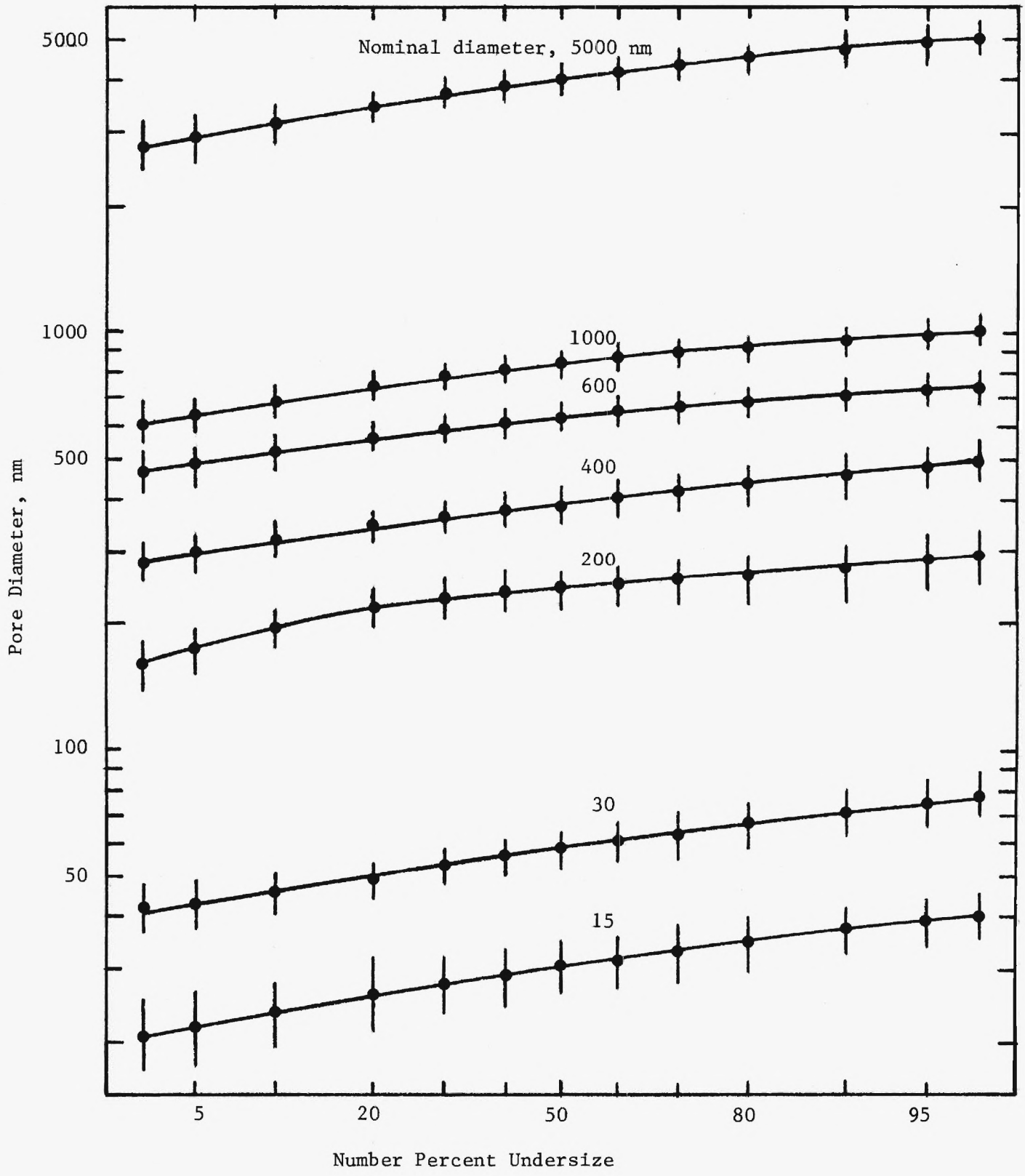

Figure 7. Pore Distribution for Nuclepore Material from Electron Microscopy

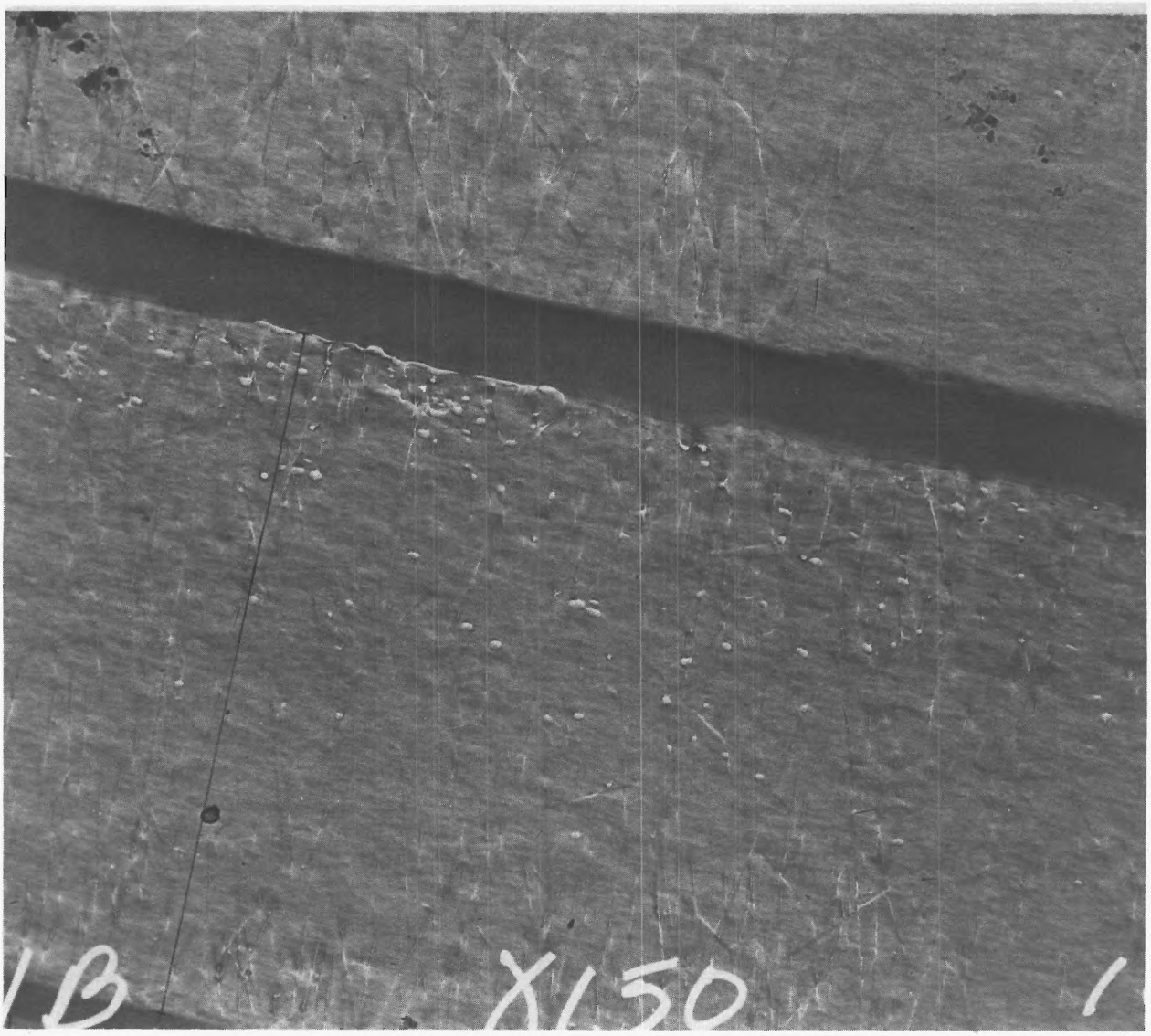

1,000 nm 12,800x

Figure 8. Transmission Electron Micrograph of Cross Section of Nominal 15 nm Nuclepore Membrane Using Ultramicrotomy. The line marks one membrane thickness.

1,000 nm 20,500x

Figure 9. Transmission Electron Micrograph of Cross Section of Nuclepore Membrane Using Ultramicrotomy.

were well represented as regular cylinders. The larger Nuclepore membranes were sized on both their rough and smooth sides; no statistical difference in the size distribution of the pores was found with the side of the membrane examined. Pore densities were determined by counting pores on specific micrographed areas for all Nuclepore membrane sizes. Table I presents electron microscopic data pertaining both to the controlled pore glasses and the Nuclepore materials.

Mercury Porosimetry: These experiments were conducted using a Micrometrics Mercury Penetration Porosimeter, Model 905-1. All samples were dried in an oven at 100 $\pm$ 5°C for at least 48 hours prior to testing. All samples were evacuated for at least 12 hours to a pressure of not more than 1.33 Nm^{-2} after being placed in the instrument sample cell. The mercury was triply distilled.

Repetative analyses were made with all porous glasses, excellant reproducibility being achieved in all cases. Figure 10 is a plot of typical intrusion and extrusion data while Table II presents mean pore diameters calculated from the intrusion results. Due to the comparatively low pore volume and limited quantities of Nuclepore materials, repetitive analyses were achieved only with the 15, 30, and 1,000 nm samples. Where repetitive analyses were conducted good reproducibility was achieved, however. Figure 11 presents typical intrusion and extrusion data for one of the Nuclepore materials, and mean pore diameters calculated from the intrusion data are also summarized in Table II. In addition, Table II contains mean diameter results corrected for material compressibility as described subsequently. It should be noted that all distributions including both those from electron microscopy and mercury penetration in their central tendencies were so sharp and so symmetrical that modal, average, and mean diameters could not be distinguished within the accuracy of the data. Mean diameter as used herein is thus really a composite; it is the

Table I. Results of Electron Microscopic Examination

Nominal Pore Diameter (nm)	Measured Number Mean Diameter (nm)	Pore Density (Pores/cm^2 x 10^{-9})
Porous Glass		
7.5	8.0	-
16.0	12.0	-
17.0	16.0	-
21.5	23.2	-
35.0	34.8	-
47.5	48.3	-
109.3	120.0	-
122.3	137.0	-
193.3	199.5	-
Nuclepore Membrane		
15	30.3	3.5
30	58.0	4.3
200	242	0.40
400	388	0.12
600	628	0.028
1000	843	0.023
5000	4040	0.0004

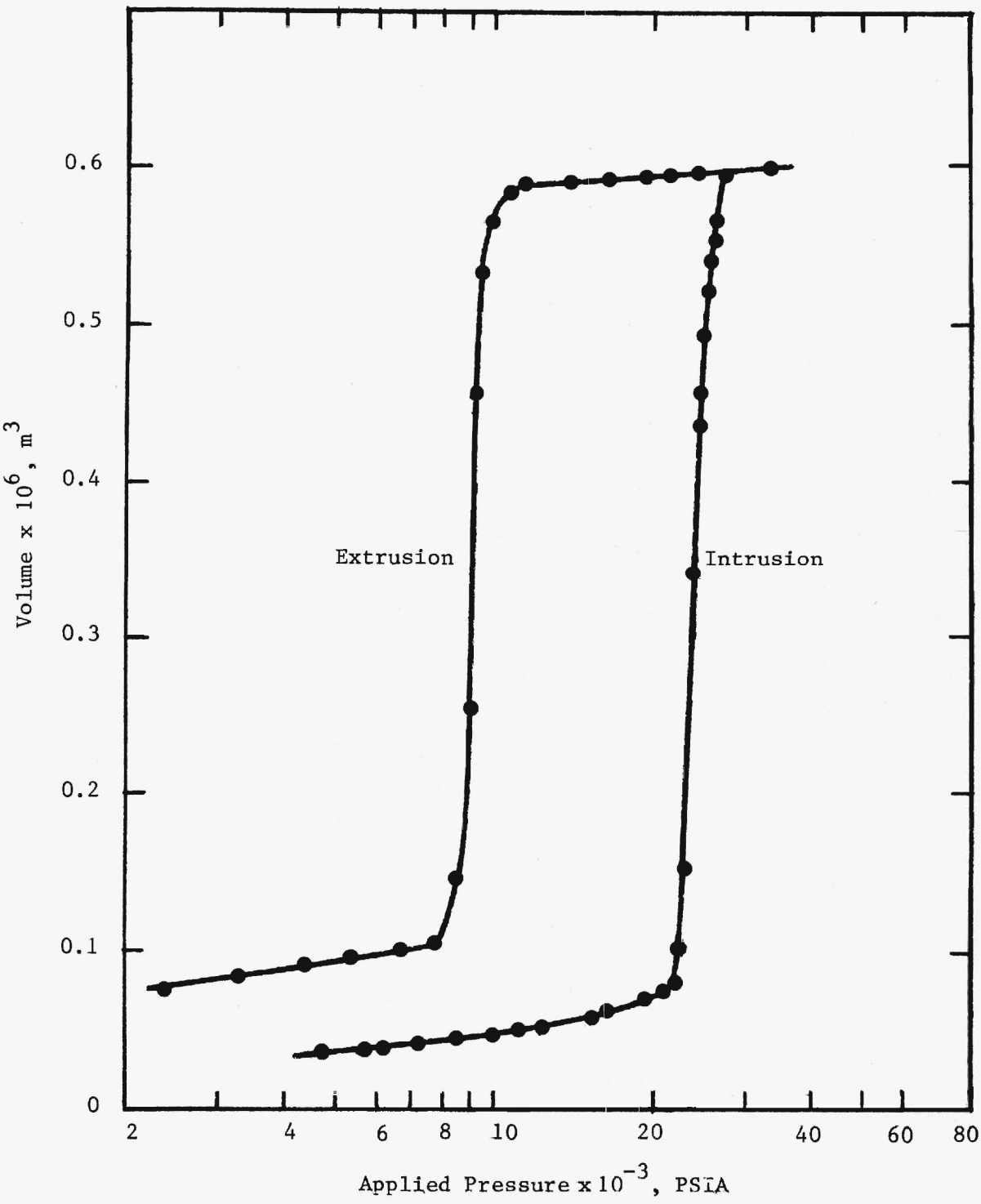

Figure 10. Experimental Mercury Penetration into 7.5 nm, Controlled Pore Glass

Table II. Mercury Porosimetry Results

Nominal Pore Diameter	Measured Mean Diameter	Corrected* Mean Diameter
(nm)	(nm)	(nm)
Porous Glass		
7.5	7.5	-
16.0	11.9	-
17.0	16.8	-
21.5	21.8	-
35.0	37.2	-
47.5	49.3	-
109.3	124.2	-
122.3	131.2	-
193.3	200.9	-
Nuclepore Membrane		
15	19.9	30.3
30	42.8	58.2
200	217	242
400	406	413
600	693	679
1000	769	747
5000	4160	4040

* For pressure, as described in text.

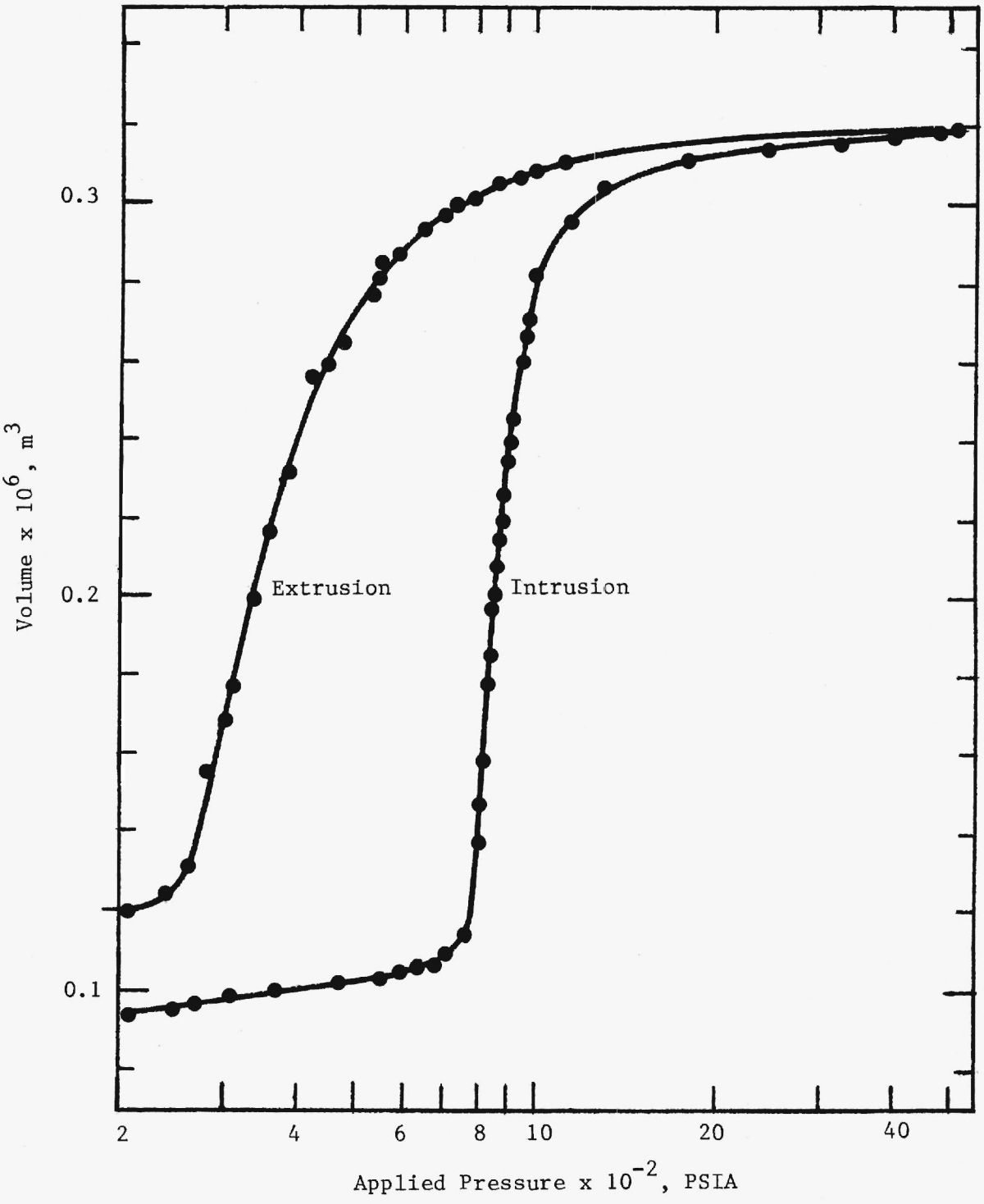

Figure 11. Experimental Mercury Penetration into 200 nm Nuclepore Material.

diameter that, all elements considered, is believed most representative.

DISCUSSION

General The technique of mercury intrusion under pressure to determine pore size distributions was first proposed by Washburn[5]. Since that time the technique has been developed and improved to the extent that it is theoretically possible also to determine the quantity of pore spaces in porous materials, the density of both solid objects and powders, the pore specific surface area, a measure of particle size distribution in the case of porous powders, and information about the shape and structure of pores.[6-9,11]

Experimentally the instrumentation employed in conducting mercury intrusion and extrusion analyses indicates the volume of liquid mercury (nonwetting) forced under pressure into the pores and extruded from the pores as the pressure is released. The material to be analyzed is first dried and evacuated to remove adsorbed gases and vapors. Mercury will then enter, or intrude, the pores in response to their size and to the applied pressure.

The surface tension of mercury opposes its entrance into pores and it is this opposition the externally applied pressure must overcome. Whenever a liquid exhibits an angle of contact with a solid of greater than 90° it resists wetting the solid and entering into pore spaces. Mercury exhibits a greater contact angle with a larger number of materials than any other conveniently usable liquid. Thus, it is a most suitable liquid for the evaluation of porous materials.

If a pore is assumed to be right cylindrical, then the surface tension σ of the mercury acts along the circle of contact for a length equal to the perimeter of the circle. If d is the pore diameter, the force tending to squeeze the liquid out of the pore normal to the plane of the circle of contact may be

written as $-\pi\sigma d \cos\theta$, where θ is the angle of contact between the liquid and the solid. The opposing force, i.e., the force due to the externally applied pressure, acts over the area of the circle of contact and is given by $\pi Pd^2/4$, where P is the applied pressure. At equilibrium the two forces must be equal, thus

$$-\pi\sigma d \cos\theta = \pi Pd^2/4 \qquad (1)$$

or

$$Pd = -4\sigma \cos\theta \qquad (2)$$

Equation 2 relates the pore diameter with the pressure required to intrude mercury into the pore. Use of eq. 2 presumes both the surface tension σ and the contact angle θ are pressure independent.

Reported measurements[9,10] of contact angles between mercury and a large variety of materials range from about 112° to 142°, with 130° being the most frequently encountered value. In the absence of specific information about the contact angle, a value of 130° is usually adopted; however, use of an incorrect value can give rise to large differences in apparent pore diameter[6]. On the other hand, the value of the surface tension and its temperature dependence give a much smaller effect on apparent pore diameter; the value[6] used in this work for the surface tension was 0.474 Nm^{-1}.

The pore size distribution may be determined by designating the volume of pores having diameters between d and d + dd by dV, such that

$$dV = F(d)dd \qquad (3)$$

where F(d) is the pore size distribution function. Differentiating eq. 3 with σ and θ assumed constant and combining the result with eq. 3 leads to

$$dV = -\frac{d}{P} F(d)dP \qquad (4)$$

Since experimental data are obtained as the volume of all pores having diameters

greater than d, the total pore volume V_t is thus diminished by the volume V of pores having diameters greater than d. The pressure-volume experimental data are therefore actually values of $(V_t - V)$ and P. When plotted they yield a curve having the slope $d(V_t - V)/dP$, or $-dV/dP$ since V_t is constant. Thus, eq. 4 may be rewritten as

$$F(d) = \frac{P}{d} \frac{d(V_t - V)}{dP} \tag{5}$$

the terms on the right side being readily assessable from the experimental pressure-volume data.

The cylindrical pore model and experimental data may also be used to calculate a value for the surface area of the sample.[6,7] Assuming there are n cylindrical pores of length L and mean diameter d, pore volume V_p is equal to $n\pi d^2 L/4$; pore area A_p is equal to $n\pi dL$ (assuming pores open at both ends); and hence the pore area can be expressed by

$$A_p = 4V_p/d \tag{6}$$

A relationship first used by Kiselev[11] for gas adsorption was applied by Rottare and Prenzlow[12] to obtain surface area from experimental mercury penetration data which involves no assumptions regarding a pore shape model. They stated that since work was required to force mercury into pores and was described by the PV term, this could be related to the total surface area of the pores, the work required to immerse an area dA of solid surface in mercury being given by

$$dW = -PdV = \sigma \cos\theta \, dA \tag{7}$$

Because the work required to immerse a surface in mercury demands integration over the entire range of pressures necessary to fill the pores, eq. 7 may be rearranged and integrated, yielding

$$A_p = -\frac{\int_{V_{rmin}}^{V_{rmax}} P dV}{w \sigma \cos\theta} \tag{8}$$

where w is the weight of the sample. Equation 8 when rearranged gives

$$\theta = \cos^{-1} \frac{\int_{V_o}^{V_m} P dV}{\sigma A} \qquad (9)$$

which can be used to evaluate the contact angle if the sample surface area is known. This latter quantity might, for example, be determined independently by the B.E.T. method.[13]

The assumption of goodness of fit for the cylindrical pore shape model may be evaluated by the relationship of eq. 6 written

$$4\ V_p/dA_p = K \qquad (10)$$

the closer the value of the expression being to unity the better the assumption.

The question of hysteresis exhibited in mercury porosimetry also arises. It has been suggested that the presence of hysteresis is due primarily to the existance of ink bottle pores.[7,8,12,14] However, both the porous glasses and Nuclepore membranes which have few, if any, ink bottle pores exibit hysteresis (see Figs. 10 and 11).

Porous Glass: Once information is available regarding the true size distribution of pores as obtained from careful electron microscopic examination, the correctness of the values used for the surface tension and the contact angle in the mercury penetration analyses can be tested. If the values employed are correct and there are no pressure effects, a plot of either true, i.e., from electron microscopy, diameter d_T versus the diameter obtained from mercury intrusion d_I should be a straight line with a slope of unity, or d_I/d_T versus d_T should be a straight line with a slope of zero and intercept of unity. Figure 12 shows the above plots for controlled pore glass and indicates that there are no discernable pressure effects. Figure 13, also for the controlled pore glass, shows the volume percent pores and number percent pores versus

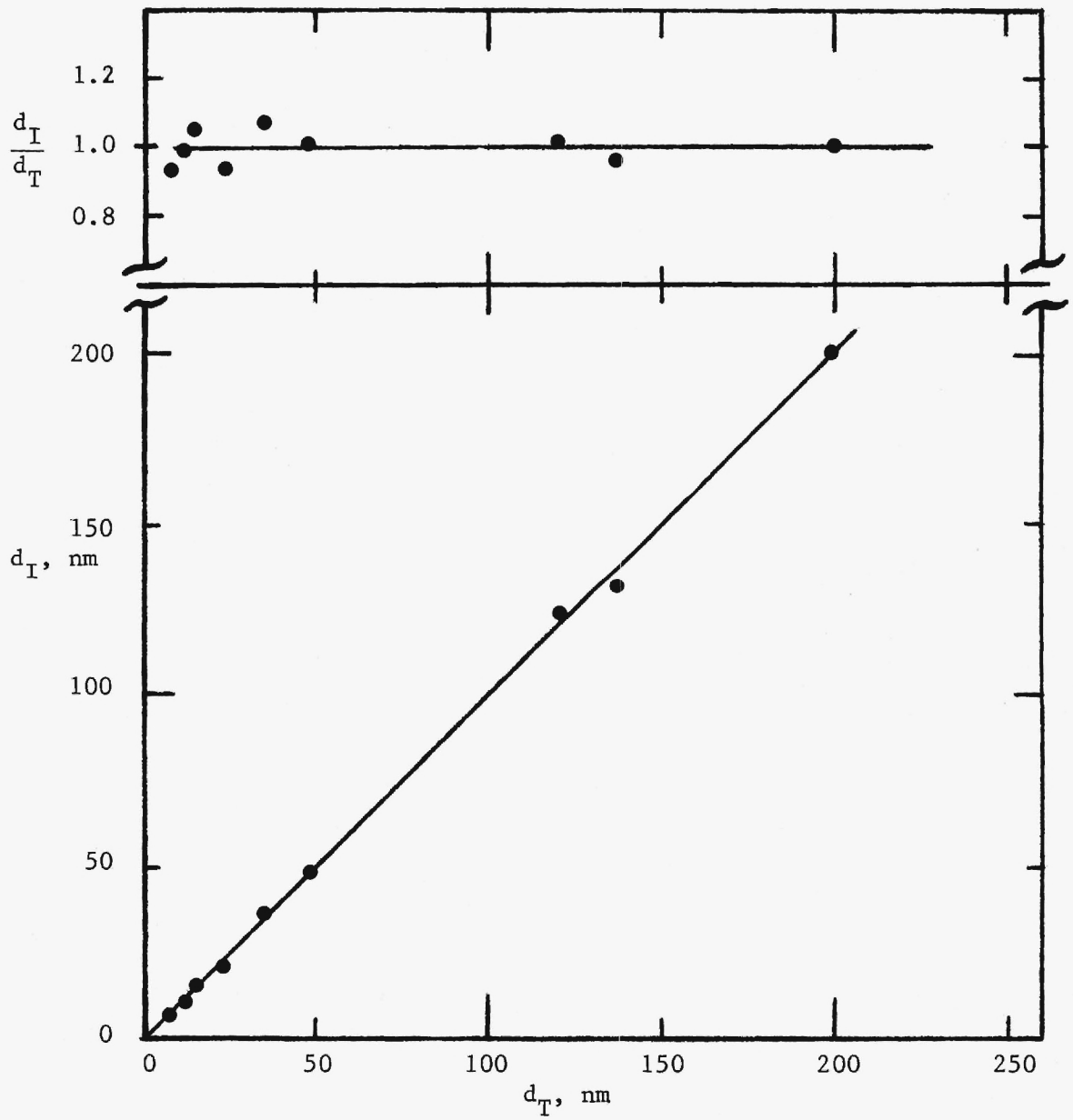

Figure 12. Relationship of Penetration and Microscopic Diameters for Controlled Pore Glass.

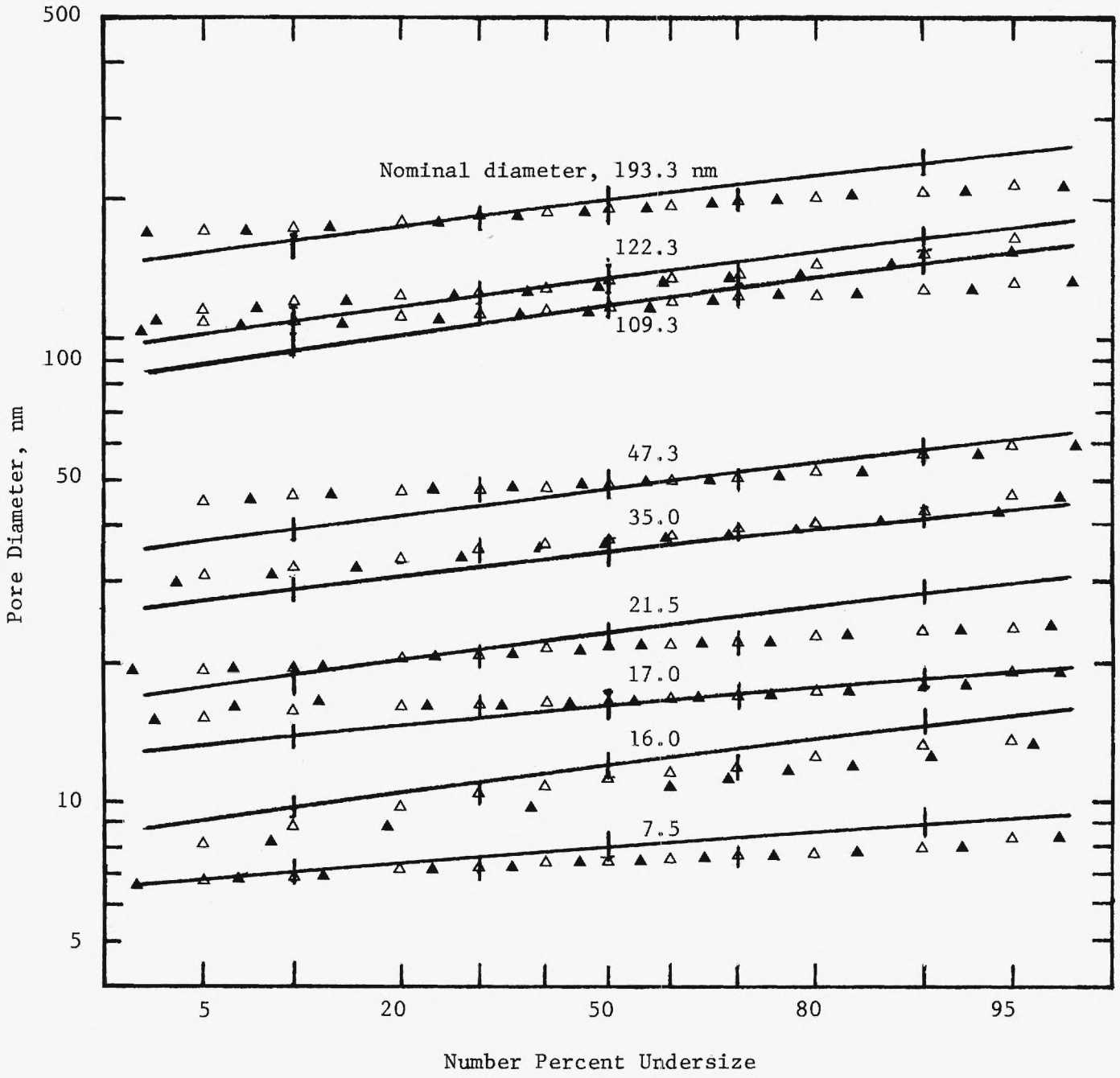

Figure 13. Volume (△) and Number (▲) Pore Distributions from Mercury Penetration Compared with Number (solid line) Distribution from Microscopy for Controlled Pore Glass.

diameter compared to the number percent true diameter from the electron micrographs (see Figure 6). The number percent pores was calculated from the volume percent pores by assuming all pores to be the same average length. These results indicate that both sets of calculated data fit equally well within the experimental error.

Table III contains the volume, area, and mean diameter of pores obtained from mercury porosimetry as well as the area of pores calculated using eq. 6 and the goodness of fit criterion, K, calculated using eq. 10. These results also indicate the cylindrical pore model is appropriate for the porous glass.

All the glass samples exhibited hysteresis. Figure 14 shows a plot of the ratio of the mean diameter determined from both mercury intrusion and extrusion d_I/d_E *versus* the pressure corresponding to the pore diameter from electron microscopy as related through eq. 2. The plot indicates that a decided change of slope takes place over the pressure range 1000-2000 psi, suggesting that a general change in pore filling and emptying occurs as pores become smaller than approximately 100 nm.

Nuclepore Membrane Plots similar to Figure 12 of true diameter d_T *versus* the diameter obtained from mercury intrusion d_I and of d_I/d_T *versus* d_T for the Nuclepore materials are shown in Figure 15. These indicate that the Nuclepore material is subject to pressure effects as would be expected. If the correct contact angle is used, the plot of d_I/d_T *versus* d_T should asymptotically approach unity as d_T approaches infinity ($P \rightarrow 0$). To make this so, it was found that the value for the contact angle should be 126.3°.

A pressure correction curve as shown in Figure 16 was also developed. The true pressure was calculated using the microscopically determined mean pore diameter in eq. 2. The experimental mercury intrusion data were corrected for compressibility using the curve of Figure 16, and a volume and number percent

Table III. Other Parameters Determined by Mercury Penetration

Nominal Pore Diameter	From Mercury Penetration		Calculated*	Goodness of**
	Pore Volume	Pore Area	Pore Area	Fit Criterion
(nm)	(cm^3/g)	(cm^2/g)	(cm^2/g)	
Porous Glass				
7.5	0.515	276	273	0.988
16.0	0.617	228	206	1.000
17.0	0.571	136	139	0.999
21.5	0.858	158	156	0.989
35.0	0.986	113	111	0.978
47.5	1.080	84.6	88.6	1.047
109.3	0.906	30.3	29.7	0.982
122.3	0.864	26.9	25.9	0.963
193.3	0.812	16.8	16.4	0.973
				Avg. 0.991
Nuclepore Membrane				
15	0.042	5.63	5.60	0.994
30	0.119	7.82	8.23	1.054
200	0.208	3.44	3.43	0.997
400	0.303	2.69	2.84	1.054
600	0.150	0.92	0.96	1.043
1000	0.211	1.07	1.00	0.937
5000	0.0765	0.0767	0.0757	0.988
				Avg. 1.010

* From eq. 6.

** From eq. 10. Should be unity.

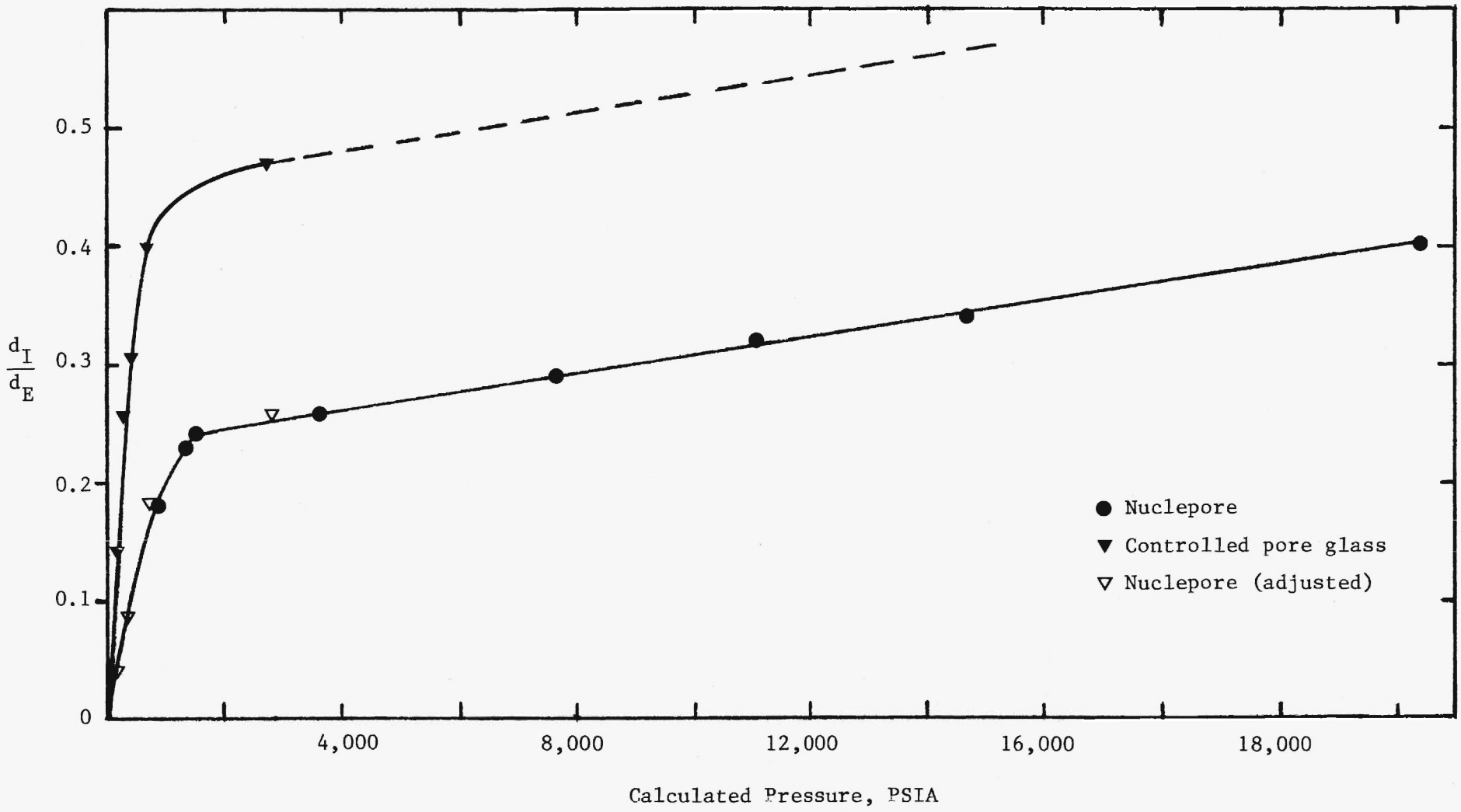

Figure 14. Mean Intrusion and Extrusion Diameter Ratio as a Function of Calculated Pressure Corresponding to Pore Diameter from Microscopy.

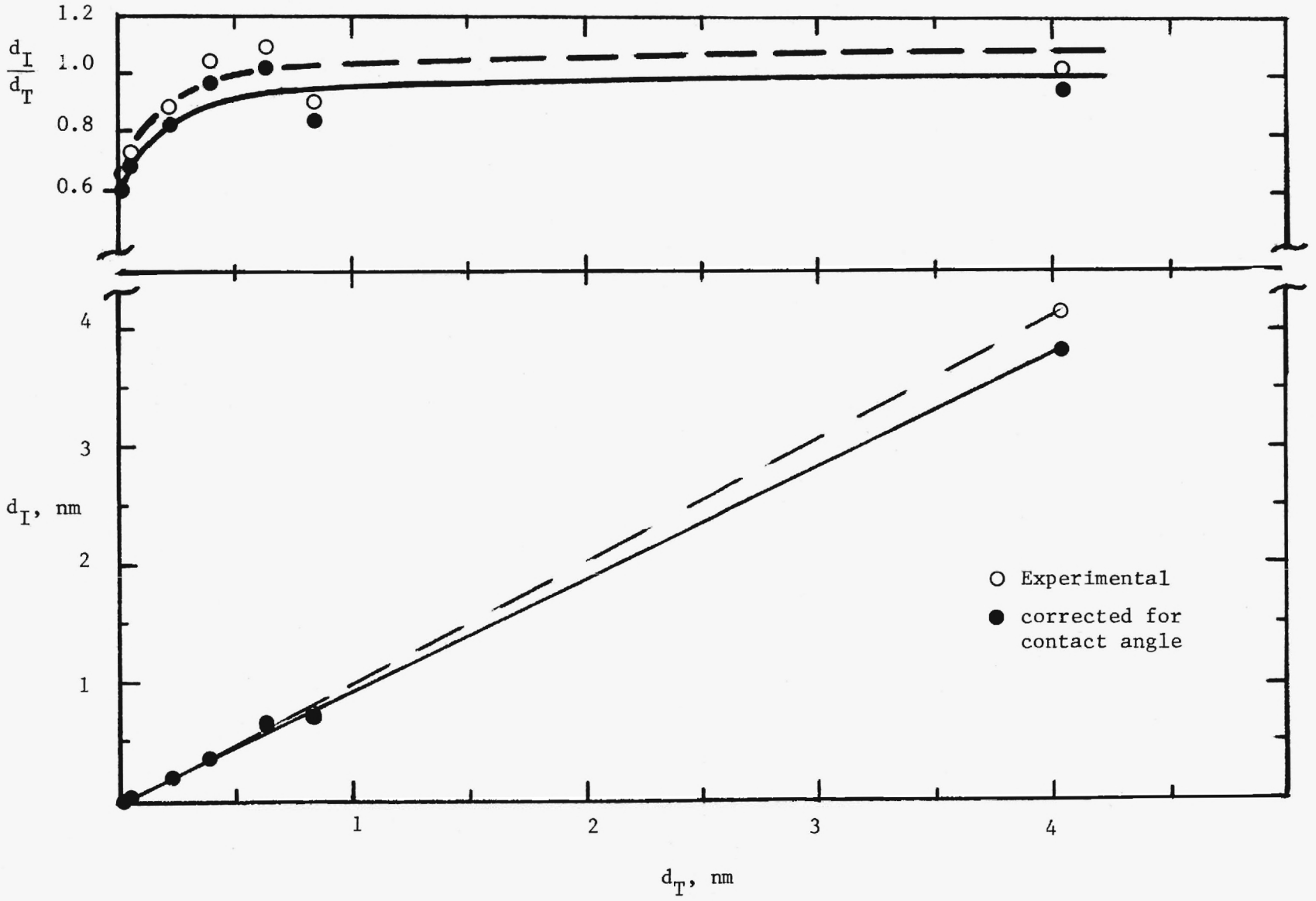

Figure 15. Relationship of Penetration and Microscopic Diameters for Nuclepore Material.

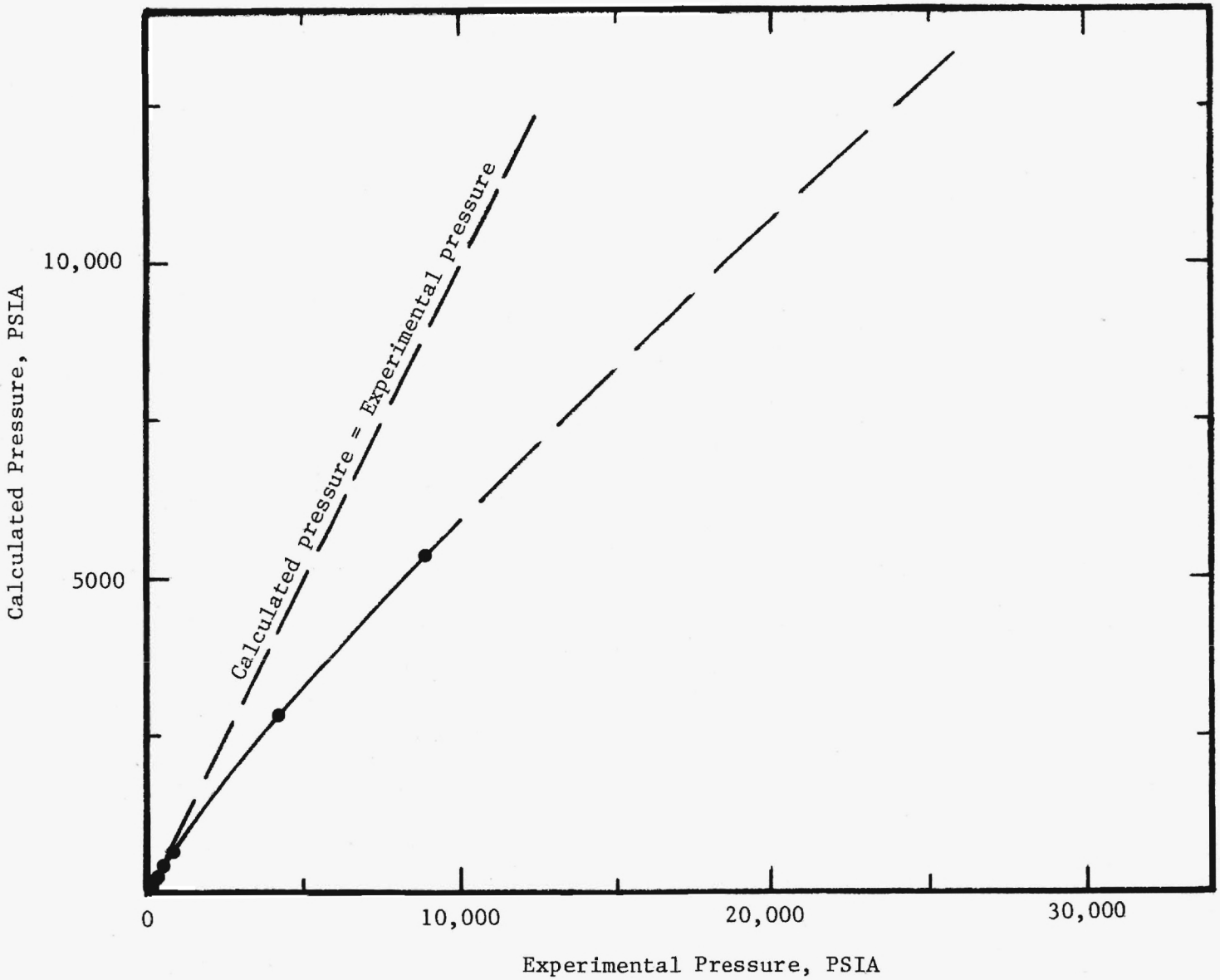

Figure 16. Pressure Corresponding to Model Pore Diameter from Mercury Penetration Compared with Calculated Pressure Corresponding to Pore Diameter from Microscopy for Nuclepore Material.

pore distribution was then determined. These latter data, upon being compared with the true number percent pore distribution as originally presented by Figure 7, indicated a compressibility correction alone was insufficient. Next a simple pressure correction was applied, and Figure 17 on which the original data are repeated (solid lines) show the resulting volume percent pores and number percent pores versus diameter compared to the number percent true pore distribution (from electron micrographs). This comparison indicates the appropriate correction is a simple pressure correction, the reason possibly being explained by either of two models. One model assumes the pores are distorted in such a way that, while the total volume remains essentially the same, the pores take on a hour-glass shape. The other, and favored model, supposes pores are compressed to an hour-glass shape thereby exhibiting a effectively smaller diameter until mercury actually enters them. Upon the entrance of mercury, they expand due to the equalization of hydrostatic pressure and resume something near their original volume. The partial closing and reduction in diameter accounts for the apparent entry of mercury into pores smaller than they actually are, and the subsequent return to shape explains correct volume measurement and why a simple pressure correction is sufficient. Further investigation of this model of behavior is currently underway.

Table III contains the pore volume and area obtained from mercury porosimetry along with the area of pores calculated using eq. 6 and the goodness of model fit calculated using eq. 10. The results of the model fit calculation also indicate the cylinderical pore model is correct for Nuclepore membranes.

All the Nuclepore membranes exhibited hysteresis even though their pores are exceptionally good straight cylinder models. Figure 14, as presented earlier, indicates that a change of slope for the Nuclepore materials takes place over the pressure range 700-2800 psi (also observed with porous glass), suggesting

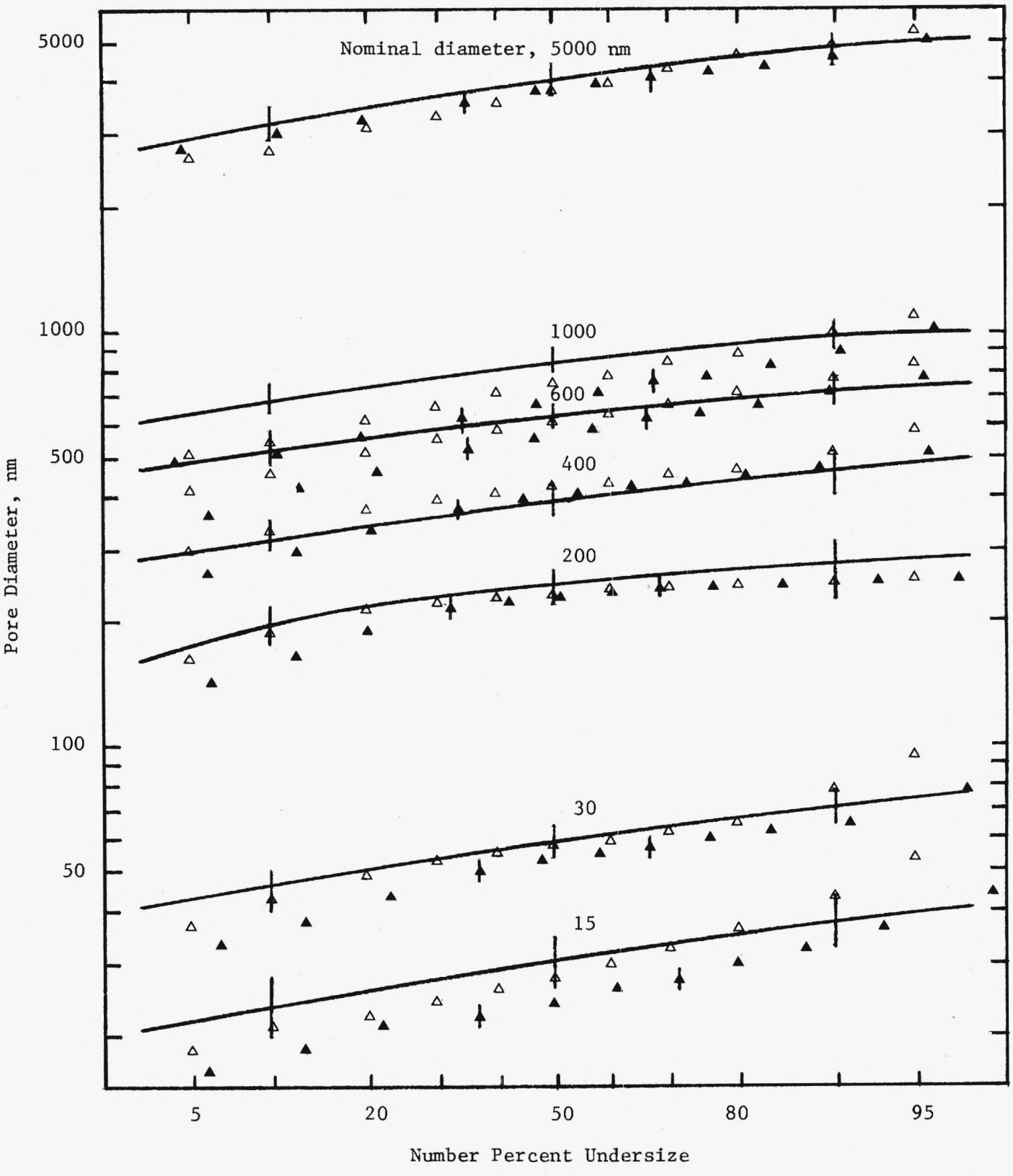

Figure 17. Volume (△) and Number (▲) Pore Distributions from Mercury Penetration Compared with Number (solid line) Distribution from Microscopy for Nuclepore Material.

again that a general change in pore filling and emptying occurs as pores become smaller than approximately 100 nm. Furthermore, if a constant value for d_I/d_E (= 0.215) is subtracted from the Nuclepore curve it is shifted downward and becomes identical to that for the controlled pore glasses. This may indicate that the mechanism of pore filling and emptying is similar regardless of the material and differs only by some constant property of the mercury or solid, possibly surface roughness. It will be necessary to examine other materials before carrying this observation further.

REFERENCES

1. R. L. Fleischer, H. W. Alter, S. C. Furman, P. B. Price and R. M. Walker Technological Applications of Science: The Case of Particle Track Etching, Report No. 72CRD107, March 1972, General Electric Company Corporate Research and Development, Schenectady, N.Y.

2. M. Wantanabe, H. Noake, and T. Aiba, "Electron Micrographs of Some Borosilicate Glasses and Their Internal Structure", J. Am. Ceramic Soc., 42, 593 (1959).

3. A. P. Karnaukhov, "Combined Investigation of the Pore Structure of Catalysts. I. Some Problems in the Contemporary State of the Sorption Method," Kinetika in Kataliz, 8, 172 (1967).

4. E. M. Barrall and J. H. Cain, "Optical and Electron Microscopy of Bio-Glass Chromatography Substrates," J. Polymer Sci., 21, 253 (1968).

5. E. W. Washburn, "Note on a Method of Determining the Distribution of Pore Sizes in a Porous Material", Proc. Nat. Acad. Sci., 7, 115 (1921).

6. H. M. Rootare, "A Short Literature Review of Mercury Porosimetry as a Method of Measuring Pore-Size Distributions in Porous Materials, and a Discussion of Possible Sources of Errors in this Method," Aminco Laboratory News, 24, No. 3, Fall 1968.

7. C. Orr Jr., "Application of Mercury Penetration to Material Analyses", Powder Technology, 3, 117 (1969).

8. M. Svatá, "Determination of Pore Size and Shape Distribution from Porosimetric Hystersis Curves," Powder Technology, 5, 345 (1971).

9. C. Orr, Jr., and J. M. DallaValle, Fine Particle Measurement, Macmillan, New York, 1959.

10. A. H. Ellison, R. B. Klemm, A. M. Schwartz, L. S. Grubb, and D. A. Petrash, "Contact Angles of Mercury on Various Surfaces and the Effect of Temperature", J. Chem. Eng. Data, 12, 607 (1967).

11. D. H. Everett and F. S. Stone (eds.), The Structure and Properties of Porous Materials, P. 130, Butterworths Scientific Publications, London, 1958.

12. H. M. Rootare and C. F. Prenzlow, "Surface Areas from Mercury Porosimeter Measurements", J. Phys. Chem., 71, 2734 (1967).

13. S. Brunauer, P. H. Emmett, and E. Teller, "Adsorption of Gases in Multimolecular Layers", J. Am. Chem. Soc., 60, 309 (1938).

14. N. M. Kamakin, "Metody issledovaniya struktury vysokodispersnych i poristych tel", Izd Akad. Nauk. SSSR, Moskva. P. 48 (1958).

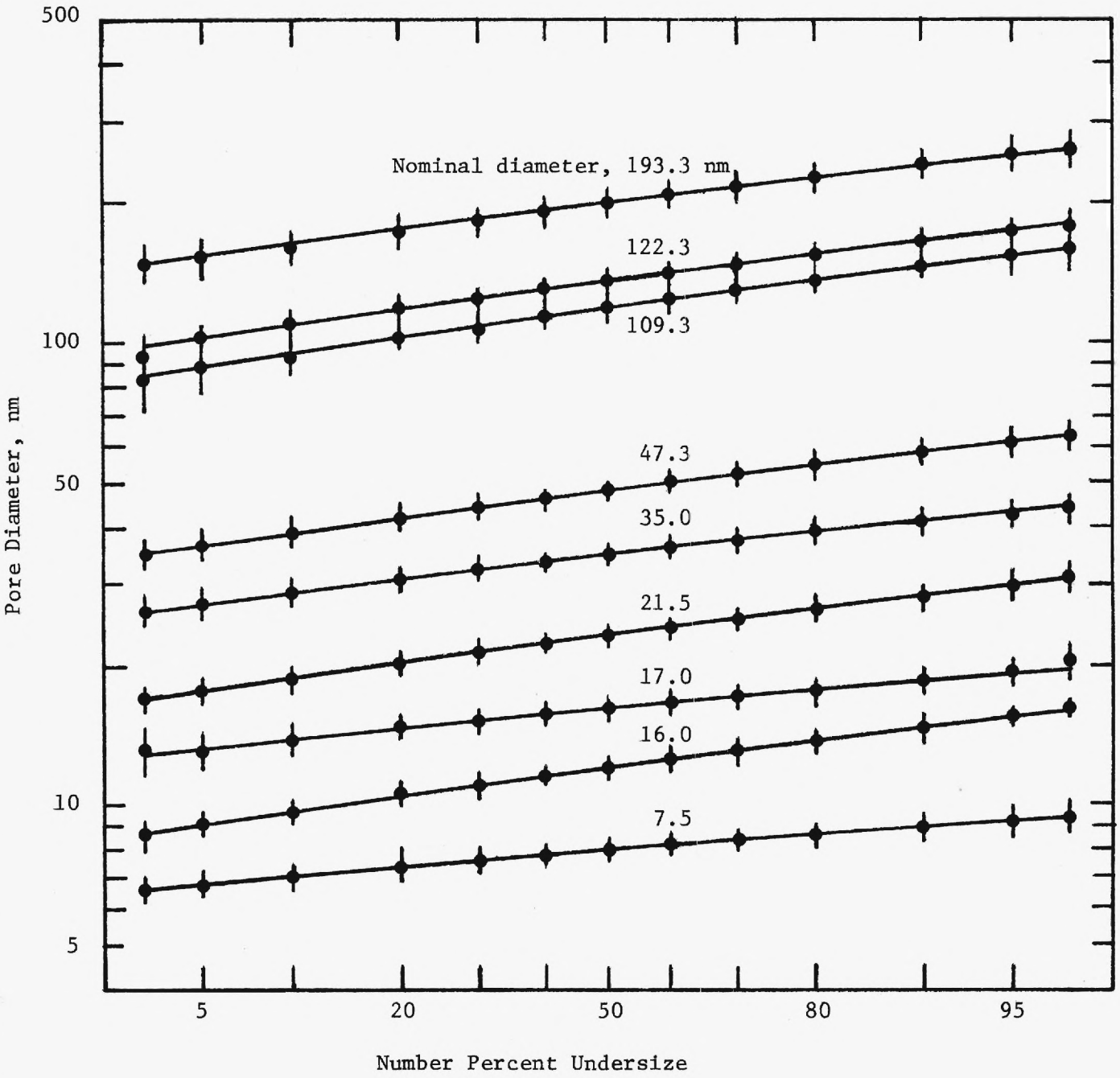

Figure 6. Pore Distribution for Controlled Pore Glass from Electron Microscopy.

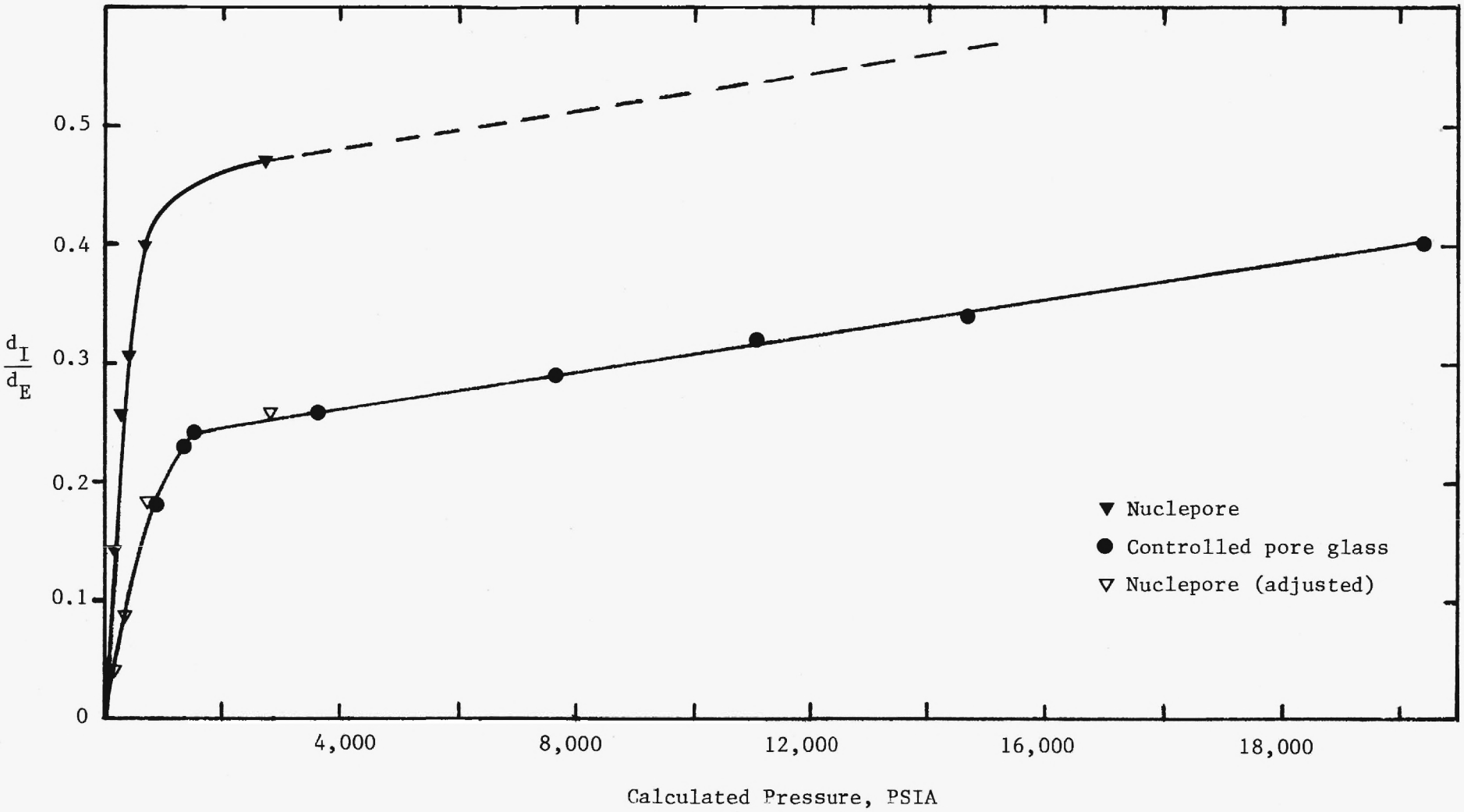

Figure 14. Mean Intrusion and Extrusion Diameter Ratio as a Function of Calculated Pressure Corresponding to Pore Diameter from Microscopy.